

THE EFFECTS OF VALPROIC ACID ON MOTOR IMPAIRMENT, OXIDATIVE  
STRESS PARAMETERS, APOPTOTIC MARKERS AND EPIGENETIC  
MECHANISMS IN A 6-HYDROXYDOPAMINE RAT MODEL OF PARKINSON'S  
DISEASE



by  
Meltem Dağdelen

Submitted to Graduate School of Natural and Applied Sciences  
in Partial Fulfillment of the Requirements  
for the Degree of Doctor of Philosophy in  
Biotechnology

Yeditepe University  
2016

THE EFFECTS OF VALPROIC ACID ON MOTOR IMPAIRMENT, OXIDATIVE  
STRESS PARAMETERS, APOPTOTIC MARKERS AND EPIGENETIC  
MECHANISMS IN A 6-HYDROXYDOPAMINE RAT MODEL OF PARKINSON'S  
DISEASE

APPROVED BY:

Prof. Dr. Ece Genç  
(Thesis Supervisor)

  
.....

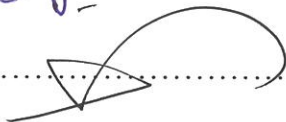
Prof. Dr. Ertuğrul Kılıç

  
.....

Prof. Dr. Zafer Gören

  
.....

Assoc. Prof. Dr. Ünal Uslu

  
.....

Assist. Prof. Dr. Alev Cumbul

  
.....

DATE OF APPROVAL: ...../...../2016

## ACKNOWLEDGEMENTS

This study would not have been possible without the support of many people. First of all, I would like to gratefully thank to my supervisor, Prof. Dr. Ece Genç, who has supported me throughout my thesis with her patience and knowledge.

I am very grateful to Assoc. Prof. Dr. Ünal Uslu and Assist. Prof. Dr. Alev Cumbul for their invaluable guidance and giving me the opportunity to use their laboratories. I would like to thank Prof. Dr. Bayram Yılmaz and YUDETAM personnel Vet. Engin Sümer, technicians Selim Doğan and Uğur Akdaş for opening their laboratories and giving me full support during my animal experiments.

I would like to gratefully thank to my dear friends, Dr. Hatice Akkaya, Sığnem Eyüboğlu, Başak Şentürk, Eray Şahin, Dr. Burcu Şeker and Sinem Ethemoglu for their endless support; cooperation and friendship that I always feel.

Last but not the least; I would like to especially express my deepest gratitude to my family. I would like to thank to my parents Fatma Dağdelen and Ali Dağdelen, my sister Meral Dağdelen Alagöz, my nephew and niece Seyhan and İlayda Alagöz, and especially to my fiancé Hasan Sazak for their endless love, confidence, unconditional support and understanding throughout my life. This thesis would not be possible without their support and motivation.

I would like to acknowledge that this study was financially supported by Yeditepe University Research Center, through the research grant no: 120800002.

## **ABSTRACT**

### **THE EFFECTS OF VALPROIC ACID ON MOTOR IMPAIRMENT, OXIDATIVE STRESS PARAMETERS, APOPTOTIC MARKERS AND EPIGENETIC MECHANISMS IN A 6-HYDROXYDOPAMINE RAT MODEL OF PARKINSON'S DISEASE**

Parkinson's Disease (PD) is characterized by the progressive loss of dopaminergic neurons resulting in deteriorated motor activity in patients. Currently, there is only symptomatic treatment; therefore, developing effective neuroprotective and neurorestorative therapies is needed. Studies indicate neuroprotective effects of histone deacetylase inhibition in PD models. Valproic acid (VPA), which is used in the treatment of epilepsy, is a histone deacetylase inhibitor and there is limited information on the effects of VPA in PD. The aim of this study is to use VPA post-acutely and compare its potential effects on neuronal survival, motor activity, oxidative stress parameters, apoptotic mechanisms and histone acetylation levels in the brain with the effects of gold standard therapeutic agent levodopa in a 6-hydroxydopamine animal model of PD. The results of this study demonstrated that VPA treatment decreased the number of apoptotic neurons and slightly increased the number of dopaminergic neurons. VPA treatment reduced oxidative stress by decreasing the level of malondialdehyde and increasing the activities of superoxide dismutase, glutathione S-transferase and reduced glutathione. The phosphorylation of both p90RSK and ribosomal S6 protein, which are involved in cell survival and proliferation process, are increased in VPA treated groups. Furthermore, histone acetylation was slightly increased in VPA treated groups. Although the locomotor activity parameters were slightly improved, they were still lower than sham operated groups. Over all, these results indicate that VPA may have therapeutic potential in the treatment of PD, but further research should be performed in order to fully understand its limitations and potential therapeutic effects.

## ÖZET

### **6-HİDROKSİDOPAMİN SIÇAN PARKİNSON MODELİNDE VALPROİK ASİDİN MOTOR AKTİVİTE, OKSİDATİF STRES PARAMETRELERİ, APOPTOTİK MEKANİZMALAR VE EPİGENETİK MEKANİZMALAR ÜZERİNDEKİ ETKİLERİ**

Parkinson Hastalığı (PH), dopaminerjik nöronların ölmesi sonucu hastaların motor aktivitesinin kötüleşmesi ile karakterize olur. Günümüzde yalnızca semptomatik tedavi mevcuttur, bu sebeple nörokoruyucu ve nörorestoratif tedavi geliştirilmesine ihtiyaç duyulmaktadır. PH modellerinde yapılan çalışmalar histon deasetilaz inhibisyonunun olası nörokoruyucu etkilerini göstermiştir. Epilepsi hastalarının tedavisinde kullanılan Valproic asit, bir histon deasetilaz inhibitörüdür ve PH modellerindeki etkisini araştıran kısıtlı sayıda çalışma mevcuttur. Bu çalışmanın amacı, 6-hidroksidopamin PH hayvan modelinde post akut olarak kullanılan valproik asidin; nöronal sağkalım, motor aktivite, oksidatif stres parametreleri, apoptotik mekanizmalar ve histon asetilasyonu üzerindeki etkilerini günümüz tedavisindeki altın standart levodopa ile karşılaştırmaktır. Bu çalışmanın sonuçları, valproik asit tedavisinin apoptotik nöron sayısını düşürdüğünü ve dopaminerjik nöron sayısını arttırdığını göstermiştir. Valproik asit tedavisi malondialdehit seviyesini düşürerek ve superoksit dismutaz, glutatyon s-transferaz ve redükte glutatyon aktivitelerini arttırarak oksidatif stresi azaltmıştır. Hücre sağkalımı ve çoğalmasında önemli olan p90 RSK ve ribozomal S6 protein fosforilasyonları valproik asit tedavisi ile artmıştır. Ayrıca histone asetilasyonu da valproik asit tedavisi ile bir miktar artmıştır. Lokomotor aktivite parametrelerinde iyileşme görülse de, kontrol gruplarına göre lokomotor aktiviteler düşük kalmıştır. Bu sonuçlar PH tedavisinde valproik asidin tedavi potansiyeli olabileceğini göstermektedir, ancak valproik asidin tedavideki sınırlarını ve potansiyel etkilerini tam olarak anlayabilmek için ek çalışmalara ihtiyaç duyulmaktadır.

## TABLE OF CONTENTS

ACKNOWLEDGEMENTS.....	iii
ABSTRACT.....	iv
ÖZET .....	v
LIST OF FIGURES .....	ix
LIST OF TABLES.....	xii
LIST OF SYMBOLS/ABBREVIATIONS.....	xiii
1. INTRODUCTION.....	1
1.1. THE ANATOMY OF THE BASAL GANGLIA .....	1
1.1.1. Circuits Through the Basal Ganglia with Special Emphasis to Nigrostriatal Pathway 2	
1.2. PARKINSON’S DISEASE.....	5
1.2.1. Clinical Features of Parkinson’s Disease.....	5
1.2.2. Etiology of Parkinson’s Disease.....	8
1.2.3. Pathology of Parkinson’s Disease.....	11
1.2.4. Nigral Degeneration - Involvement of Apoptosis.....	18
1.2.5. Therapeutic Approaches for Parkinson’s Disease .....	23
1.3. ANIMAL MODELS OF PARKINSON’S DISEASE .....	25
1.3.1. Neurotoxin Induced Models .....	25
1.3.2. Genetic Models .....	29
1.4. RIBOSOMAL S6 KINASE (RSK) FAMILY.....	30
1.4.1. Phospho p90RSK Protein .....	30
1.4.2. Phospho Ribosomal S6 Protein.....	32
1.5. EPIGENETIC MECHANISMS .....	32
1.5.1. Histone Modifications.....	33
1.6. AIM OF THE STUDY.....	34
2. MATERIALS .....	36
2.1. CHEMICALS AND REAGENTS .....	36
2.2. ANTIBODIES.....	38

2.3.	COMMERCIAL KITS.....	38
2.4.	LABORATORY EQUIPMENTS .....	38
2.5.	LABORATORY TECHNICAL INSTRUMENTS.....	39
3.	METHODS.....	41
3.1.	EXPERIMENTAL SETUP AND GROUPS .....	41
3.2.	INTRANIGRAL 6-HYDROXYDOPAMINE INJECTIONS .....	42
3.3.	APOMORPHINE INDUCED ROTATION TEST .....	44
3.4.	SPONTANEOUS LOCOMOTOR ACTIVITY.....	45
3.5.	DRUG TREATMENT .....	46
3.6.	SACRIFICATION OF THE ANIMALS .....	47
3.7.	HISTOLOGY .....	47
3.7.1.	Cryosectioning.....	47
3.7.2.	Immunohistochemistry for Tyrosine Hydroxylase.....	47
3.7.3.	TUNEL Assay.....	49
3.7.4.	Cresyl Violet Staining.....	51
3.7.5.	Hematoxylin Eosin Staining.....	51
3.7.6.	Analysis by Light Microscopy.....	52
3.8.	BIOCHEMICAL ANALYSIS OF OXIDATIVE STRESS.....	54
3.8.1.	Sample Preparation.....	54
3.8.2.	Determination of Protein Concentration (Lowry Method).....	54
3.8.3.	Determination of Lipid Peroxide Level.....	55
3.8.4.	Determination of Superoxide Dismutase (SOD) Activity .....	55
3.8.5.	Determination of Reduced Glutathione (GSH) Activity .....	56
3.8.6.	Determination of Glutathione S-transferase (GST) Activity.....	57
3.9.	WESTERN BLOTTING.....	58
3.9.1.	Sample Preparation.....	58
3.9.2.	Determination of Protein Concentration (Qubit Assay).....	58
3.9.3.	Sodium Dodecyl Sulfate Polyacrylamide Gel Electrophoresis (SDS-PAGE) 59	
3.9.4.	Blotting .....	60
3.9.5.	Immunostaining .....	61
3.9.6.	Imaging .....	61

3.10.	STATISTICS .....	62
4.	RESULTS .....	63
4.1.	APOMORPHINE INDUCED ROTATION TEST .....	63
4.2.	HISTOLOGY .....	64
4.2.1.	Immunohistochemistry for Tyrosine Hydroxylase .....	64
4.2.2.	TUNEL Assay .....	66
4.2.3.	Hematoxylin Eosin and Cresyl Violet Stainings .....	69
4.3.	SPONTANEOUS LOCOMOTOR ACTIVITY .....	71
4.3.1.	Distance Travelled .....	71
4.3.2.	Stereotypic Activity .....	72
4.3.3.	Ambulatory Activity .....	73
4.3.4.	Horizontal Activity .....	74
4.3.5.	Vertical Activity .....	75
4.4.	BIOCHEMICAL ANALYSIS OF OXIDATIVE STRESS .....	76
4.4.1.	Lipid Peroxide (MDA) Level .....	77
4.4.2.	Superoxide Dismutase (SOD) Activity .....	78
4.4.3.	Reduced Glutathione (GSH) Activity .....	79
4.4.4.	Glutathione S-transferase (GST) Activity .....	80
4.5.	WESTERN BLOTTING .....	81
4.5.1.	Acetyl Histone H3 (Lys9) .....	81
4.5.2.	Phospho p90RSK (Ser380) .....	82
4.5.3.	Phospho-S6 Ribosomal Protein (Ser235/236) .....	84
5.	DISCUSSION .....	86
6.	CONCLUSION .....	94
	REFERENCES .....	95



## LIST OF FIGURES

Figure 1.1. The anatomy of the basal ganglia.....	1
Figure 1.2. The direct and indirect pathways of the basal ganglia .....	3
Figure 1.3. The disrupted direct and indirect pathways of the basal ganglia in PD .....	4
Figure 1.4. The possible mechanisms for the pathogenesis of PD .....	12
Figure 1.5. Schematic diagram of the toxicity of the dopamine metabolism in substantia nigra pars compacta .....	18
Figure 1.6. Schematic diagram for the summary of the crosstalk between the intrinsic and extrinsic pathways of apoptosis .....	21
Figure 1.7. Schematic diagram of the toxicity of the 6-OHDA metabolism in substantia nigra pars compacta .....	27
Figure 1.8. Schematic representation of the structure of RSK proteins .....	30
Figure 1.9. Schematic representation of the RSK activation.....	31
Figure 3.1. The rats were fixed in a stereotaxic frame and Bregma and lambda points were located.....	43
Figure 3.2. Stereotaxic operation.....	44
Figure 3.3. Apomorphine induced rotation test.....	45
Figure 3.4. Spontaneous locomotor activity test.....	46

Figure 3.5. Schematic representation of Labeled streptavidin biotin (LSAB) method .....	48
Figure 3.6. Figure representing the right and left substantia nigra pars compacta .....	53
Figure 3.7. Color Prestained Protein Standard .....	60
Figure 3.8. Schematic representation of blotting .....	61
Figure 4.1. Graphs comparing apomorphine induced rotational behavior of the animals...	63
Figure 4.2. Photomicrographs demonstrate Tyrosine Hydroxylase immunoreactivity in right substantia nigra pars compacta .....	65
Figure 4.3. Graphs comparing Tyrosine Hydroxylase immunoreactivity in right substantia nigra pars compacta .....	66
Figure 4.4. Photomicrographs demonstrate TUNEL positive neurons in right substantia nigra pars compacta .....	67
Figure 4.5. Graphs comparing TUNEL positive neurons in right substantia nigra pars compacta .....	68
Figure 4.6. Photomicrographs demonstrate Hematoxylin Eosin staining in right substantia nigra pars compacta .....	69
Figure 4.7. Photomicrographs demonstrate cresyl violet staining in right substantia nigra pars compacta .....	70
Figure 4.8. Graphs comparing distance traveled by the animals .....	72
Figure 4.9. Graphs comparing stereotypic movement of animals .....	73

Figure 4.10. Graphs comparing ambulatory movement of animals .....	74
Figure 4.11. Graphs comparing horizontal movement of animals .....	75
Figure 4.12. Graphs comparing vertical movement of animals.....	76
Figure 4.13. Graphs comparing MDA level in the striatum .....	77
Figure 4.14. Graphs comparing SOD activity in the striatum .....	78
Figure 4.15. Graphs comparing GSH activity in the striatum .....	79
Figure 4.16. Graphs comparing GST activity in the striatum.....	80
Figure 4.17. Western blot analysis for 17 kDa band of Acetyl-Histone H3 (Lys9) in striatal tissue .....	81
Figure 4.18. Graph comparing Acetyl-Histone H3 (Lys9) level in striatum.....	82
Figure 4.19. Western blot analysis for 90 kDa band of phospho p90RSK (Ser380) in striatal tissue .....	83
Figure 4.20. Graph comparing phospho p90RSK (Ser380) level in striatum.....	83
Figure 4.21. Western blot analysis for 32 kDa band of phospho S6 ribosomal protein (Ser235/236) in striatal tissue .....	84
Figure 4.22. Graph comparing phospho S6 ribosomal protein (Ser235/236) level in striatum .....	85

## LIST OF TABLES

Table 1.1. A summary of the clinical symptoms of PD.....	6
Table 1.2. Genes implicated in inherited PD.....	8
Table 1.3. Putative risk factors directly or indirectly associated with PD.....	10
Table 1.4. Major antioxidant enzymes and summary of the catalyzed reactions.....	15
Table 1.5. Haber-Weiss and Fenton reactions.....	16
Table 1.6. BCL-2 family of proteins.....	19
Table 3.1. The experimental groups and number of animals.....	41
Table 3.2. The time schedule of the experiments.....	42
Table 3.3. NuPAGE Novex Bis Tris Gels (1.0 mm, 12 well) properties.....	59

## LIST OF SYMBOLS/ABBREVIATIONS

6-OHDA	6-hydroxydopamine
MEK 1/2	Mitogen activated protein kinase kinase
AADC	Aromatic amino acid decarboxylase
AAV2	Adeno-associated viral vector serotype 2
AP	Anteroposterior from bregma
APAF1	Apoptotic protease activating factor 1
APS	Ammoniumpersulphate
BAK	BCL-2 antagonist or killer
BAX	BCL-2-associated X protein
BCL-2	B cell lymphoma 2
BID	BCL-2 homology 3 (BH3)-interacting domain death agonist
BSA	Bovine serum albumin
CDNB	1-chloro-2,4-dinitrobenzene
COMT	Catechol-o-methyl transferase
DA	Dopamine
DAB	3,3- diaminobenzidine
DAT	Dopamine transporter
DTNB	5,5-dithiobis(2-nitrobenzoic acid)
DV	Dorsoventral from the skull
ERK 1/2	Extracellular signal regulated kinases
GABA	$\gamma$ -aminobutyric acid
GPe	Globus pallidus external
GPi	Globus pallidus internal
GSH	Reduced glutathione
GSHPx	Glutathione peroxidase
GST	Glutathione S-transferase
H <sub>2</sub> O <sub>2</sub>	Hydrogen peroxide
HATs	Histone acetyltransferases
HCl	Hydrochloric acid

HDACs	Histone deacetylases
i.m	Intramuscular
i.p	Intraperitoneal
IgG	Immunoglobulin G
IMS	Intermembrane space
LB	Lewy body
L-DOPA	Levodopa
LDS	Lithium dodecyl sulfate
LRRK2	Leucine-rich repeat kinase 2
MAO	Monoamine oxidase
MDA	Malondialdehyde
MES	2-(N-morpholino) ethane sulfonic acid
ML	Mediolateral from the midline
MOMP	Mitochondrial outer membrane permeabilization
MPTP	1-methyl-4-phenyl-1,2,3,6-tetrahydropyridine
NaCl	Sodium chloride
NaOH	Sodium hydroxide
NBT	Nitroblue tetrazolium
NSAID	Non-steroidal anti-inflammatory
O <sub>2</sub> <sup>-</sup> .	Superoxide anion
OH.	Hydroxyl radical
p90RSK	MAPK-activated protein kinase
PBS	Phosphate buffered saline
PD	Parkinson's disease
POD	Peroxidase
PVDF	Polyvinylidene difluoride
REM	Rapid eye movement
RIPA	Radio-Immunoprecipitation Assay
sc	Subcutaneous
SDS-PAGE	Sodium dodecyl sulfate polyacrylamide gel electrophoresis
SMAC	Second mitochondria-derived activator of caspase
SNpc	substantia nigra pars compacta

SNpr	Substantia nigra pars reticulata
SOD	Superoxide dismutase
STN	Subthalamic nucleus
TBA	Thiobarbituric acid
TBS-T	Tris Buffered Saline plus Tween 20
TCA	trichloro acetic acid
TNB	5-thio-2-nitrobenzoic acid
TUNEL labeling	Terminal deoxynucleotidyl transferase-mediated dUTP nick-end
UCHL1	Ubiquitin carboxy-terminal hydrolase L1
VPA	Valproic acid
XIAP	X-linked inhibitor of apoptosis protein

## 1. INTRODUCTION

### 1.1. THE ANATOMY OF THE BASAL GANGLIA

Basal ganglia comprise of a group of nuclei located deep in the cerebral hemispheres [1]. The nuclei are the striatum, globus pallidus, the subthalamic nucleus and the substantia nigra (Figure 1.1). Basal ganglia control voluntary motor movements and dysfunction of basal ganglia leads to many motor disorders such as Parkinson's Disease and Huntington's Chorea [2,3].

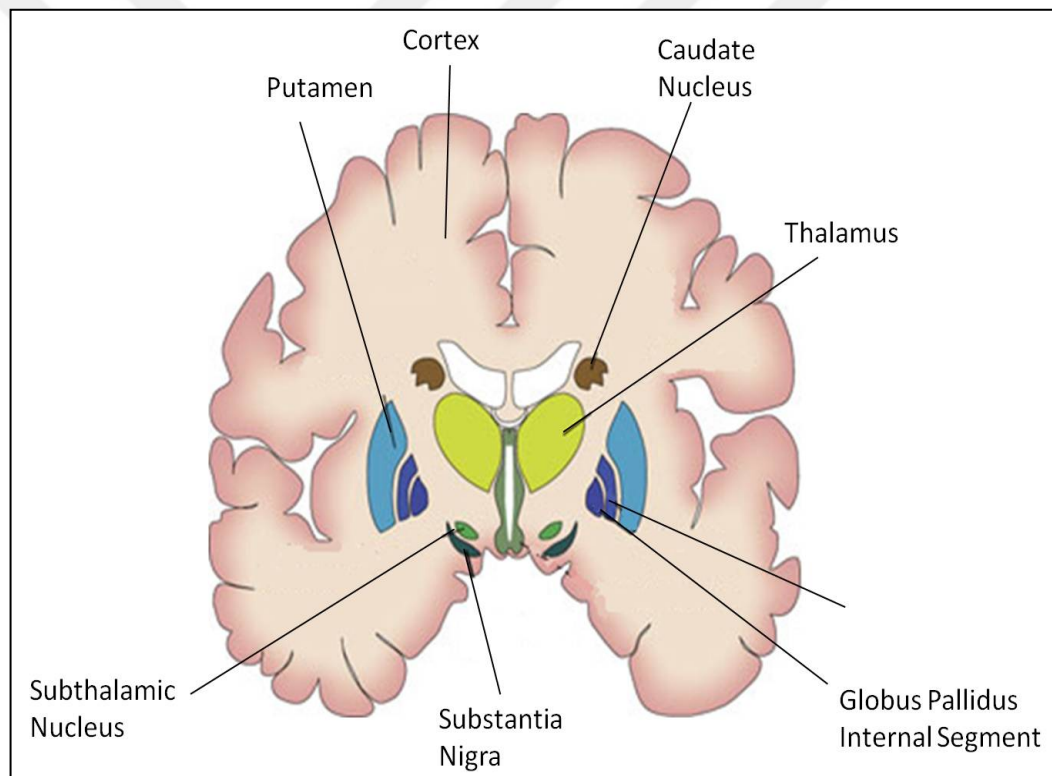


Figure 1.1. The anatomy of the basal ganglia.

The striatum consists of caudate nucleus and putamen. The caudate and putamen are separated by an internal capsule in the primates, whereas in rats there is no internal capsule [4]. The striatum receives glutamatergic input from cortex and sends inhibitory GABAergic output to globus pallidus since 90 per cent of the neurons of striatum are medium spiny neurons which produce  $\gamma$ -aminobutyric acid (GABA) [5, 6]. The globus



pallidus includes an internal and external segment. While the globus pallidus external segment sends GABAergic output to subthalamic nucleus, internal segment sends GABAergic output to thalamus. Subthalamic nucleus is located between thalamus and substantia nigra. It is the only nucleus that has glutamatergic projections in the basal ganglia [7]. Substantia nigra lies below subthalamic nucleus and consists of substantia nigra pars reticulata and substantia nigra pars compacta which has different histological and functional characteristics. Substantia nigra pars compacta sends dopaminergic projections to striatum, as substantia nigra pars reticulata sends GABAergic projections to many brain regions [8].

### **1.1.1. Circuits Through the Basal Ganglia with Special Emphasis to Nigrostriatal Pathway**

The basal ganglia have two major circuits, direct and indirect pathway that control motor movement. The dopaminergic modulation of these pathways has important functions in the regulation of motor movement. Disruption of this modulation leads to hypokinetic or hyperkinetic motor behaviors.

The direct pathway positively regulates motor behavior. When the cortical projections excite striatum via glutamate, the GABAergic neurons of striatum inhibits the GABAergic neurons in globus pallidus internal. Therefore, ventrolateral thalamus receives less inhibition (dis-inhibition) and thalamus sends excitatory glutamatergic projections to motor cortex to facilitate movement [9]. On the other hand, the indirect pathway suppresses the unwanted movements. The excited striatal neurons by cortical projections inhibit the GABAergic neurons in globus pallidus external. Consequently glutamatergic neurons of the subthalamic nucleus receives less inhibition (dis-inhibition) which results in more excitation of the GABAergic neurons of globus pallidus internal. Therefore, glutamatergic neurons in ventrolateral thalamus receive more inhibition and decreased excitatory activity to motor cortex suppresses motor activity (Figure 1.2) [9,10].

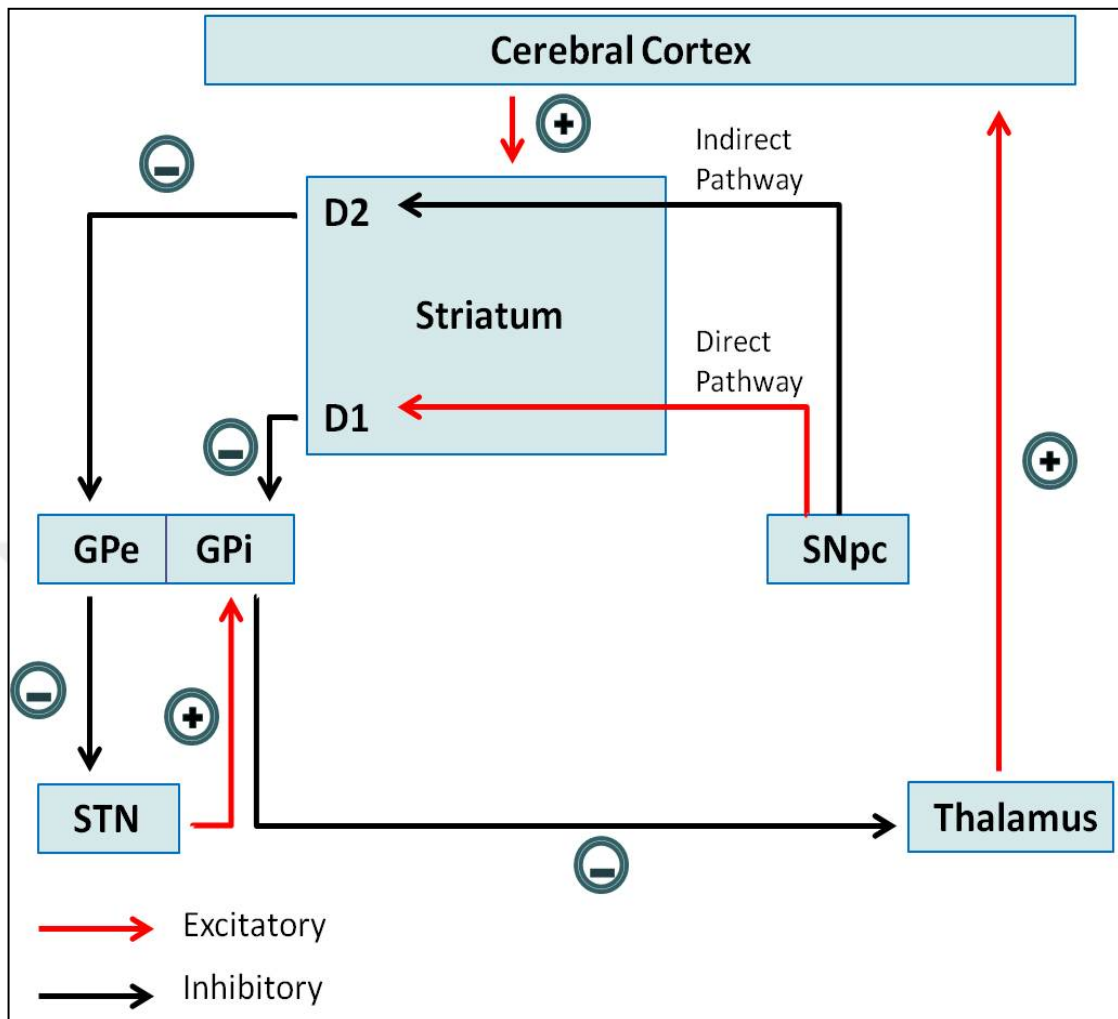


Figure 1.2. The direct and indirect pathways of the basal ganglia. Black arrows indicate inhibitory GABAergic projections and red arrows indicate excitatory glutamatergic projections. (GPe, globus pallidus external; GPi, globus pallidus internal; STN, subthalamic nucleus; SNpc, substantia nigra pars compacta; D1, D1 receptor; D2, D2 receptor).

Dopamine has modulatory effects on these corticostriatal pathways. Dopamine is released from the dendrites of the substantia nigra pars compacta dopaminergic neurons to the striatum. Striatum interneurons have two dopamine receptors, such that dopamine has excitatory effect via D1 receptors on direct pathway and inhibitory effects via D2 receptors on indirect pathway [11]. The overall effect of dopamine is increased motor behavior. The degeneration of the dopaminergic neurons leads to hypokinetic symptoms of Parkinson's

Disease such as akinesia, bradykinesia, hypertonia, masklike face, postural instability, since the stimulatory effect of dopamine on motor activity is disrupted (Figure 1.3).

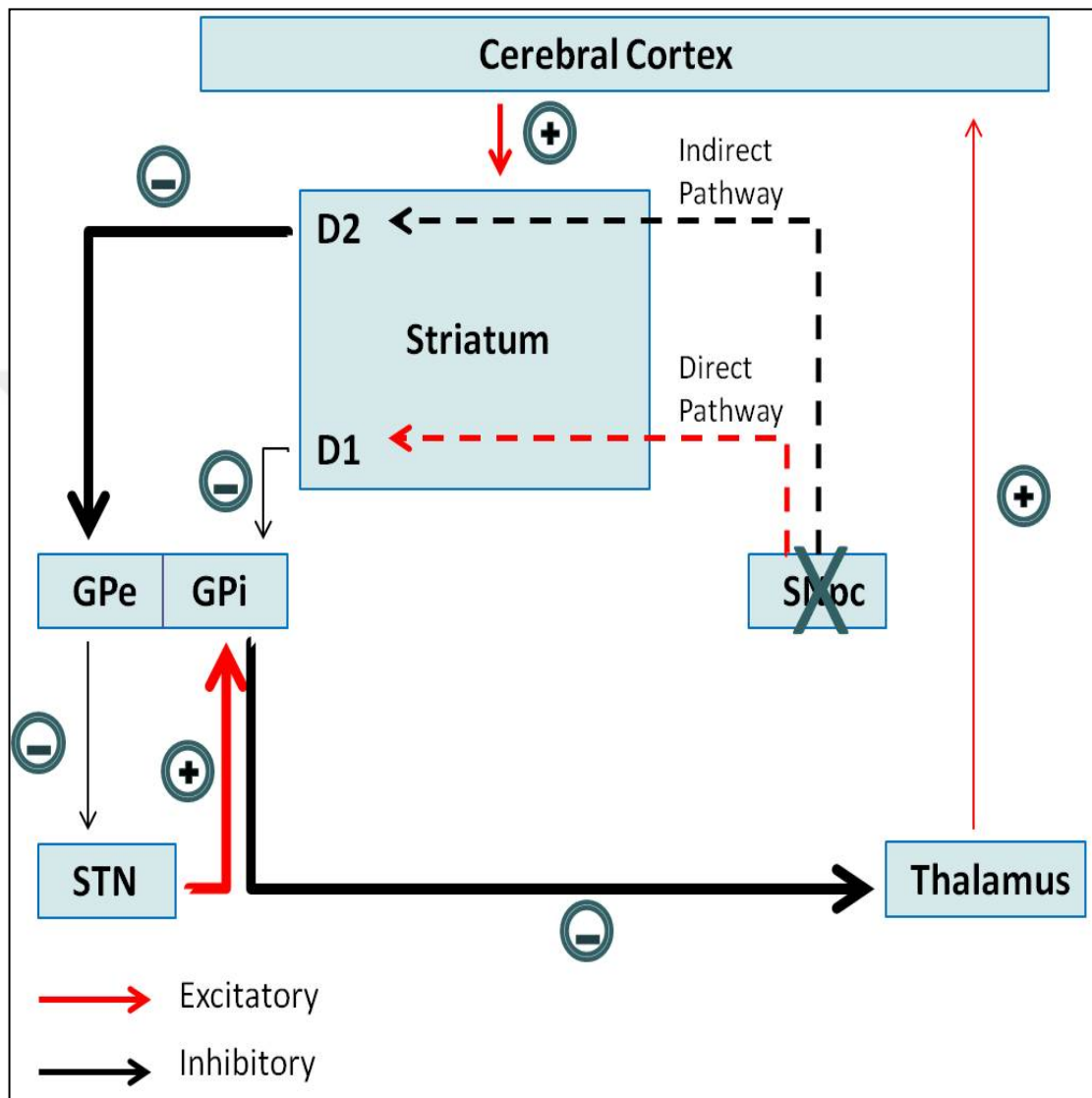


Figure 1.3. The disrupted direct and indirect pathways of the basal ganglia in PD. Black arrows represent inhibitory GABAergic projections and red arrows are excitatory glutamatergic projections. Dashed arrows indicate the loss of dopaminergic modulation, thick arrows indicate increased output and thin arrows indicate decreased output. (GPe, globus pallidus external; GPi, globus pallidus internal; STN, subthalamic nucleus; SNpc, substantia nigra pars compacta; D1, D1 receptor; D2, D2 receptor).

## **1.2. PARKINSON'S DISEASE**

Parkinson's Disease (PD) is the second most common neurodegenerative disease worldwide and the incidence is increasing with the aging population with a prevalence of 0.3 per cent in entire population and 2 per cent over the age of 65 [12]. PD was first described by English doctor James Parkinson in his book 'Essay on the Shaking Palsy' in 1817 [13]. It is characterized by the progressive degeneration of the dopaminergic neurons in substantia nigra pars compacta resulting in the loss of dopaminergic innervation to the striatum [14, 15]. Epidemiological studies imply that environmental and genetic factors are important in the development of PD. Although the pathogenesis of the disease is not fully understood, mechanisms related to free radical stress, mitochondrial dysfunction, apoptosis and protein aggregation are the major factors in the degeneration of dopaminergic neurons. The major clinical features are bradykinesia, akinesia, tremor, postural instability and dementia [16]. Currently, the available treatment of PD is only symptomatic which focuses on the replacement of the dopamine in the brain so that novel neuroprotective or neurorestorative treatments are needed. Therefore, understanding the molecular mechanisms of PD pathogenesis is crucial in the development of the novel therapies for PD.

### **1.2.1. Clinical Features of Parkinson's Disease**

Although PD is known as a motor system disorder, it also has many non-motor symptoms (Table 1.1.). Bradykinesia, rigidity, resting tremor, postural instability are the major motor symptoms, whereas dementia, depression, sleep disturbances, constipation are some of the non-motor clinical features of PD [17, 18, and 19].

Since there is no definite diagnostic test for PD, the diagnosis is made based on the clinical symptoms of PD. The Hoehn and Yahr scale and the Unified Parkinson's Disease Rating scale (UPDRS) are the most frequently used rating scales for the diagnosis of the disease [20, 21].

Table 1.1. A summary of the clinical symptoms of PD.

<b>Motor symptoms</b>	<b>Non-motor symptoms</b>
Tremor, rigidity, postural instability	Cognitive impairment
Bradykinesia	Depression
Hypomimia	Sensory symptoms
Shuffling gait	Sleep disorders
Micrographia	Dysautonomia

### ***1.2.1.1. Motor Symptoms***

Bradykinesia is the slowness of the movements and it is the most prominent symptom of PD and other basal ganglia disorders [22]. Studies show that bradykinesia is highly associated with the degree of dopamine loss in the brain and therefore, the disrupted motor cortex activity [23, 24]. The patient finds it difficult to initiate and execute a movement, also loses facial expressions [22]. The spontaneous movements (swallowing and eye blinking) are decreased. Interestingly, when a patient is excited by an external stimulus, he can easily make quick movements (kinesia paradoxa).

Tremor is the rhythmic movements of the body organs such as hands and most common clinical symptom of PD. Tremor increases at resting state and decreases in action, writing and mental concentration. The tremor frequency is 4-6 Hz. It can spread to other body areas such as limbs, jaw, chin and legs [25].

Rigidity is the increased resistance of the passive movement of the limbs such as flexion and extension which is associated with the increased muscle tone [26].

Postural instability is caused by the disturbances in the postural reflexes and occurs in the late stages of PD [27]. To evaluate the degree of postural instability, pull test is performed in which the patient is pulled back and forth from the shoulders. Postural instability is the main cause of the hip fractures, as the patients fall frequently [28].

Speech abnormalities in PD patients are called as ‘tip-of-the-tongue’ phenomenon [29]. Furthermore, neuro-ophthalmological symptoms such as visual hallucinations and decreased blink rate are commonly seen in PD patients [30].

### ***1.2.1.2. Non-motor Symptoms***

Non-motor symptoms of PD are important as they decrease the quality of life of the patients. They generally occur before the diagnosis of the disease and include neuropsychiatric symptoms, sleep abnormalities and autonomic dysfunction [31].

Depression, dementia, confusion, hallucinations and panic attacks are among the neuropsychiatric symptoms of PD. Depression characterized by sadness, remorse and lack of self-esteem is seen in 10-45 per cent of the patients [32]. PD patients have six fold higher risk for dementia as compared with healthy people [33]. Furthermore, half of the patients develop dementia 15 years after the disease diagnosis [34]. Interestingly, in PD patients who have dementia, the hippocampal volume is decreased as in Alzheimer’s disease [35]. Psychotic symptoms such as hallucination, delusion, delirium are seen in 40 per cent of PD patients and as the disease progresses they become more pronounced. Apart from these symptoms, the use of dopaminergic drugs in the treatment of PD leads to many obsessive-compulsive behaviors such as pathological gambling, craving for foods and compulsive shopping [36].

Excessive sleepiness in daytime, rapid eye movement (REM) sleep behavior disorder, vivid dreams are the major sleep disorders commonly seen in PD patients [37]. One of the three PD patients suffers from REM sleep behavior disorder. REM sleep behavior disorder occurs before the PD onset so it is considered as an important risk factor for PD development. Violent dream contents are seen in PD patient such as talking, yelling, punching and kicking which affect the patient adversely [38]. Excessive sleepiness in daytime is another important marker for PD diagnosis and affects around 50 per cent of the PD patients [39].

Bladder dysfunctions, sweating, dry eyes and sexual dysfunction are the major autonomic dysfunctions in PD [40]. Furthermore, constipation is commonly seen in PD patients as gastrointestinal symptom [41].

### 1.2.2. Etiology of Parkinson's Disease

Although the exact cause of PD is still not understood, environmental, genetic, dietary factors and ageing are strongly implicated in the etiology of PD. Probably the combination of many factors is involved in the etiology and pathogenesis of PD since it is a complex disorder [42].

#### 1.2.2.1. Genetic Factors

Several genes ( $\alpha$ -synuclein, parkin, UCHL-L1, PINK1, DJ-1, LRRK-2, ATP13A2 and HTRA2) have been implicated in the pathogenesis of the Parkinson's Disease (Table 1). However, these genes are only responsible for around 30 per cent of the familial cases and 3 per cent of the sporadic cases of PD [43].

Table 1.2. Genes implicated in inherited PD [44].

<b>Locus</b>	<b>Gene</b>	<b>Inheritance</b>	<b>Function</b>
PARK1	$\alpha$ -synuclein	Autosomal Dominant	Lewy body
PARK2	Parkin	Autosomal Recessive	Ubiquitin E3 ligase
PARK5	UCHL-L1	Autosomal Dominant	Ubiquitin C-terminal hydrolase
PARK6	PINK1	Autosomal Recessive	Mitochondrial kinase
PARK7	DJ-1	Autosomal Recessive	Antioxidant
PARK8	LRRK-2	Autosomal Dominant	Mixed lineage kinase
PARK9	ATP13A2	Autosomal Recessive	Unknown
PARK13	HTRA2	Unknown	Mitochondrial serine protease

Aggregated  $\alpha$ -synuclein protein is the main component of Lewy Bodies in PD [45].  $\alpha$ -synuclein is preferentially expressed in substantia nigra and composed of an N-terminal amphipathic region,  $\alpha$  hydrophobic middle region and an acidic C-terminal region.  $\alpha$ -synuclein is normally a presynaptic protein and has important functions in storage of neurotransmitters and vesicle recycling [46]. However, the missense mutations (A53T, A30P and E46K) of  $\alpha$ -synuclein gene located in locus PARK1 disrupts its function and

cause Lewy bodies [47]. Studies show that dopaminergic neurons selectively affected by the mutated  $\alpha$ -synuclein since it preferentially expressed in dopaminergic neurons [48]. Some of the detrimental effects of abnormal  $\alpha$ -synuclein to dopaminergic neurons are disruption of vesicular trafficking [49], mitochondrial dysfunction [50] and impaired microtubule-dependent trafficking [51].

Mutations in the parkin gene cause early-onset PD [52]. Parkin gene is an E3 ubiquitin ligase which degrades the misfolded proteins and structurally has an N-terminal ubiquitin like domain, a C-terminal RING domain and a central linker region in between [53]. Disruption of parkin's ubiquitin ligase activity leads to the accumulation of the substrates that should be degraded such as synphilin 1 which is important in Lewy body formation, glycosylated form of  $\alpha$ -synuclein, microtubule proteins and cell cycle proteins [54].

Ubiquitin carboxy-terminal hydrolase L1 (UCHL1) is a neuron specific ubiquitin C-terminal hydrolase which degrades the damaged proteins. Mutation (I93M) in the UCHL1 gene disrupts the ubiquitin proteasome system and eventually toxic effects on dopaminergic neurons occur [55].

Mutations in phosphatase and tensin (PTEN) homolog-induced putative kinase 1 (PINK1) gene is associated with early-onset PD. PINK1 structurally has an N-terminal serine threonine kinase domain and a C-terminal auto regulatory domain [56]. Mutation of PINK1 leads to dopaminergic degeneration as a consequence of mitochondrial dysfunction, while the overexpression of PINK1 prevents apoptosis by inhibiting cytochrome c release from mitochondria [57].

Mutations in the DJ-1 gene cause 1-2 per cent of early-onset PD [58]. DJ-1 is widely expressed in the brain with a specific localization to mitochondria and has important antioxidant and chaperone activities [59]. Studies show that overexpression of DJ-1 protects dopaminergic neurons against oxidative stress induced neuronal death [60]. Furthermore, DJ-1 acts as a chaperone to disrupt  $\alpha$ -synuclein aggregation and neuronal death [61]. Interestingly, DJ-1 knockout mice show motor abnormalities such as hypokinesia without significant dopaminergic neuron loss [62].

Leucine-rich repeat kinase 2 (LRRK-2) or dardarin gene is associated with late-onset PD. LRRK2 has a leucine rich repeat domain and a protein kinase domain [63]. LRRK2 protein is mainly located in golgi apparatus, lysosome, mitochondria and plasma membrane.



Mutation of LRRK2 interferes with vesicle recycling and neurite outgrowth. Mutated LRRK2 is found to be localized to Lewy bodies in PD [64].

### ***1.2.2.2.Environmental and Other Factors***

A number of toxins such as pesticides, MPTP, cyanide, manganese and organic solvents are involved in the development of PD. Furthermore, occupations, dietary intake and head trauma are among the putative factors [65]. High fat diet and milk consumption are risk factors in PD development. Interestingly, nicotine intake via cigarette smoking has protective effects. Similarly, high coffee or tea consumption, alcohol intake and non-steroidal anti-inflammatory (NSAID) drugs decrease the risk of PD (Table 1.3) [66].

Table 1.3. Putative risk factors directly or indirectly associated with PD.

<b>Directly associated factors</b>	<b>Indirectly associated factors</b>
Pesticide exposure	Smoking
Metals	Caffeine intake
Increasing age	NSAID use
Dietary factors	Alcohol

Many studies indicate that pesticide exposure such as herbicides, insecticides, paraquat, wood preservatives and dieldrin are widely associated with the development of PD by disrupting mitochondrial electron transport and ATP synthesis [67]. Heavy metals such as iron, manganese and lead can accumulate in substantia nigra and cause dopaminergic neuron death by increasing oxidative stress. People working at certain occupations such as farming, dry cleaning and metal degreasing have higher risk for the development of PD [68].

Aging is one of the biggest risk factor for the development of PD. The prevalence of PD is strongly associated with age as PD is seen in 1 per cent of the individuals over the age of 60 and 5 per cent of the individuals over the age of 80 [69]. Brain cells are particularly affected from age related cellular damage, disrupted cellular repair and defense

mechanisms. Furthermore, similar pathological features are seen amongst PD patient's brains and aging brains of older people [70].

### **1.2.3. Pathology of Parkinson's Disease**

The loss of dopaminergic neurons and the presence of Lewy bodies in substantia nigra pars compacta are the major pathological features of PD [71].

The progressive loss of dopaminergic neurons results in loss of striatal dopamine amount. Around 60 per cent of the dopaminergic neurons are lost which accounts for 80 per cent loss of dopamine in the striatum until physiological symptoms emerge. The degeneration of the dopaminergic neurons specifically occurs in the ventrolateral part of the substantia nigra pars compacta [72]. However, the brain has compensatory mechanisms for the degeneration of dopaminergic neurons. To compensate for the dopamine depletion, the dendrites of the remaining neurons and dopamine production are increased; also D2 receptors in striatum are proliferated in PD brain. Furthermore, dopamine transporters are down regulated to decrease dopamine reuptake thereby increase presynaptic dopamine amount for compensation [73]. Apart from the dopaminergic neuron degeneration in the nigrostriatal pathway, catecholaminergic neurons in the locus coeruleus, serotonergic neurons in the raphe nuclei and neurons in dorsal motor nucleus of the vagus regions of the brain are most affected in PD [74]. Of note, the loss of cholinergic neurons in the nucleus basalis of Meynert is probably responsible for the dementia frequently seen in PD patients [75].

The presence of Lewy bodies in PD brains was first identified by Frederich Lewy in 1912 [76]. Lewy bodies are round shaped, 5-25  $\mu\text{m}$  in diameter, eosinophilic inclusions with an eosinophilic core structure. They are found in cell soma and neurites of degenerating neurons specifically in substantia nigra, locus coeruleus, nucleus basalis of Meynert and dorsal motor nucleus of the vagus [77]. Ubiquitin, cytoskeletal elements, cell stress proteins, synaptic vesicle proteins and some enzymes are the protein components of Lewy bodies. Importantly, abnormal aggregates of  $\alpha$ -synuclein and associated synphilin proteins are major components of Lewy bodies [78].

Although the exact mechanism for the pathogenesis of PD is not known, several mechanisms such as oxidative stress, mitochondrial dysfunction, protein aggregation and misfolding, inflammation and loss of trophic factors all of which trigger cell death mechanisms such as apoptosis have been suggested (Figure 1.4).

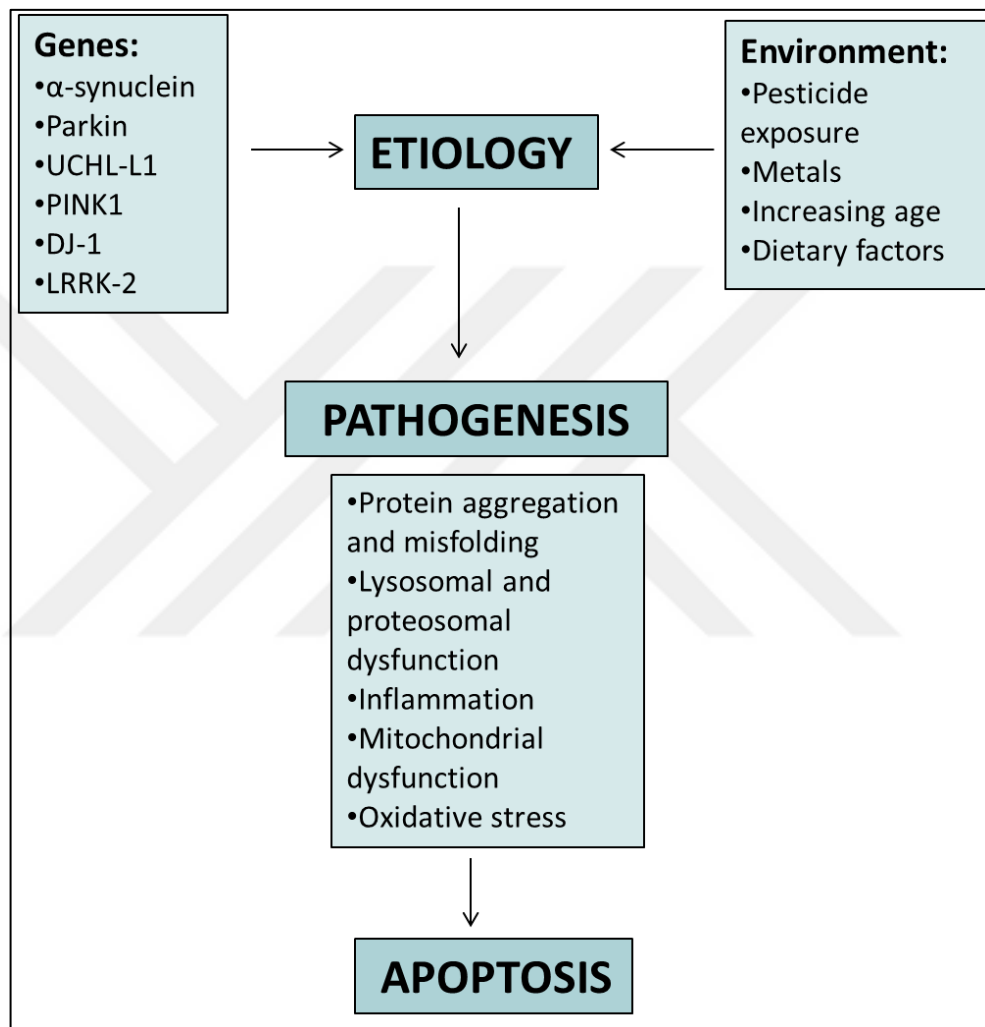


Figure 1.4. The possible mechanisms for the pathogenesis of PD.

### ***1.2.3.1. Protein Aggregation and Misfolding***

Aggregation and misfolding of  $\alpha$ -synuclein is strongly implicated in the pathogenesis of both sporadic and hereditary PD.  $\alpha$ -synuclein is a natively unfolded protein specially expressed in substantia nigra [79]. When it forms  $\beta$ -sheet oligomers through a process

called fibrillation, it is precipitated and these aggregations form Lewy bodies [80]. Although the exact role of  $\alpha$ -synuclein is not fully understood, according to studies conducted in animals, it has important roles in synaptic plasticity and regulation of dopamine neurotransmission [81]. Abeliovich et al [82], suggest that  $\alpha$ -synuclein regulates presynaptic release of dopamine. Furthermore, a study conducted in  $\alpha$ -synuclein overexpressing fly model of PD indicate that, nigrostriatal neuron degeneration and motor impairment were induced due to  $\alpha$ -synuclein overexpression [83]. Therefore, there is a great interest for developing therapies to halt  $\alpha$ -synuclein aggregation. In addition, scientists are trying to figure out whether  $\alpha$ -synuclein aggregation could be used as a biomarker in the diagnosis of PD.

#### ***1.2.3.2. Lysosomal and Proteosomal Dysfunction***

Lysosomal and proteosomal dysfunction are also important hallmarks in the pathogenesis of PD. Lysosomes have proteolytic enzymes and function to degrade aggregated proteins and damaged proteins. The dysfunction of ubiquitin proteasome system, which are particularly controlled by Parkin and PINK1, leads to accumulation of defective mitochondria and proteins such as  $\alpha$ -synuclein [84]. Impaired lysosomal function causes  $\alpha$ -synuclein aggregation, decreased striatal dopamine, motor deficits and increased dopaminergic degradation [85]. A study conducted in mice indicates that, lysosomal dysfunction leads to dopaminergic degradation, but rapamycin treatment to reactivate lysosomal function, decreases dopaminergic degradation by increasing the number of active lysosomes [86, 87].

#### ***1.2.3.3. Inflammation***

Inflammatory mechanisms are also implicated in the PD pathogenesis. The levels of microglia and cytokines are elevated in PD brains [88]. Studies show that anti-inflammatory agents decrease dopaminergic degeneration. An epidemiological study indicates that the incidence of PD is decreased by approximately 45 per cent, by the chronic usage of nonsteroidal anti-inflammatory drugs [89]. Microglia are normally in resting state in the brain, but when they are activated they are involved in the inflammatory

processes. In PD brains, specifically in substantia nigra and striatum, the microglia levels are significantly elevated [90]. Importantly, reactive microglia increase superoxide radicals which lead to increased amounts of oxidative stress and subsequent dopaminergic cell death [91]. Of note, inflammatory cytokines such as tumor necrosis factor alpha, interleukin-1 and interleukin-6 are seen in PD brains. McGeer et al report that [92], inflammatory cytokine levels have been elevated in PD brains specifically in basal ganglia region.

#### ***1.2.3.4.Mitochondrial Dysfunction***

Mitochondrial dysfunction is strongly implicated in PD pathogenesis. The importance of the mitochondria in PD pathogenesis was first understood when it is found that mitochondrial toxins such as MPTP (1-methyl-4-phenyl-1,2,3,6-tetrahydropyridine) and paraquat may cause Parkinsonism. Langston et al [93], showed that MPP<sup>+</sup> which is a toxic metabolite of a synthetic drug MPTP, is selectively taken up by dopaminergic neurons and causes parkinsonism. Studies with autopsy tissues of PD patients revealed that mitochondrial complex I activity is significantly diminished [94]. Complex I also known as nicotinamide adenine dinucleotide coenzyme Q reductase is a part of electron transport chain and involved in oxidative phosphorylation and ATP production. During electron transport, electrons may escape and form superoxide anions. Therefore, mitochondrial dysfunction causes oxidative stress and insufficient energy supply which are detrimental for dopaminergic neurons [95]. In addition, mitochondrial DNA is more susceptible than nuclear DNA such that mutations are more frequently seen. Dopaminergic neurons in substantia nigra pars compacta have elevated amounts of mitochondrial DNA mutations [96, 97]. Apart from the cause of mitochondrial defect, in the end mitochondrial membrane potential is disrupted in a way that death proteins are released and apoptosis occurs [98]. Therefore, mitochondrial dysfunction has tremendous effects in dopaminergic neuron degeneration and is subject of intensing research.

### 1.2.3.5. Oxidative Stress

Oxidative stress occurs as a result of the disruption of the balance between oxidants and antioxidants for the benefit of oxidants. Loss of protective mechanisms and increased levels of reactive oxygen species play detrimental roles in PD pathogenesis.

Reactive oxygen species such as hydrogen peroxide ( $H_2O_2$ ), hydroxyl radical ( $OH\cdot$ ), superoxide anion ( $O_2\cdot^-$ ) occur during the cellular metabolism and overproduction of them causes oxidative stress. In normal physiological conditions, enzymatic antioxidants such as superoxide dismutase (SOD), catalase (CAT), glutathione peroxidase (GTPx) and glutathione-s-transferase (GST) fight with reactive oxygen species [99]. As discussed, as a result of the damaged mitochondrial complex I activity, electrons escape from the system to form superoxide anions. Superoxide anions are very toxic to the cells and they are converted to less toxic hydrogen peroxide ( $H_2O_2$ ) by superoxide dismutase in a reaction called dismutation [100]. Hydrogen peroxide is then reduced to water by other enzymatic antioxidants, catalase and glutathione peroxidase [101, 102]. Since glutathione is the substrate for the glutathione peroxidase catalyzed reactions, GSH:GSSG ratio is an important indicator of the redox state of the cell. Increasing amounts of hydroxyl radicals are formed as a result of the decreased GSH:GSSG ratio. Glutathione-s-transferases [103] are involved in the inactivation process of the secondary metabolites of oxidative reactions such as unsaturated aldehydes (Table 1.4).

Table 1.4. Major antioxidant enzymes and summary of the catalyzed reactions.

Antioxidants	Catalyzed reaction
Superoxide dismutase (SOD)	$M^{(n+1)+}\text{-SOD} + O_2\cdot^- \rightarrow M^{n+}\text{-SOD} + O_2$ $M^{n+}\text{-SOD} + O_2\cdot^- + 2H^+ \rightarrow M^{(n+1)+}\text{-SOD} + H_2O_2$
Glutathione peroxidase (GTPx)	$2GSH + H_2O_2 \rightarrow GSSG + 2H_2O$
Catalase (CAT)	$2H_2O_2 \rightarrow O_2 + 2H_2O$
Glutathione-s-transferase (GST)	$RX + GSH \rightarrow HX + R\text{-S-GSH}$

On the other hand, in excess amounts of metals such as iron, hydrogen peroxide can be broken down to hydroxyl radicals ( $\text{OH}\cdot$ ) in Haber-Weiss and Fenton reactions causing further damage to the cells (Table 1.5).

Table 1.5. Haber-Weiss and Fenton reactions

Haber-Weiss	$\text{Fe}^{3+} + \cdot\text{O}_2^- \rightarrow \text{Fe}^{2+} + \text{O}_2$
Fenton reaction	$\text{Fe}^{2+} + \text{H}_2\text{O}_2 \rightarrow \text{Fe}^{3+} + \text{OH}^- + \cdot\text{OH}$

The activity of mitochondrial isoform of SOD (SOD2) is increased in PD brains, but there is no significant change in cytosolic SOD. This elevated activity indicates high amounts of reactive oxygen species in PD brains since SOD is in the first line of antioxidant defense system. It is also interesting to note that, high concentrations of mitochondrial isoform of SOD probably indicate mitochondrial dysfunction is responsible for the increased amounts of SOD [104]. On the other hand, the activities of glutathione peroxidase and catalase are found to be lower in PD brains [105, 106]. Decreased levels of glutathione is also found in substantia nigra pars compacta of PD patients [107]. Numerous studies demonstrate the involvement of excessive amounts of iron in substantia nigra pars compacta of PD brains, iron levels are higher in substantia nigra pars compacta as compared with other brain regions [108]. The GSH/GSSG ratio is also decreased in PD brains, contributing to hydroxyl radical formation and leading to further degeneration of dopaminergic neurons.

All of these pathologic features lead to overproduced reactive oxygen species that have deleterious effects on cellular macromolecules such as proteins, lipids and nucleic acids. Reactive oxygen species attack cellular macromolecules leading to their peroxidation.

Damage to the proteins lead to their peroxidation and they become more vulnerable to proteolysis. It has been shown that protein carbonyl, which is a marker for protein oxidation, is significantly increased in substantia nigra of PD brains of the patients [109].

Likewise, nucleic acids are very vulnerable to oxidative stress. Reactive oxygen species cause modifications of DNA. Mutated DNA eventually leads to cell death via apoptosis. 8-hydroxyguanosine which is a marker for oxidized nucleic acids (DNA and RNA) is found to be higher in substantia nigra of PD brains [110].

Furthermore, reactive oxygen species attack polyunsaturated fatty acids in a successive of chain reactions causing lipid peroxidation. In the first step, hydroxyl radicals attack and abstract a hydrogen atom from polyunsaturated fatty acids. A set of reactions are initiated such that another hydrogen atom is abstracted from another lipid leading to formation of numerous compounds. It is important to note that; a lipid peroxidation product malondialdehyde can be easily measured from tissue and blood samples to measure the level of oxidative stress. Lipid hydroperoxides, markers for lipid peroxidation, are found in increased amounts in PD brains of patients [111]. Accordingly, increased levels of thiobarbituric acid reactive compounds commonly seen in substantia nigra pars compacta of PD brains, indicates lipid peroxidation [112].

Dopaminergic neurons are highly susceptible to oxidative stress due to their special structural organization. Degradation of dopamine itself is an important source of oxidative stress (Figure 1.5). There are two main mechanisms for dopamine degradation as enzymatic and non-enzymatic degradation. Monoamine oxidase (MAO) enzymatically degrades dopamine to produce hydrogen peroxide ( $H_2O_2$ ) as by-product [113]. In normal conditions, hydrogen peroxide is converted to water by glutathione peroxidase. Glutathione peroxidase (GSHPx) uses glutathione (GSH) as a reducing agent in this process.

Unfortunately, glutathione is present in very low levels in substantia nigra pars compacta as compared with the other regions of the brain. Therefore, hydrogen peroxide clearance by glutathione peroxidase is very low in substantia nigra pars compacta [114]. Of note, as the age increases, monoamine oxidase levels increase and glutathione levels further decrease to cause selective dopaminergic neuron death. In addition, dopamine can be degraded by auto-oxidation process. The non-enzymatic auto-oxidation of dopamine is catalyzed by iron and hydroxyl radicals, superoxide radicals and hydrogen peroxide are produced which further increase oxidative stress.



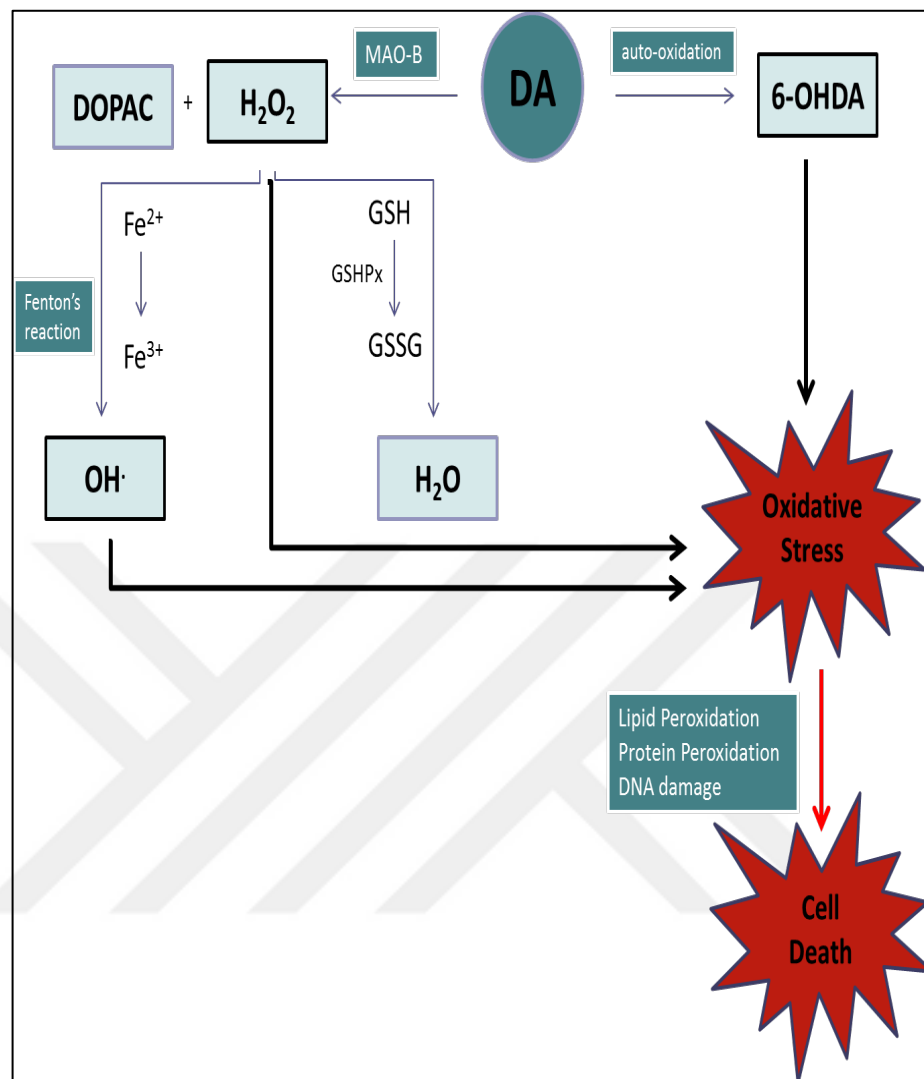


Figure 1.5. Schematic diagram of the toxicity of the dopamine metabolism in substantia nigra pars compacta. DA, dopamine; MAO, Monoamine oxidase; H<sub>2</sub>O<sub>2</sub>, hydrogen peroxide; GSHPx, Glutathione peroxidase; GSH, glutathione; GSSG, oxidized glutathione; 6-OHDA, 6-hydroxydopamine; DOPAC, dihydroxyphenylacetic acid.

#### 1.2.4. Nigral Degeneration - Involvement of Apoptosis

Progressive degeneration of the dopaminergic neurons in substantia nigra pars compacta leads to Parkinson's Disease. Although the pathogenesis of the disease is not fully understood, mechanisms related to free radical stress, mitochondrial dysfunction and proteosomal dysfunction are the major factors in the degeneration of dopaminergic neurons.

Neuronal death mainly occurs in two ways; as apoptosis and necrosis. Necrosis occurs in response to external stimuli such as trauma or infection. It could be detrimental to the cell, since the cell content is released into the extracellular space after the rupture of the cell membrane [115]. On the other hand, apoptosis is a programmed cell death mechanism which occurs in many organisms normally during development and aging and as a homeostatic mechanism to maintain cell populations in tissues. Some prominent changes in morphology of the cell occur during apoptotic process, such as cell shrinkage, nuclear fragmentation, chromatin condensation, membrane blabbing. At the end phagocytosis recognize the dying cell and remove it [116]. It is speculated that the decision to go to apoptosis or necrosis is determined by the amount of oxidative stress. Huge amounts of reactive oxygen species cause necrotic cell death in dopaminergic neurons, while trace amounts of reactive oxygen species leads to apoptosis [117].

In the apoptotic process there are two main pathways termed the intrinsic and extrinsic pathways. The intrinsic pathway is under the regulation of mitochondria. BCL-2 (B cell lymphoma 2) family of proteins strictly regulates apoptotic process [118]. They are a large class of proteins mainly divided into 2 subclasses as, anti-apoptotic and pro-apoptotic BCL-2 proteins (Table 1.6).

Table 1.6. BCL-2 family of proteins

<b>Antiapoptotic BCL-2 proteins</b>	<b>Proapoptotic BCL-2 proteins</b>	
	<i>Effectors</i>	<i>BH3 only proteins</i>
BCL-2	BAK	BID
BCL-XL	BAX	BIM
BCL-W	BOK	BAD
MCL-1		PUMA, NOXA

Pro-apoptotic BCL-2 proteins are also divided into two subclasses as follows; effectors and BH-3 only proteins. Anti-apoptotic BCL-2 proteins bind to pro-apoptotic proteins to neutralize their function and prevent apoptosis by inhibiting the formation of mitochondrial outer membrane permeabilization (MOMP). On the other hand, pro-apoptotic proteins increase the rate of apoptosis. Effector pro-apoptotic proteins are stongly involved in

MOMP formation. Conformational changes and homo-oligomerization of BAX and BAK proteins are crucial for MOMP formation as mutation of each of them prevents MOMP formation [119]. The other subclass, BH3 only proteins, supports the functions of effector proteins by sending apoptotic signals to them, also they try to inhibit the functions of anti-apoptotic proteins.

Apoptotic cell death is a highly complex process which involves interactions of numerous proteins as seen in Figure 1.6 [120]. Normally in the cell the anti-apoptotic Bcl-2 proteins bind to Bax (BCL-2-associated X protein) or Bak (BCL-2 antagonist or killer) proteins and neutralize their function. When an apoptotic stimulus comes, BH3 only proteins bind to anti-apoptotic Bcl-2 proteins so that pro-apoptotic BCL-2 family proteins such as BAX or BAK get free and come together in the outer mitochondrial membrane to form MOMP (mitochondrial outer membrane permeabilization).

Following MOMP formation, intermembrane space (IMS) proteins such as cytochrome c, second mitochondria-derived activator of caspase (SMAC) and OMI are released from the mitochondria. Cytochrome c binds to apoptotic protease activating factor 1 (APAF1) and induces its oligomerization such that a heptameric structure is formed termed as apoptosome. Apoptosome complex recruits the initiator procaspase 9 and activates it. Caspase 9 in turn cleaves and activates executioner caspases, caspase 3 and caspase 7, which leads to apoptosis. X-linked inhibitor of apoptosis protein (XIAP) inhibits the activity of caspases. IMS proteins such as SMAC and OMI block the antagonizing activity of XIAP.

In the extrinsic apoptotic pathway, the death receptors such as Fas or Tnf- $\alpha$  is involved. When a ligand binds to its death receptor, the death domain in its cytoplasmic part is exposed and recruits an adaptor protein. Adaptor protein then recruits procaspase 8. Procaspase 8 proteolytically cleaves and activates itself. The dimerized and activated caspase 8 either directly activates executioner caspases, caspase 3 and caspase 7 which leads to apoptosis. Activated caspase 8 also activates BCL-2 homology 3 (BH3)-interacting domain death agonist (BID) by cleaving it into tBID, which leads to crosstalk between intrinsic and extrinsic apoptotic pathways [121].

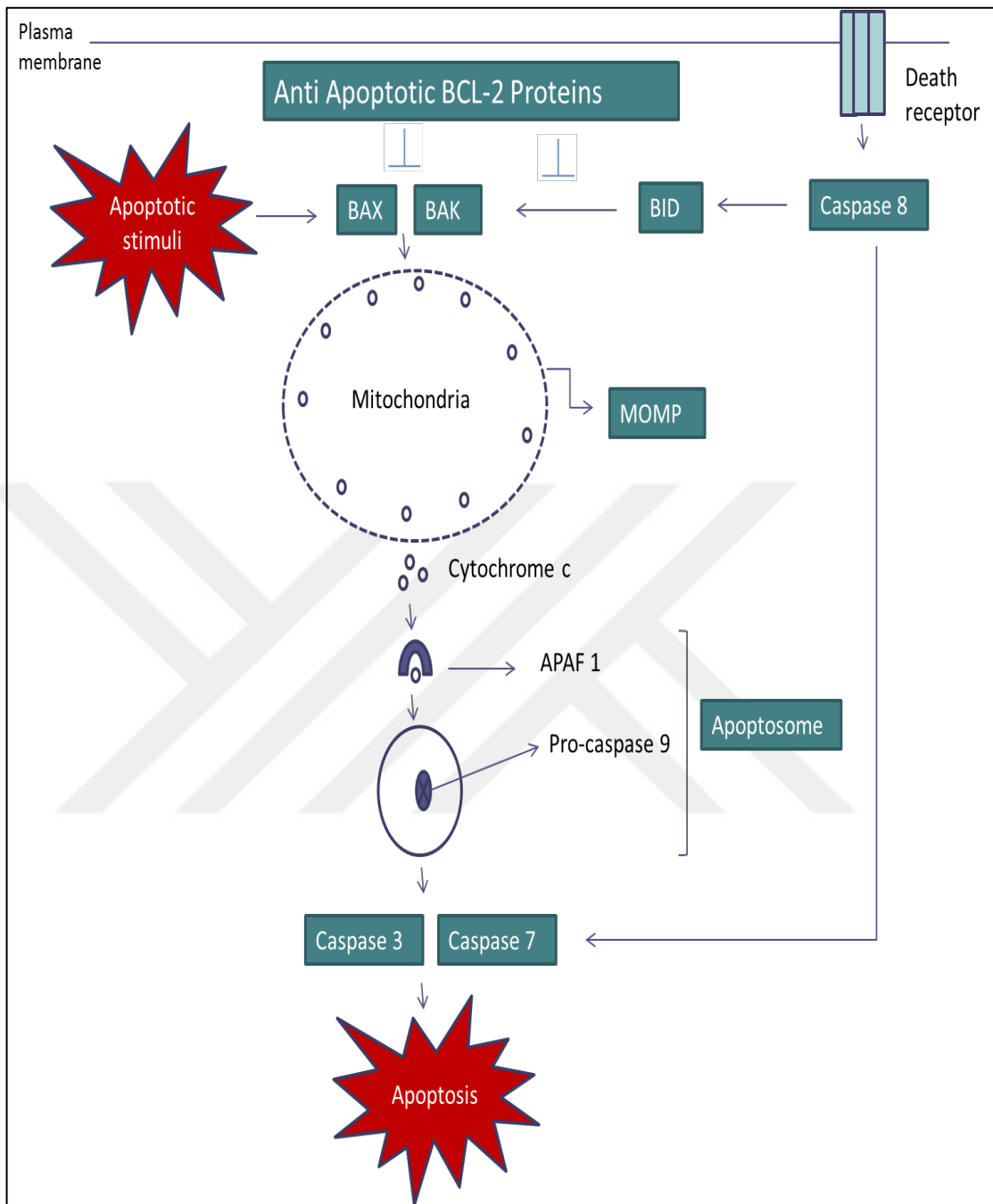


Figure 1.6. Schematic diagram for the summary of the crosstalk between the intrinsic and extrinsic pathways of apoptosis (adapted from ref. 120) BCL-2, B cell lymphoma 2, Bax, BCL-2-associated X protein; Bak, BCL-2 antagonist or killer; BID, BCL-2 homology 3 (BH3)-interacting domain death agonist; APAF1, apoptotic protease activating factor 1.

Detection of apoptotic neurons in PD is very difficult, because of the relatively slow rate of substantia nigra pars compacta dopaminergic cell loss and the rapid clearance of apoptotic cells. Apoptotic cell death only lasts for 1-2 hours and the rate of apoptosis is predicted to be only 5 per cent per year [122]. In addition, neurodegeneration lasts for many years before the symptoms occur in PD, such that apoptotic cells may be at very low quantities at a certain time point. Therefore, fixation of brain tissue for detecting apoptosis may be long after apoptosis occur in the dopaminergic neurons.

In the lights of these informations, many researchers have had hard time detecting apoptotic neurons in postmortem PD brains [123, 124]. On the other hand, many other researchers detected apoptotic neurons in PD brains using very sensitive methods and microscopes. Mochizuki et al [125] were able to show apoptotic neurons by using very sensitive TUNEL (Terminal deoxynucleotidyl transferase dUTP nick end labeling) method. They have demonstrated apoptotic neurons in eight out of eleven patients. Likewise, many studies have shown the presence of the morphological signs of apoptosis in substantia nigra of PD brains [126, 127]. Furthermore, Anglade et al [128] have implicated the presence of apoptotic neurons in substantia nigra of PD brains by using electron microscopy. Similarly, the molecular markers of apoptosis have been demonstrated in PD brains. It is important to note that executioner caspase 3 is significantly elevated in dopaminergic neurons of PD brains of patients [129]. Similarly, increased amounts of initiator caspases, caspase 8 and caspase 9, have been shown in substantia nigra of PD brains [130].

Given the difficulties in detecting the way of neuronal death associated with PD pathogenesis by examination of post-mortem tissues, researchers have turned to in vitro and animal models of the disease to understand the molecular mechanisms of apoptosis. The majority of animal and in vitro models of PD demonstrate morphological apoptosis and activation of caspases. In a MPTP animal model of PD, BAX has been reported to be increased [131]. Of note, Bim expression is required for death in the MPTP animal model. Another BH3-only protein, PUMA is induced and required for death in several in vitro models of PD [132]. A genetically engineered mice lacking BAX, has been durable to MPTP induced toxicity [133]. An elegant study demonstrated that, vectoral overexpression of BCL-2 prior to 6-hydroxydopamine injection to the animals, increased the number of

surviving dopaminergic neurons, indicating the importance of anti-apoptotic BCL-2 proteins [134].

These data emphasize the importance of apoptosis in the degeneration of dopaminergic neurons in PD pathogenesis. A clear understanding of the molecular mechanisms of apoptosis is very crucial in developing potential neuro-protective therapies for PD. Therefore, a huge number of studies are going on to fully understand apoptotic process and halt the degeneration of dopaminergic neurons in PD.

### **1.2.5. Therapeutic Approaches for Parkinson's Disease**

#### ***1.2.5.1. Pharmacotherapy***

As discussed, decreased amounts of dopamine in striatum is a hallmark of PD, therefore, the researchers target to bring dopamine amounts to normal conditions to alleviate the motor symptoms. Levodopa discovery is a breakthrough in the treatment of PD and is considered as a gold standard therapy [135]. In physiological conditions, tyrosine hydroxylase converts tyrosine to L-dopa. Levodopa is then converted into dopamine by the enzyme dopa decarboxylase therefore, it is a precursor for dopamine. It can cross blood brain barrier but most of it is metabolized in the peripheral system. In order to increase the bioavailability of levodopa in the brain, peripheral dopa decarboxylase inhibitors such as carbidopa or benserazide are commonly used to prevent the formation of dopamine in peripheral tissues since dopamine cannot cross blood brain barrier. After levodopa is converted into dopamine, dopamine can be degraded by the enzymes such as catechol-o-methyl transferase (COMT). To overcome this, tolcapone or entacapone, which inhibits COMT enzyme, is used as complement therapy to increase bioavailability of levodopa [136].

Although levodopa is the gold standard therapy, it does not revert dopaminergic neuron death. Therefore, motor complications occur when levodopa is used for a long time. Involuntary movements such as dyskinesia are commonly seen in levodopa treated PD patients affecting their quality of life. To overcome the motor complications, dopamine agonists such as apomorphine, pergolide, pramipexole or ropinirole are used. As a common practice, dopamine agonists are used in the first line of therapy to delay the onset

of levodopa induced motor complications. On the other hand, dopamine agonist treatment may lead to impulse control disorders such as gambling, pathological shopping and eating [137]. In addition, MAO-B inhibitors such as selegiline or rasagiline are used to inhibit the metabolism of dopamine and increase the effectiveness of levodopa. MAO-B inhibitors may also be used as a monotherapy to delay the onset of levodopa, but have a limited therapeutic effect [138].

#### ***1.2.5.2. Functional Neurosurgery***

Surgical operations were widely used in the treatment of PD before the discovery of levodopa. Many years after levodopa, in order to treat motor complications, again a common interest occurred for surgical operations, as the techniques were improved. In deep brain stimulation a medical device, which sends electrical signals to the specific parts of the brain, is implanted to subthalamic nucleus, globus pallidus interna or thalamus. Deep brain stimulation does not damage healthy brain tissue by destroying nerve cells. Instead the procedure blocks electrical signals from targeted areas in the brain. Thalamus, subthalamic nucleus and globus pallidus interna are main targets in deep brain stimulation. Deep brain stimulation has two important advantages: The period of time the patient does not give any response to medication is significantly decreased. In addition, it allows the physician to reduce the dose of medication thereby decreasing its unwanted side effects such as tremor, rigidity and bradykinesia [139]. Rodriguez-Oroz et al [140] has demonstrated that the effect of deep brain stimulation lasts for four years.

#### ***1.2.5.3. Gene Therapy***

Many clinical trials involve gene therapy approaches for the treatment of PD. Adeno-associated viral vector serotype 2 (AAV2) is commonly used for the delivery of specific genes into nigrostriatal pathway of the brain. In one clinical trial, aromatic amino acid decarboxylase (AADC) is administered to the brain using AAV2. Aromatic amino acid decarboxylase is responsible for the conversion of levodopa to dopamine and present in low amounts in PD brain. Although it provides continuous expression of dopamine in nigrostriatal pathway, it is not known how it will affect the motor complications occurring

in levodopa treatment [141]. Another trial investigates the effect of the delivery of the glutamic acid decarboxylase, an enzyme which synthesizes an inhibitory neurotransmitter  $\gamma$ -aminobutyrate, to the subthalamic nucleus. The aim is to have an inhibitory response as seen in deep brain stimulation [142]. Glial cell derived neurotrophic factor (GDNF) analog neurturin is also delivered to nigrostriatal pathway. The main target is to provide neuroprotection to dopaminergic neurons [143].

On the light of these informations, currently there is no known effective neuroprotective or neurorestorative therapy for PD. Finding novel therapies that halt the degeneration of the dopaminergic neurons and replace the degenerated neurons in the brain is the main target of continuous research. Of note, discovery of biomarkers are also the target of increasing number of research since biomarkers may be used to predict the disease before the symptoms occur.

### **1.3. ANIMAL MODELS OF PARKINSON'S DISEASE**

Experimental models of PD are commonly used to understand the possible pathological mechanisms of the disease. In addition, they are also used to develop and test novel therapeutic strategies. The target is to have animal models which extensively mimic pathological and clinical characteristics of PD. To this end, neurotoxin induced, genetically engineered and pharmacological models are used as animal models of PD [144].

#### **1.3.1. Neurotoxin Induced Models**

Various neurotoxins such as 6-hydroxydopamine, MPTP (1-methyl-4-phenyl-1,2,3,6-tetrahydropyridine), rotenone and paraquate are used to mimic PD in animals. The entire toxin based models increase reactive oxygen species production in the brain thereby promoting dopaminergic neuron death. Each model has advantages and disadvantages over each other as will be discussed in detail in the below sections.



### ***1.3.1.1.6-hydroxydopamine (6-OHDA) Model***

6-hydroxydopamine (6-OHDA) is a catecholaminergic neurotoxin and also a by-product of dopamine auto-oxidation. 6-hydroxydopamine is taken into the cell via dopamine transporters (DAT) therefore, it particularly damage catecholaminergic neurons [145].

6-hydroxydopamine cannot cross blood brain barrier, therefore, it is stereotactically injected into specific brain regions as follows, substantia nigra pars compacta, medial forebrain bundle or striatum. When it is injected into substantia nigra pars compacta, the degeneration of the dopaminergic neurons begin after 24 hours of injection [146]. On the other hand, injection of 6-hydroxydopamine into the striatum leads to a more slow degeneration pattern as weeks [147].

The 6-hydroxydopamine model is widely used to investigate the mechanism of dopaminergic neuron death since it causes oxidative stress and mitochondrial dysfunction which are strongly implicated in PD pathogenesis as well (Figure 1.7). Enzymatic deamination of 6-hydroxydopamine by MAO leads to formation of  $H_2O_2$ . Fenton reaction further increases the amount of various reactive oxygen species. It is important to note that, non-enzymatic auto-oxidation of 6-hydroxydopamine further increases the levels of  $H_2O_2$  and reactive oxygen species [148]. Furthermore, the concentration of iron in substantia nigra pars compacta is significantly increased after 6-hydroxydopamine injection [149]. As a result of these reactions, 6-hydroxydopamine increases MDA level which is a marker for lipid peroxidation, while decreasing GSH and SOD activity which are antioxidant defense mechanisms [150]. It has also been shown that 6-hydroxydopamine is toxic to mitochondrial complex I. 6-hydroxydopamine also induces ROS dependent apoptosis in dopaminergic cells [151].

The major drawback of this model is that no Lewy body like inclusions are seen the brain in 6-hydroxydopamine model. In addition, 6-hydroxydopamine causes a dramatic loss of dopaminergic neurons within hours, although in humans there is a progressive loss lasting for years [152].

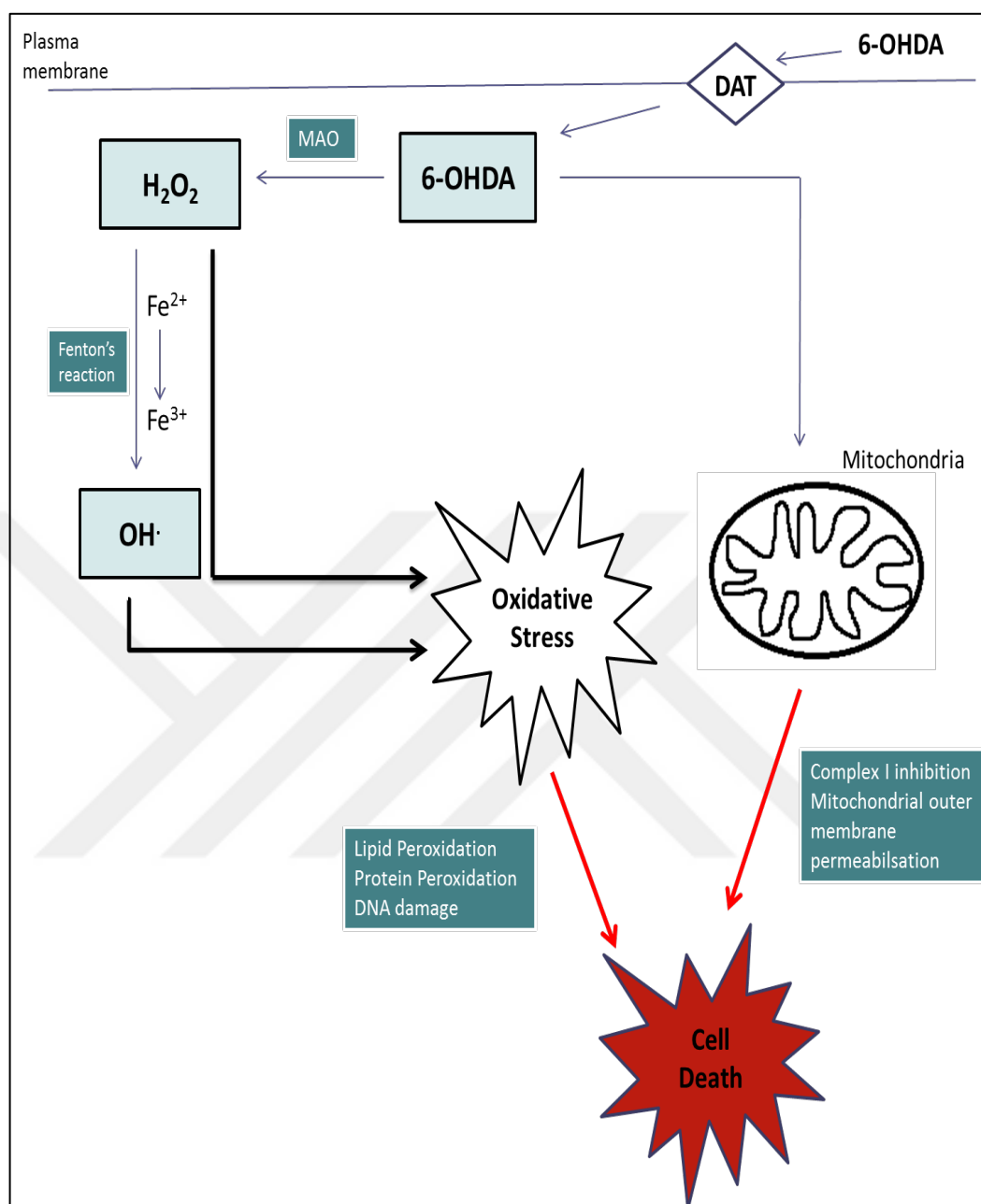


Figure 1.7. Schematic diagram of the toxicity of the 6- hydroxydopamine metabolism in substantia nigra pars compacta. 6-OHDA, 6-hydroxydopamine; MAO, Monoamine oxidase; H<sub>2</sub>O<sub>2</sub>, hydrogen peroxide; DAT, dopamine transporter.

Generally researchers prefer to inject 6-OHDA in one hemisphere while the other hemisphere of the brain serves as an internal control. Studies indicate that bilateral injections increase the rate of animal death after surgery. Although in human PD neurons die bilaterally, unilateral injections of 6-OHDA is preferred as compared to bilateral

injections when testing a therapeutic agent. Unilateral injections 6-hydroxydopamine cause circling motor behavior after administration of the dopaminergic drugs such as apomorphine, due to physiologic imbalance between the lesioned and unlesioned site [153]. Subcutaneous injections of apomorphine cause contralateral rotations of the animal, while amphetamine leads to ipsilateral rotations. The most important advantage of this circling behavior is that, the number of turnings correlates with the severity of the lesion and cell death. Therefore, 6-hydroxydopamine PD model may be a good model for the discovery of novel therapeutics which specifically target survival of dopaminergic neurons.

Various other behavioral tests are used to assess the effect of 6-hydroxydopamine on motor activities [154]. For example paw retraction test, adjusting steps test and forelimb use asymmetry test are used to examine akinetic behavior of PD animals. Reaction time task and catalepsy test are used for the assessment of motor activity initiation. It is important to note that, locomotor activity test gives reliable data of the motor activities of the PD animals since locomotor activity is under the control of dopaminergic pathways. In this test, stereotypic, ambulatory, vertical activities and the distance travelled by the animal are measured [155]. Distance travelled is the measurement of the area travelled by the animal in the activity cage as centimeter. Stereotypic activity is the number of times the rat licking the fore legs, moving them over its head and bites its own fur. Ambulatory activity is the number of squares crossed in the activity cage. Vertical activity is the number of times the rat stands on its hind feet.

### ***1.3.1.2.MPTP Model***

A synthetic drug 1-methyl-4-phenyl-1,2,3,6-tetrahydropyridine (MPTP) causes PD in humans [156]. Although rats are somehow resistant to MPTP toxicity, the systemic administration of MPTP leads to PD in various animals such as mice and primates [157]. Of note, MPTP is able to cross the blood brain barrier. It is selectively taken up into the dopaminergic neurons via DAT. Subsequently, MPTP is converted to its active form  $MPP^+$  by the activity of MAO.  $MPP^+$  inhibits mitochondrial complex I which also results in oxidative stress and cell death. Although  $\alpha$ -aggregations are seen in MPTP animal models, they are not similar to Lewy bodies seen in PD patients [158].

### ***1.3.1.3. Paraquat Model***

Paraquat is an herbicide and a risk factor for human for developing PD [159]. It is a lipophilic compound and it can also cross the blood brain barrier although it is limited and slow. It is systemically injected to the animals. Paraquat selectively kills dopaminergic neurons by inhibiting mitochondrial complex I. Of note, it causes LB like pathology and decreased locomotor activity.

### ***1.3.1.4. Rotenone Model***

Rotenone is also an environmental toxin like paraquat. It is an insecticide which has lipophilic properties. Systemically administered rotenone to the animals leads to degeneration of dopaminergic neurons and PD [160]. It specifically inhibits complex I of mitochondria. It also causes LB like structures and diminished motor activity.

## **1.3.2. Genetic Models**

Although PD is a sporadic disease, a small number of patients have familial PD with an earlier onset. Developing of genetically engineered animals is an interesting area of research to study familial PD. To this end, in order to understand why mutations of specific genes cause PD, the mutations of genes involved in PD etiology such as  $\alpha$ -synuclein and parkin are specifically expressed in animal models.

Controversial results are present between transgenic mouse and rat models over expressing  $\alpha$ -synuclein. A transgenic mice model over expressing  $\alpha$ -synuclein has failed to show dopaminergic degeneration. On the other hand, it clearly shows the presence of lewy body like inclusions [161]. On the contrary, viral over expression of human  $\alpha$ -synuclein in rats leads to dopaminergic degeneration. In addition, lewy body like inclusions are present in those models [162].

Further research is needed in order to extensively understand the genetic basis of PD and discover new therapeutic approaches.

## 1.4. RIBOSOMAL S6 KINASE (RSK) FAMILY

Ribosomal S6 kinase (RSK) is a family of serine threonine kinase which has important functions in cell proliferation, differentiation, survival and motility [163]. RSKs are regulated by Ras/mitogen-activated protein kinase pathway (MAPK) and have two main classes p90RSK (MAPK-activated protein kinase) and p70RSK (s6 kinase).

### 1.4.1. Phospho p90RSK Protein

p90RSK family has three isoforms all of which are highly conserved. p90RSK (MAPK-activated protein kinase) have two distinct kinase domains namely N-terminal kinase domain which phosphorylates substrates and C-terminal kinase domain which is responsible for auto-activation. These two kinase domains are connected via a linker region [164]. The phosphorylation sites of p90RSK are depicted in Figure 1.8 in detail.

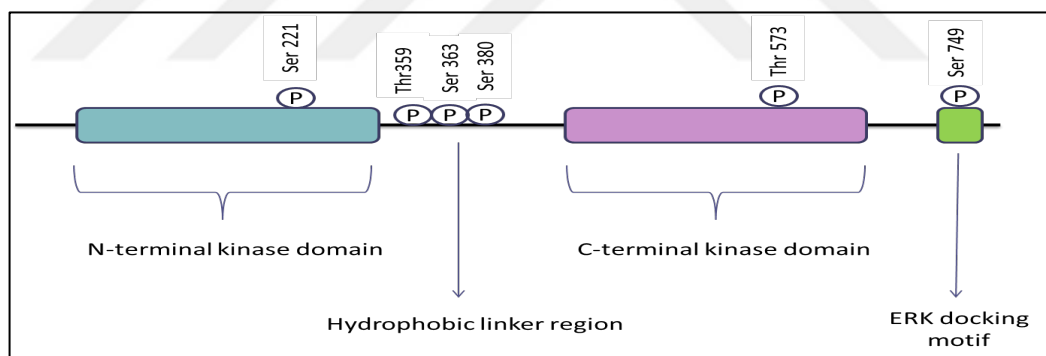


Figure 1.8. Schematic representation of the structure of RSK proteins. Ser, serine; thr, threonine.

When a stimulus such as growth factor, hormone or neurotransmitter is present, MAPK cascade is initiated upstream of RSK (Figure 1.9). Growth factor receptor-bound proteins (GRB2) serves as an interaction between auto-phosphorylated and activated receptors and guanine nucleotide-exchange factor son of sevenless (SOS). GTP-bound Ras via a reaction catalyzed by SOS, binds and activates Raf protein kinases. Activated Raf kinase in turn activates mitogen activated protein kinase kinase (MEK 1/2) via phosphorylation. Phosphorylated MEK 1/2 subsequently phosphorylates extracellular signal regulated

kinases (ERK 1/2). ERK 1/2 then phosphorylate and activate C-terminal kinase domain of RSK which subsequently auto-phosphorylates hydrophobic region of RSK. Then, PDK1, which is a serine/threonine kinase, interacts with phosphorylated hydrophobic domain to phosphorylate N-terminal kinase domain. The active N-terminal kinase domain targets and phosphorylates various downstream targets such as; NF- $\kappa$ B, CREB-1 and ribosomal protein S-6 (rpS6) [165-168].

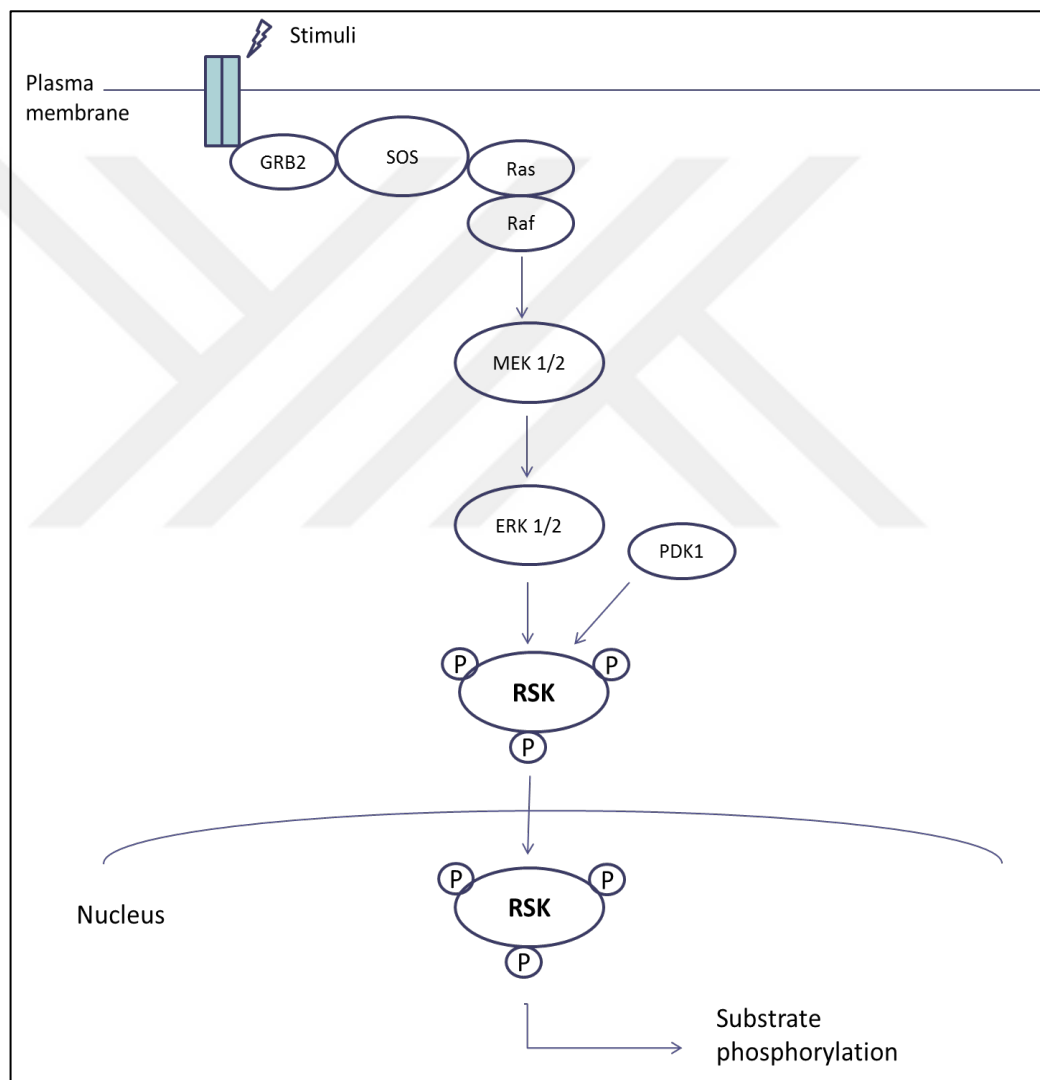


Figure 1.9. Schematic representation of the RSK activation. GRB2, Growth factor receptor-bound proteins; SOS, guanine nucleotide-exchange factor son of sevenless; MEK 1/2, mitogen activated protein kinase kinase; ERK 1/2, extracellular signal regulated kinases.

Activated p90RSK phosphorylates and inactivates pro-apoptotic protein BAD thus inhibits apoptotic pathways and DNA fragmentation [169]. It is important to note that, activated p90RSK proteins also inhibit apoptotic proteins such as BIM, p53 and caspases.

Neise et al [170], also demonstrated that inhibition of p90RSK leads to apoptosis via p53 independent accumulation of p21 protein. On the other hand, in PD, the role of p90RSK is not extensively studied therefore, there is limited knowledge. Activation of p90RSK prevents 6-hydroxydopamine-induced apoptotic death in SH-SY5Y cells through MEK1/2-ERK1/2 mediated pathways [171]. Therefore, p90RSKs are strongly implicated in cell survival processes by inhibiting cell death mechanisms. Further research should be done in order to fully understand the role of RSK proteins in the pathogenesis of PD.

#### **1.4.2. Phospho Ribosomal S6 Protein**

Either phosphorylation of p90RSK (Ser380, Thr359, Ser363) or p70 S6 kinase (Ser235/236) leads to their activation as discussed, which in turn leads to phosphorylation of the S6 ribosomal protein. Phosphorylated S6 ribosomal proteins increase the translation of mRNAs which encode proteins involved in cell cycle progression and translational process such as ribosomal proteins. The phosphorylation sites are Ser235, Ser236, Ser240, Ser244 all of which are located in carboxy terminal domain [172]. Various studies indicate that the phosphorylation of ribosomal s6 protein is involved in synaptic plasticity [173]. There is limited knowledge about the role of ribosomal S6 protein in PD, so that further research should be conducted in this area.

### **1.5. EPIGENETIC MECHANISMS**

The modification of gene expression without alteration of DNA sequence is named as epigenetic mechanisms. Epigenetic mechanisms include DNA methylation and histone post translational modifications. During DNA methylation, DNA methyltransferases covalently add methyl groups to 5' position of the cytosine residues within CpG dinucleotide. Post translational histone modifications include acetylation, methylation, phosphorylation, ubiquitination, and ADP-ribosylation [174]. Epigenetic mechanisms may be influenced from environmental, factors such as chemical, nutritional or social factors

[175]. Increasing number of studies indicate the important role of epigenetic mechanisms in PD pathogenesis [176]. Therefore, it is an interesting area of research to develop new therapeutic agents for PD treatment.

### **1.5.1. Histone Modifications**

There are 5 types of histone molecules as follows; H1, H2A, H2B, H3, H4 and H5. Two of each H2A, H2B, H3, H4 proteins form the core octomeric structure. DNA (147 base pairs) is then wrapped around this core structure in order to form nucleosome. The role of H1 is to hold this nucleosome complex together. This densely packaged histone proteins and DNA form chromatin [177].

Among the post translational modifications of core histone proteins acetylation is particularly important. Histone acetylation is controlled by two enzymes as follows; histone deacetylases (HDACs) and histone acetyltransferases (HATs) [178]. Histone acetyltransferases transfers an acetyl group from acetyl Co-A to lysine residues in histone tails so that N-acetyl lysine is formed. This acetylation neutralizes the positive charge of the histone tails thus reducing the ionic interaction between DNA and histone proteins. Therefore, histone tail acetylation is associated with chromatin relaxation and transcriptional activation. Because positively charged lysine residue is neutralized and its interaction with negatively charged phosphate residue of DNA is disrupted. On the other hand, histone deacetylation is mediated by histone deacetylases (HDACs) which removes the acetyl groups. Thus histone deacetylation is related to a more condensed chromatin state and transcriptional repression. The relaxed chromatin also known as euchromatin leads to gene transcription, whereas condensed chromatin also known as heterochromatin represses gene transcription [179]. Therefore, the balance between the activities of histone deacetylases and histone acetyltransferases is important in the regulation of genes. There are four classes of histone deacetylases. Histone deacetylases target various non-histone proteins such as transcription factors, cytoskeleton proteins and cellular proteins as well [180].

Histone deacetylase inhibitors are particularly important in PD. Increasing number of studies show the effectiveness histone deacetylase inhibitors in treatment of neurodegenerative disorders. Promising studies show that histone deacetylase inhibitors



increase the acetylation levels in the brain and provide neuroprotection via affecting many genes involved in cell cycle regulation, apoptosis and DNA repair process. A recent study shows that class I/II histone deacetylase inhibitors block Bax-dependent apoptosis in mouse cortical neurons via both p53 dependent and independent mechanisms [181].

Valproic acid (VPA) is a class I and class IIa inhibitor HDACs, but not class IIb [182]. Valproic acid has been used in the treatment of epilepsy, migraine, schizophrenia and bipolar disorders. It can cross blood brain barrier. Its bioavailability is 100 per cent in human beings, but a bit lower in rodents. It is important to mention that, valproic acid has well established pharmacokinetic and pharmacodynamic properties. It increases GABA activity, blocks Ca and Na channels and decreases NMDA mediated excitatiton [183, 184]. In addition, there are several studies on the valproic acid's effect on dopamine levels. A chronic treatment leads to increased amounts of dopamine in rodents [185]. Valproic acid treatment prevents MPP<sup>+</sup>-induced death of dopaminergic neurons in an in vitro model of midbrain neuron-glia cocultures [186]. Importantly, Kidd et al [187] showed that, prophylactic valproic acid treatment has protective effects in a MPTP mouse model of PD. Of note, it is commercially available, cheap and easy to use. All of these data make it tempting to test the efficacy of valproic acid in the treatment of PD.

## **1.6. AIM OF THE STUDY**

Increasing number of studies indicate that histone deacetylase inhibition has potential neuroprotective effects in both in vivo and in vitro models of brain disorders. Valproic acid, which is used in the treatment of epilepsy and bipolar disorder, is a histone deacetylase inhibitor. Although there are many studies regarding the neuroprotective effects of histone deacetylase inhibitors in various in vitro models of Parkinson's Disease, there is limited information on the potential effects of the valproic acid in in vivo models.

The hypothesis of this study is that, valproic acid will be an adjuvant therapy to levodopa for the treatment of PD. To test this hypothesis, valproic acid was used post acutely to compare its potential effects with the effects of gold standard therapeutic agent levodopa on neuronal survival, motor activity, oxidative stress parameters, apoptotic mechanisms and histone acetylation levels in the brain in a 6-hydroxydopamine animal model of Parkinson's Disease.

In the light of this target, surgical operations were completed with a stereotaxic frame. All rats were evaluated for apomorphine induced rotations to validate the model. Stereotypic, ambulatory, vertical, horizontal motor activities and distance travelled by the animal were measured with an activity monitoring system. Coronal sections were taken through the substantia nigra on a cryostat. Afterwards, immunohistochemistry for tyrosine hydroxylase, TUNEL assay and cresyl violet and hematoxylin eosin staining were performed. Biochemical analysis of oxidative stress parameters were measured from striatal tissue of the rats. Finally, western blot analysis for phospho p90RSK, phospho S6 ribosomal protein, histone acetylation were performed from striatal tissue.



## 2. MATERIALS

Chemicals, reagents, antibodies, commercial kits and technical equipments used in this study are listed below.

### 2.1. CHEMICALS AND REAGENTS

- 1-Chloro-2,4 dinitrobenzene (Acros Organics)
- 20X TBS Tween-20 Buffer (Thermo Scientific)
- 2-propylpentanoic acid sodium(Sigma)
- 2-Thiobarbituric acid (Sigma)
- 5,5'-Dithiobis (2-nitrobenzoic acid) (Alfa Aesar)
- 6-hydroxydopamine hydrochloride (Sigma)
- Acetic acid (100 per cent) (Riedel-de Haen)
- Ammonium sulfate (Sigma)
- Benserazide hydrochloride (Sigma)
- Blotto, non-fat dry milk (Santa Cruz)
- Cell cleaning solution for UV/VIS (Agilent Technologies)
- Color Protein Standard (11-245 kDa) (New England Biolabs)
- Copper (II) chloride (Sigma)
- Copper (II) sulfate pentahydrate (Riedel-de Haen)
- Cresyl violet aetate (Santa cruz Biotechnology)
- DAB Chromogen (Thermo Fisher Scientific)
- DAB Substrate Buffer (Thermo Fisher Scientific)
- Di-sodium hydrogen phosphate (Merck)
- Entellan Mounting medium (BioMount)
- Eosin Y solution alcoholic(Sigma)
- Ethylenediaminetetraacetic acid (Fluka)
- Folin-Ciocalteu's phenol reagent (Sigma)
- Formaldehyde solution (37 per cent) (Merck)
- Frozen section compound (Leica Microsystems)

- Hydrogen peroxide solution 30 per cent (Sigma)
- Ketazol 10 per cent (Richter Pharma)
- L-3,4 di-hydroxy phenyl alanine (Sigma)
- L-Ascorbic acid, (Bioshop)
- Mayer's Hematoxylin (Thermo Fisher Scientific)
- Metaphosphoric acid (Alfa Aesar)
- Nitroblue Tetrazolium (Fisher Bioreagents)
- Phosphate buffered saline tablets (Sigma)
- Potassium cyanide (Merck)
- Potassium sodium tartrate tetrahydrate (Acros Organics)
- Potassium dihydrogen phosphate (Merck)
- Potassium hexacyanoferrate (III) (Alfa Aesar)
- R-(-)-Apomorphine hydrochloride (Sigma)
- Rhompun 2 per cent flakon (Bayer)
- Saline (Isotonic 9 per cent NaCl) (Polifarma)
- Sodium acetate(Sigma)
- Sodium carbonate anhydrous (Riedel-de Haen)
- Sodium chloride (Sigma)
- Sodium dihydrogen phosphate (Sigma)
- Sodium hydroxide pellets (Sigma)
- Titriplex III (Merck)
- Trichloroacetic acid (Fisher Chemical)
- Tris Base (Fisher Bioreagents)
- Tri-sodium citrate dihydrate (Merck)
- Triton X-100 (Roche)
- Xanthine (Alfa Aesar)
- Xylene(Sigma)

## 2.2. ANTIBODIES

- Anti-acetyl-histone H3 (Lys9) (Millipore)
- Anti-rabbit IgG HRP-linked antibody (Cell signaling)
- Anti-tyrosine hydroxylase (Millipore)
- Pathscan Multiplex Western Cocktail II - phospho p90RSK, phospho S6 ribosomal protein (Cell signaling)
- $\beta$ -actin antibody (Cell signaling)

## 2.3. COMMERCIAL KITS

- Amersham ECL Advance Western Blotting Detection Kit, GE Healthcare (Lumigen TMA A solution, Lumigen TMA B solution)
- In situ cell death detection kit, POD, Roche (Terminal deoxynucleotidyl transferase enzyme solution, Nucleotide mixture in reaction buffer, Anti-fluorescein antibody conjugated with horse-radish peroxidase)
- NuPAGE MES SDS Buffer Kit (for Bis-Tris Gels), Life Tech (NuPAGE MES SDS Running Buffer, NuPAGE LDS Sample Buffer, NuPAGE Antioxidant, NuPAGE Reducing Agent)
- Qubit Protein Assay Kit, Life Tech (Qubit protein reagent, Qubit protein buffer, Qubit protein Standard #1, Qubit protein Standard #2, Qubit protein Standard #3)
- RIPA Lysis Buffer System, Roche (Lysis Buffer, PMSF, Protease inhibitor cocktail, sodium orthovanadate)
- Vectastin Universal Quick Kit, Vectastin (Normal Horse Serum, Biotinylated Universal Secondary antibody, Streptavidin/Peroxidase preformed complex)

## 2.4. LABORATORY EQUIPMENTS

- 4-12 per cent Bis-Tris Protein Gels (Life Tech)
- Low profile blades (Richard-Allan Scientific)
- iBLOT Transfer Stack, PVDF (Life Tech)

- M-polylysine slides (25\*75\*1,0 mm) (Thermo Scientific)
- Qubit Assay Tubes, 500 tubes (Life Tech)
- Propylene centrifuge tubes; 50 mL, 15 mL, 2 mL, 0.5 mL (Isolab)
- Micropipettes 10  $\mu$ L, 100  $\mu$ L, 200  $\mu$ L, 1000  $\mu$ L (Eppendorf)

## 2.5. LABORATORY TECHNICAL INSTRUMENTS

- Automatic Glass Cover slipper (Leica)
- Balance (OHAUS Adventurer)
- Biological Safety Cabinet (Thermo)
- Stereological workstation and light microscope (Leica)
- Blot transfer (iBlot 2 Dry Blotting System)
- Computer-based gel imaging instrument (DNR)
- Cryostat (Leica)
- Gel electrophoresis (Biorad)
- Heater (Thermo)
- Homogenizer (Waring)
- Incubator (Mettler)
- Locomotor activity cage (Commat, MAY)
- Magnetic stirrer (IKAMAG)
- Microcentrifuge (Sigma)
- Micromotor system (Mannas, Strong 204-102L)
- Microscope (Leica)
- pH meter (Hanna instruments PH211, Germany)
- Power supply (Biorad)
- Qubit 2.0 Fluorometer (Life Technologies)
- Refrigerator (Arçelik, Ugur)
- Autoclave (Sanyo MLS 3780)
- Shaker (Heidolph)
- Staining Automat (Leica)
- Stereotaxic frame (Stoelting)

- Ultracentrifuge (Sigma)
- Ultrasonicator (Bandelin)
- UV spectrophotometer (Agilent 8453)
- Vortex (MS1 Minishaker)
- Water bath (Grant)



### 3. METHODS

#### 3.1. EXPERIMENTAL SETUP AND GROUPS

Adult male Wistar albino rats (250-300 g) were obtained from Yeditepe University Experimental Research Center (YUDETAM). All of the experiments were approved by the Ethical Committee of Yeditepe University Experimental Research Center and the use of animals was in compliance with US National Institutes of Health Guide for Care and Use of Laboratory Animals. Animals were maintained in standard housing conditions with constant temperature, humidity, 12-h light/dark cycles, and free access to food and water.

42 rats were randomly divided into 7 experimental groups as follows: sham operated (S), sham operated and VPA treated (SV), sham operated and L-DOPA treated (SL), nigraly 6-OHDA injected (PD), nigraly 6-OHDA injected and VPA treated (PV), nigraly 6-OHDA injected and L-DOPA treated (PL), nigraly 6-OHDA injected and VPA and L-DOPA treated (PVL). Each group has 6 animals (Table 1).

Table 3.1. The experimental groups and number of animals.

<b>Groups</b>	<b>Number</b>
Sham operated (S)	n=6
Sham operated and VPA treated (SV)	n=6
Sham operated and L-DOPA treated (SL)	n=6
Nigraly 6-OHDA injected (PD)	n=6
Nigraly 6-OHDA injected and VPA treated (PV)	n=6
Nigraly 6-OHDA injected and L-DOPA treated (PL)	n=6
Nigraly 6-OHDA injected and VPA and L-DOPA treated (PVL)	n=6

The sequence of operation, locomotor activity, apomorphine test and drug treatments are explained in Table 2. All rats were pretrained on locomotor activity. Locomotor activity test was repeated at one, two and three weeks postoperation. Apomorphine test was carried out twice after the operation. All animals were admitted to drug treatment meanwhile.



Table 3.2. The time schedule of the experiments.

<b>Days</b>	<b>Procedure</b>
-2	Locomotor activity
0	Operation
7	Locomotor activity
10	Apomorphine test
12	The beginning of the treatment with Valproic acid, L-DOPA or saline.
15	Locomotor activity
21	The ending of the treatment with Valproic acid, L-DOPA or saline, Locomotor activity
22	Apomorphine test
23	Animal sacrifice

### 3.2. INTRANIGRAL 6-HYDROXYDOPAMINE INJECTIONS

All animals were anesthetized by intramuscular (im) injections of xylazine (10 mg/kg) and ketamine (80 mg/kg). After they are deeply anesthetized, rats were fixed in a stereotaxic frame in the flat skull position. The scalp was shaved and a small central incision was made to expose the skull. Bregma and lambda points were located (Figure 3.1).

A small hole was drilled with a micromotor using the following coordinates of substantia nigra pars compacta: anteroposterior from bregma (AP) = -4.8 mm, mediolateral from the midline (ML) = -1.8 mm and dorsoventral from the skull (DV) = -8.2 mm [188]. The coordinates were confirmed according to rat brain atlas [189].

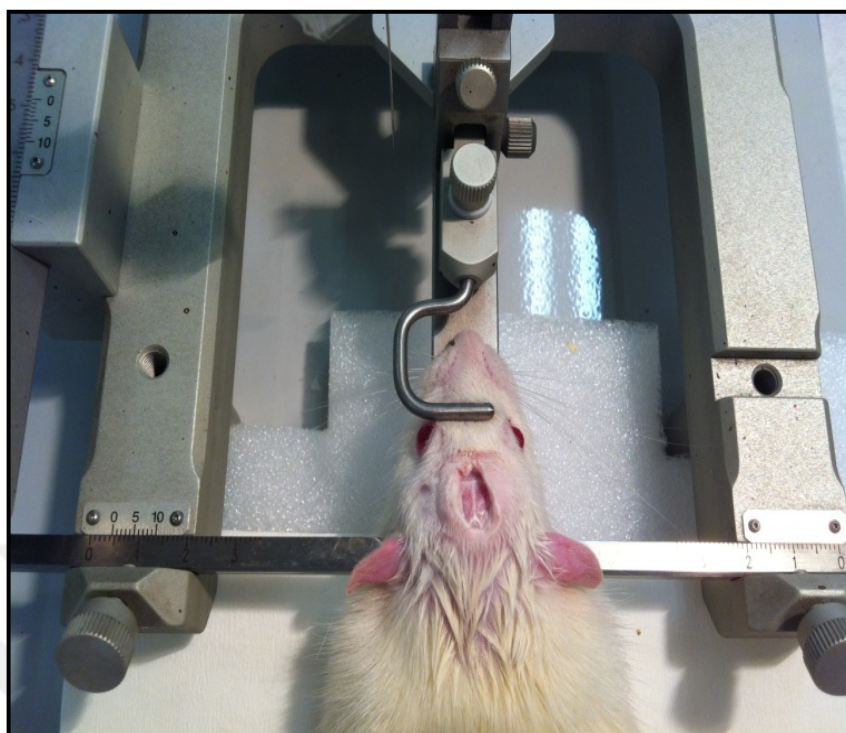


Figure 3.1. The rats were fixed in a stereotaxic frame and Bregma and lambda points were located.

6-hydroxydopamine ( $8 \mu\text{g}/\text{per rat}$  in  $2 \mu\text{l}$  saline with 0.1 per cent ascorbic acid) was infused with a  $5 \mu\text{L}$ , 26 gauge hamilton syringe at a flow rate of  $0.2 \mu\text{l}/\text{min}$  into the right substantia nigra pars compacta (Figure 3.2). Sham operated animals were submitted to the same procedure but instead of 6- hydroxydopamine,  $2 \mu\text{l}$  vehicle (0.9 per cent saline containing 0.1 per cent w/v ascorbic acid) was injected into the substantia nigra pars compacta. The needle was left in place for an additional 5 minutes before retraction. Then the surgical area was sutured. All operations were performed under aseptic conditions.

Of note, 6- hydroxydopamine was freshly prepared just before the surgical operation and kept in dark since it quickly oxidizes.



Figure 3.2. Stereotaxic operation. Intranigral 6-hydroxydopamine injections were performed with Stoelting stereotaxic frame.

### 3.3. APOMORPHINE INDUCED ROTATION TEST

Unilateral injection of 6-hydroxydopamine leads to asymmetric circling motor behavior after administration of the dopaminergic drugs such as apomorphine, due to physiologic imbalance between the lesioned and unlesioned site. This circling behavior gives reliable information on the degree of lesion in substantia nigra pars compacta. [154]

10 days after 6-hydroxydopamine or saline injection to the substantia nigra pars compacta, all rats were evaluated for apomorphine induced rotations (Figure 3.3). All animals were injected 0.5 mg/kg apomorphine subcutaneously (sc) and placed in the plastic cylinders. The rotational behavior was monitored for 30 minutes. All observations were made between 9 a.m. and 12 p.m. Only the rats showing pronounced rotational behavior (more than 5 contralateral turns/min) were selected for the study. Many studies showed that more than 5 contralateral rotations account for approximately 90 per cent dopamine loss in striatum [190].

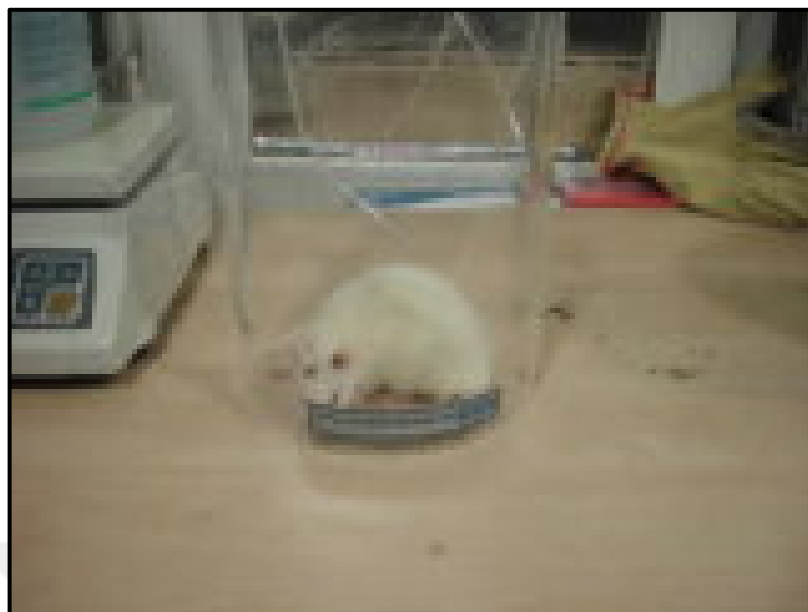


Figure 3.3. Apomorphine induced rotation test.

#### **3.4. SPONTANEOUS LOCOMOTOR ACTIVITY**

Motor activity measurements were recorded before the operation, before drug therapy commencement and twice after drug administration using an animal activity monitoring system (MAY - Activity Monitoring System - Commat Ltd., TR) (Figure 3.4). Locomotor activity cage is a rectangular frame (45x45x30 cm) containing infrared light sources on each side. The floor of the cage is an activity platform connected to an electromechanical counter. When the animal moves, the infrared beams are disrupted and the instrument counts it as a locomotor activity. To record locomotor activity, each rat was individually placed in the same area of the plexiglass cage. Spontaneous motor activity was recorded at 5 min intervals during a 10 min period. All observations were made between 9 a.m. and 12 p.m. The plexiglass cage was cleaned with a wet towel between the tests. Stereotypic, ambulatory, vertical, horizontal motor activities and distance travelled by the animal were measured [191].



Figure 3.4. Spontaneous locomotor activity test was performed using an animal activity monitoring system (COMMAT).

### 3.5. DRUG TREATMENT

All of the rats were intraperitoneally injected with either valproic acid, levodopa combined with benserazide hydrochloride or saline for 10 days after the surgical operation. Rats in S and PD groups were intraperitoneally injected with saline. In SV and PV groups the rats received intraperitoneal injections of valproic acid (300 mg/kg). The rats in SL and PL groups were treated with levodopa (10 mg/kg) combined with benserazide hydrochloride (2 mg/kg) to inhibit peripheral decarboxylation of levodopa. In the PVL group the rats received intraperitoneal injections of valproic acid (300 mg/kg) and L-DOPA (10 mg/kg) combined with benserazide hydrochloride (2 mg/kg) [192]. All of the drugs were dissolved in saline.

### **3.6. SACRIFICATION OF THE ANIMALS**

After the last measurement, animals were decapitated with a guillotine and their brains were dissected out. The brains were rapidly frozen on dry ice and stored at  $-80^{\circ}\text{C}$  until used. The striata of the brains were used for biochemical analysis of oxidative stress and western blot experiments. Coronal sections were taken through the substantia nigra on a cryostat for the histological experiments.

### **3.7. HISTOLOGY**

#### **3.7.1. Cryosectioning**

The brains of the animals were embedded in mounting medium and cut into  $16\ \mu\text{m}$  coronal sections on a cryostat (Leica) at  $-20^{\circ}\text{C}$ . Coronal sections were taken through substantia nigra ( $-4.8\ \text{mm}$  posterior to bregma) onto polylysine coated slides. The slides were dried on a slide warmer at  $40^{\circ}\text{C}$  to remove water and ensure tissue adhesion to the slides more effectively. The slides were stored at  $-80^{\circ}\text{C}$  until used.

#### **3.7.2. Immunohistochemistry for Tyrosine Hydroxylase**

Immunohistochemistry is a highly sensitive method to detect the presence and location of the interested proteins in tissues. It is a reliable method to quantify tyrosine hydroxylase positive neurons. Tyrosine hydroxylase is the rate limiting enzyme in the biosynthesis of dopamine; it catalyzes the conversion of L-tyrosine to L-DOPA, so it is a selective and specific indicator of dopaminergic neurons in substantia nigra pars compacta in Parkinson's Disease.

Labeled streptavidin biotin (LSAB) method was used for the immunohistochemical detection of tyrosine hydroxylase [193]. In this method, biotinylated secondary antibody binds to primary antibody, and then streptavidin peroxidase complex binds to secondary antibody. Finally, the reaction is visualized with a chromogen (Figure 3.6).

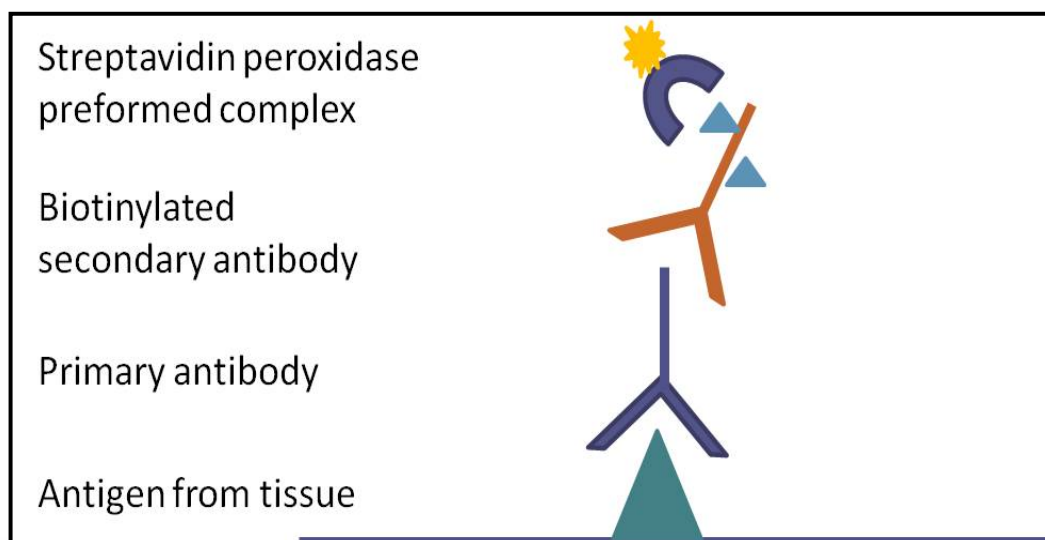


Figure 3.5. Schematic representation of Labeled streptavidin biotin (LSAB) method.

### **3.7.2.1. Fixation**

The fixative (10 per cent neutral buffered formalin) solution was prepared in advance. 4 g sodium phosphate monobasic ( $\text{NaH}_2\text{PO}_4$ ) and 6.5 g sodium phosphate dibasic ( $\text{Na}_2\text{HPO}_4$ ) were weighed out and dissolved in 900 mL distilled water. 100 mL formaldehyde (37 per cent) was added to the solution to have a final volume of 1000 mL. Furthermore, to have washing solution, 1 phosphate buffered saline (PBS) tablet (Sigma) was dissolved in 100 mL distilled water.

The sections were dried in an incubator at  $37^\circ\text{C}$  for 20 minutes. Then the sections were fixed in 10 per cent neutral buffered formalin (pH 7.4) solution for 20 minutes at room temperature and the slides were washed twice with 1X PBS (pH 7.4).

### **3.7.2.2. Permeabilisation**

During fixation of sections methylene bridges are formed which mask antigenic sides of the proteins. Therefore, antigen retrieval step is essential in immunohistochemical staining to expose antigenic sides of the proteins. The slides were incubated in permeabilisation solution (0.1 per cent tri-sodium citrate dihydrate, 0.1 per cent triton X-100 in distilled

water) for two minutes to perform antigen retrieval and washed with 1X PBS. This step was repeated twice at 4°C. To block endogenous peroxidase activity and reduce background staining, the slides were incubated in 0.3 per cent hydrogen peroxide solution for 30 minutes at room temperature which is followed by a washing step with 1X PBS.

### ***3.7.2.3. Blocking***

A hydrophobic barrier was made around the tissue with a barrier pen. The slides were incubated in blocking solution (normal horse serum) in humidified chamber at room temperature for 30 minutes to eliminate nonspecific binding of primary antibody.

### ***3.7.2.4. Immunostaining***

The sections were incubated in 1:1000 dilution of the primary antibody (rabbit anti-tyrosine hydroxylase) overnight at 4°C in a humidified chamber. Then the slides were rinsed with 1X PBS. Biotinylated secondary antibody (anti-rabbit/mouse/goat IgG) was applied to the sections for 30 minutes in humidified chambers at room temperature. The slides were washed with 1X PBS. Streptavidin peroxidase preformed complex solution was applied to the sections for 30 minutes at room temperature in humidified chambers. The slides were washed with 1X PBS. DAB (3,3'-diaminobenzidine) solution was prepared by mixing 1000 µL DAB substrate buffer with 50 µL DAB chromogen. The reaction was visualized by DAB as a chromogen. The sections were counterstained with Mayer's hematoxylin and rinsed in running tap water. The sections were dehydrated in ascending alcohol concentrations, cleared in xylene and coverslipped in Entellan mounting medium.

### **3.7.3. TUNEL Assay**

TUNEL assay is a reliable method to detect apoptotic neuron death. DNA double strand breaks which occur during apoptosis are precisely labeled and visualized with TUNEL assay. In this technique, terminal deoxynucleotidyl transferase (TdT) enzyme adds fluorescein labeled nucleotides to the free 3'-OH DNA ends which is then visualized with anti-fluorescein antibody labeled with POD and substrate reaction.



### ***3.7.3.1. Fixation***

The sections were dried in an incubator at 37°C for 20 minutes and the sections were fixed in 4 per cent paraformaldehyde (pH 7.4) solution for 20 minutes at room temperature. Then the slides were washed twice with 1X PBS (pH 7.4).

### ***3.7.3.2. Permeabilisation***

The slides are incubated in permeabilisation solution (0.1 per cent tri-sodium citrate dihydrate, 0.1 per cent triton X-100 in distilled water) to expose antigenic sites of the proteins for 4 minutes and washed with 1X PBS. This step was repeated twice at 4°C.

### ***3.7.3.3. Blocking***

A hydrophobic barrier was made around the tissue with a barrier pen. The slides were incubated in blocking solution (normal horse serum) in humidified chamber at room temperature for 30 minutes. The slides were rinsed twice with 1X PBS.

### ***3.7.3.4. Labeling***

TUNEL reaction mixture (45 µl label solution was mixed with 5 µL enzyme solution for one section) was prepared. The sections were incubated in TUNEL reaction mixture in dark, 37°C humidified chambers for 60 minutes. Then the slides were washed with 1X PBS three times for 5 minutes each. Converter-POD was added to the sections and incubated in dark, 37°C humidified chambers for 30 minutes. Then the slides were washed with PBS three times at room temperature. The reaction was visualized by using DAB (1000 µL DAB substrate buffer was mixed with 50 µL DAB chromogen) solution as a chromogen. The sections were counterstained with Mayer's hematoxylin and rinsed in tap water. Sections were dehydrated in ascending alcohol concentrations, cleared in xylene and coverslipped in Entellan mounting medium.

#### **3.7.4. Cresyl Violet Staining**

Cresyl violet is a basic dye and stains Nissl substances in cytoplasm of neurons dark blue. Cresyl violet staining is generally used to demonstrate the structural features of the neurons and in this study it was performed to determine the 6- hydroxydopamine lesion site.

Two solutions were prepared in advance. To prepare solution A, sodium acetate was dissolved in distilled water. For solution B, glacial acetic acid was diluted with distilled water. Then the two solutions were mixed together and the pH was adjusted to 3.8-4.0 with acetic acid. Cresyl violet acetate was dissolved in this solution and left on the magnetic stirrer overnight in dark. The staining solution was filtered with a filter paper before staining the sections. All of the solutions were put into coplin jars and the protocol explained below was followed:

- The sections were dried in an incubator at 37°C for 20 minutes.
- The sections were fixed in neutral formaldehyde (pH 7.4) solution for 20 minutes at room temperature.
- Then the slides were washed with distilled water for 1 minute.
- The sections were stained with Cresyl Violet for 20 minutes on a shaker.
- The slides were washed with distilled water.
- The sections were then dehydrated in ascending alcohol series (70 per cent, 80 per cent, 90 per cent, 96 per cent, and 100 per cent) for 1 minute each.
- Finally the slides were cleared in xylene I and II for 2 minutes each.
- The slides were coverslipped in Entellan mounting medium using automatic glass coverslipper.

#### **3.7.5. Hematoxylin Eosin Staining**

Hematoxylin Eosin staining is a routine stain in histology laboratory and commonly used to investigate the pathology in tissue sections [194]. Hematoxylin is a positively charged basic dye; therefore, stains negatively charged nucleic acid components in the nucleus blue color. On the contrary eosin dye is a negatively charged acidic dye, so that it stains positively charged structures such as proteins in the cytoplasm pink color.

All of the solutions were prepared in advance and put into coplin jars and the protocol explained below was followed:

- The sections were dried in an incubator at 37°C for 20 minutes.
- Then the sections were fixed in neutral formaldehyde (pH 7.4) solution for 25 minutes at room temperature.
- The slides were washed with distilled water.
- The sections were stained with Mayer's hematoxylin solution for 5 minutes and rinsed in running tap water for 2 minutes.
- The slides were decolorized in acid alcohol (99 mL 70 per cent ethanol was mixed with 1 mL glacial acetic acid) for 1 minute.
- The slides were washed in tap water for 1 minute.
- The sections were subjected to 80 per cent ethanol for 2 minutes.
- Then the sections were counterstained with Eosin for 4 minutes.
- The sections were dehydrated in ascending alcohol series (80 per cent, 96 per cent, 96 per cent, 96 per cent, and 100 per cent) for 1 minute each.
- Finally the slides were cleared in xylene I and II for 1 minute each.
- The slides were coverslipped in Entellan mounting medium using automatic glass coverslipper.

### **3.7.6. Analysis by Light Microscopy**

Each section (Figure ) was examined via a stereological workstation equipped with a CCD digital camera (Optronics Microfire 1600x1200P, Goleta, CA, USA), computer assisted motorized stage (Bioprecision, Howtrone, NY, USA), mikrokator (Heidenhein, Traunreut, Germany), image card (ATI FireGL Advance Micro Device, Camberly, UK) and light microscope (Leica DM 4000B, Wetzlar, Germany).

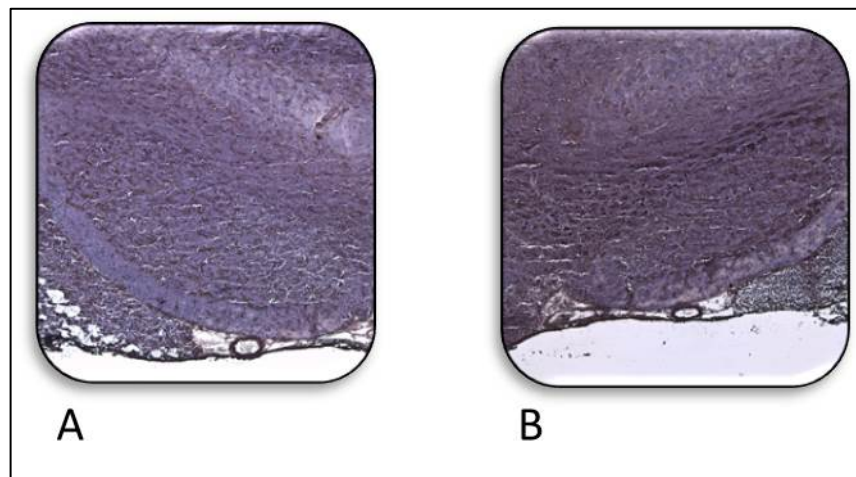


Figure 3.6. Figure representing the right and left substantia nigra pars compacta. A. Immunofluorescence image shows the tyrosine hydroxylase immunoreactivity of right substantia nigra in a 6-hydroxydopamine injected animal. B. Immunofluorescence image shows the tyrosine hydroxylase immunoreactivity of right substantia nigra in a saline injected animal.

Tyrosine hydroxylase positive neurons and TUNEL positive neurons were counted in substantia nigra pars compacta (Figure 3.6) using the above mentioned microscopy with Stereo Investigator 7.0.5 (StereoInvestigator, Microbrightfield, Williston, VT) image analysis software. Dopaminergic neurons were clearly distinguished depending on their shapes and size. Neurons were counted on both right (lesioned side) and left (internal control) substantia nigra pars compacta of the rat brains.

Histopathological evaluations were performed on the cryosections stained with hematoxylin and eosin and cresyl violet staining. Similarly, each section was examined with Stereo Investigator 7.0.5 image analysis software.

### 3.8. BIOCHEMICAL ANALYSIS OF OXIDATIVE STRESS

#### 3.8.1. Sample Preparation

The striata of the brains were homogenized on ice in appropriate volume of distilled water with a homogenizer. The homogenates were centrifuged (3500 rpm, 4°C) for 15 minutes and the supernatants were collected.

#### 3.8.2. Determination of Protein Concentration (Lowry Method)

The protein concentration was determined according to the Lowry Method [195]. According to the principle of the Lowry method, divalent copper ions interact with peptide bonds of the proteins and are reduced to monovalent ions under alkaline conditions. Monovalent copper ions react with Folin reagent and an unstable molybdenum/tungsten blue product is produced.

Alkaline copper reagent and folin reagent were prepared freshly. To prepare alkaline copper reagent appropriate amounts of sodium hydroxide (NaOH), sodium carbonate (Na<sub>2</sub>CO<sub>3</sub>), cupric sulfate (CuSO<sub>4</sub>) and sodium potassium tartrate (NaKC<sub>4</sub>H<sub>4</sub>O<sub>6</sub>) were weighed out and dissolved in distilled water. To prepare folin reagent appropriate volume of 2N folin reagent was diluted with distilled water. Since the folin reagent is light sensitive, it was kept in amber bottle.

- One volume of sample was mixed with one volume of alkaline copper reagent and for blank one volume of alkaline copper reagent was mixed with distilled water.
- The mixtures were incubated at room temperature for 10 minutes.
- Then equal volume of Folin reagent was added to the mixtures.
- The solution was incubated at 55°C for 5 minutes,
- The absorbance was measured at 650 nm.

The following formula was used for the calculation of the protein concentration:

$$\mu\text{g/mL} = \left\{ \left( \text{Optical density of the } \frac{\text{sample}}{0.125} \right) \times 50 \times \text{Dilution factor} \right\} \quad (3.1)$$

### 3.8.3. Determination of Lipid Peroxide Level

The Malondialdehyde level was determined according to the method of Placer et al [196]. Malondialdehyde formed at the final step of the lipid peroxidation interacts with thiobarbituric acid to form pink colored MDA-TBA adduct. In the method adopted from Placer et al., the pink colored product is measured spectrophotometrically.

Thiobarbituric acid (TBA) was dissolved in 10 per cent perchloric acid and trichloro acetic acid (TCA) was dissolved in distilled water. One volume of TBA solution was mixed with three volumes of 10 per cent TCA were mixed immediately before use.

- Sample and the freshly prepared solution were mixed and for blank the solution was mixed with 0.9 per cent NaCl.
- The mixtures were boiled for 20 minutes at 100°C in water bath and cooled under running tap water.
- Then the mixtures were centrifuged at 2500 rpm for 5 minutes.
- The absorbance of the supernatant was measured at 532 nm.

The formula was used for the calculation of the malondialdehyde level:

$$nmol/g = \{Optical\ density\} / 0.092\ nmol/g\ tissue \quad (3.2)$$

### 3.8.4. Determination of Superoxide Dismutase (SOD) Activity

The superoxide dismutase (SOD) activity was determined according to the method of Sun et al [197]. The principle of this experiment depends on nitroblue tetrazolium (NBT) reduction. If there is no enzyme activity, the NBT reduction occurs and a blue-purple colored product is produced. According to the SOD activity the NBT reduction is disrupted such that a lighter color is produced.

To prepare assay reactive, 0.3 mmol/L xantine, 0.6 mmol/L disodium salt dihydrate (Na<sub>2</sub>EDTA), 150 μmol/L nitroblue tetrazolium (NBT), 400 mmol/L sodium carbonate (Na<sub>2</sub>CO<sub>3</sub>), 1 g/L bovine serum albumin (BSA) were prepared and mixed in amber bottle. 2 M ammonium sulfate (NH<sub>4</sub>2SO<sub>4</sub>) was prepared in distilled water to dilute xantine oxidase

(167 U/L). 0.8 mmol/L cuprous chloride ( $\text{CuCl}_2$ ) was prepared in distilled water. 3 volumes of chloroform were mixed with 5 volumes of ethanol to prepare chloroform/ethanol solution.

- Equal volumes of sample and chloroform/ethanol solution were mixed and centrifuged at 3500 rpm for 45 minutes at 4°C.
- The supernatant was mixed with assay reactive and xantine oxidase, for the blank assay reactive was mixed with double distilled water and xantine oxidase.
- The reactions were incubated at room temperature for 20 minutes.
- Cuprous chloride was added to the tubes to stop the reaction and the absorbance was measured at 560 nm immediately.

SOD activity (U/mg protein) is expressed as the amount of SOD enzyme required for the 50 per cent inhibition of NBT reaction and the formula to calculate one enzyme unit is indicated as:

$$\text{Enzyme unit (U)} = \left\{ \left( \text{per cent of } \frac{\text{inhibition}}{50} \right) \times \text{dilution factor} \right\} \quad (3.3)$$

### 3.8.5. Determination of Reduced Glutathione (GSH) Activity

The reduced glutathione (GSH) activity was determined according to the method of Ellman et al [198]. The principle of this experiment relies on the 5,5-dithiobis(2-nitrobenzoic acid) (DTNB) reduction to 5-thio-2-nitrobenzoic acid (TNB) which is a yellow product by GSH activity.

To deproteinize the sample a precipitation solution was prepared by mixing appropriate amounts of glacial metaphosphoric acid, disodium EDTA ( $\text{C}_{10}\text{H}_{14}\text{N}_2\text{Na}_2\text{O}_8$ ), sodium chloride (NaCl) in distilled water. 0.3 M disodium hydrogen phosphate ( $\text{Na}_2\text{HPO}_4$ ) was prepared in distilled water. To prepare Ellman reagent, 0.02 per cent DTNB was dissolved in 1 per cent sodium citrate.

- The sample was mixed with the precipitation solution, for the blank distilled water was mixed with precipitation solution.

- The solutions were centrifuged at 3000 rpm for 30 minutes.
- The supernatant was mixed with appropriate volumes of disodium hydrogen phosphate and Ellman reagent.
- The absorbance of the yellow colored product was measured at 412 nm.

The formula indicated below was used for the calculation of the GSH activity:

$$(\mu\text{mol}/\text{mL}) = \left\{ \frac{[2 \times \text{Optical Density}]}{[0.175 \times 0.307]} \right\} \quad (3.4)$$

### 3.8.6. Determination of Glutathione S-transferase (GST) Activity

The glutathione S-transferase activity was determined according to the method of Habig et al [199]. The principle of this experiment relies on the conjugation reaction of glutathione with 1-chloro-2,4-dinitrobenzene (CDNB) substrate catalyzed by glutathione S-transferase. This conjugation is measured by an increase in absorbance.

100 mM Tris buffer was prepared and the pH was adjusted to 7.4 with HCl. 1 mM CDNB was prepared in ethanol absolute. 5 mM reduced glutathione (GSH) was prepared in distilled water.

- The sample was mixed with CDNB, GSH and tris buffer, for the blank CDNB, GSH and tris buffer were mixed.
- CDNB was added to the tubes at last to initiate the reaction.
- The increase in absorbance was measured at two time points (at 0 and 120 seconds) at 340 nm.

GST activity is expressed as  $\mu\text{molmin}^{-1} \text{mg}^{-1}$  protein. The formula indicated below was used for the calculation of the GSH activity:

$$(\mu\text{molmin}^{-1} \text{mL}^{-1}) = \left\{ (\text{Optical density } 2 - \text{optical density } 1) \times \frac{2500}{2} \right\} \quad (3.4)$$



### 3.9. WESTERN BLOTTING

#### 3.9.1. Sample Preparation

The tissues were homogenized in RIPA lysis buffer. To prepare 1 mL of complete RIPA (1X), 10  $\mu$ L PMSF solution in DMSO, 10  $\mu$ L protease inhibitor cocktail solution in DMSO, 10  $\mu$ L sodium orthovanadate solution and 1 mL RIPA Lysis buffer (1X) were mixed. For homogenization of 100 mg tissue, 0.3 mL complete RIPA buffer is required. The striata tissues were weighed out and homogenized in appropriate volume of complete RIPA (1X) with a razor blade on ice. The samples were incubated at 4°C for 30 minutes and centrifuged at 10000 g for 10 minutes at 4°C. To have a clear lysate, the supernatant was centrifuged one more time. The supernatant was stored at -20°C for further use.

#### 3.9.2. Determination of Protein Concentration (Qubit Assay)

The protein concentrations were determined using Qubit protein assay kit. To prepare working solution, 1:200 dilution of Qubit protein reagent was prepared by mixing 1  $\mu$ L of protein reagent with Qubit protein buffer for one sample. 190  $\mu$ L of working solution was mixed with 10  $\mu$ L of each standart #1 (0 ng/ $\mu$ L in TE buffer with 2 mM sodium azide), standart #2 (200 ng/ $\mu$ L in TE buffer with 2 mM sodium azide), standart #3 (400 ng/ $\mu$ L in TE buffer with 2 mM sodium azide) in Qubit assay tubes. Also 199  $\mu$ L of working solution was mixed with 1  $\mu$ L of each sample. The final volumes of all tubes were 200  $\mu$ L. All tubes were vortexed and incubated at room temperature for 15 minutes. Qubit 2.0 Fluorometer was calibrated with standart #1, standart #2, standart #3 solutions and then the concentrations of the proteins were measured.

The formula indicated below was used for the calculation of the protein concentration which is expressed as  $\mu$ g/mL. (QF value means the value given by the Qubit 2.0 Fluorometer and x stands for the number of  $\mu$ L of sample added to the tube.

$$(\text{Concentration of the sample}) = \{ QF \text{ value} \times (200/x) \} \quad (3.6)$$

### 3.9.3. Sodium Dodecyl Sulfate Polyacrylamide Gel Electrophoresis (SDS-PAGE)

The proteins were separated using sodium dodecyl sulfate polyacrylamide gel electrophoresis (SDS-PAGE). To prepare reduced samples, 2.5  $\mu$ L NuPAGE LDS (lithium dodecyl sulfate) sample buffer (4X), 1  $\mu$ L NuPAGE reducing agent (10X) and appropriate volume of sample were mixed and the total volume was completed to 10  $\mu$ L with distilled water. The sample solution was heated at 70°C for 10 minutes. To prepare 1X MES SDS running buffer, 50 mL 20X NuPAGE MES SDS running buffer was mixed with 950 mL distilled water.

The electrophoresis was performed with XCell SureLock Mini-Cell. The combs were removed and NuPAGE Novex Bis Tris Gels (Table 3.3) were oriented in the Mini-Cell tank.

Table 3.3. NuPAGE Novex Bis Tris Gels (1.0 mm, 12 well) properties.

Gel Type	Formulation	Stacking Gel	Separating Gel	pH
NuPAGE Novex Bis-Tris Gels	Bis-Tris-HCl buffer (pH 6.4), Acrylamide, Bis-acrylamide, APS, Ultrapure water	4 per cent	10 per cent, 12 per cent, 4-12 per cent	7.0

The upper and lower buffer chambers of XCell SureLock Mini-Cell were filled with 1X SDS running buffer. 0.5 mL antioxidant was added to the XCell SureLock Mini-Cell to prevent reoxidation of the proteins during electrophoresis. The wells of the gels were washed with running buffer containing antioxidant. 5  $\mu$ L Color Protein Standard (11-245 kDa) (Figure 3.7) and 15  $\mu$ L reduced sample were loaded onto the gels. The proteins were run at 200 V constant for 25 minutes.

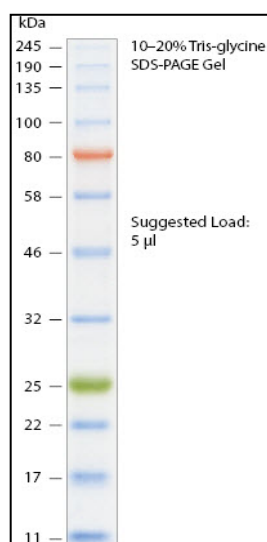


Figure 3.7. Color Prestained Protein Standard, Broad Range (11-245 kDa) New England Biolabs

#### 3.9.4. Blotting

iBLOT 2 Dry Blotting System and iBLOT transfer stack (PVDF) were used to transfer proteins from gels to the membranes. To prepare 1X TBS-T (Tris Buffered Saline plus Tween 20) washing solution, 20 mM Tris-HCL (pH 7.4) was mixed with 0.05 per cent Tween 20.

The gels were removed from XCell SureLock Mini-Cell and opened with the help of Gel knife and immersed in distilled water. iBLOT PVDF Anode Stack Bottom regular package was opened and placed onto iBLOT 2 Dry Blotting System. PVDF membrane was placed on Bottom stock. The pre-run gel was placed on the membrane. Then iBLOT filter paper was soaked in distilled water and placed on the gel. The air bubbles between the PVDF membrane and the gel were removed with the Blotting roller. iBLOT cathode stack was opened and placed on top of the filter paper (Figure 3.8). iBLOT 2 Dry Blotting System was run for 7 minutes. The PVDF membranes were immediately placed into plastic dishes containing 1X TBS-T to avoid drying and the gels were stained with Coomassie blue to check whether the proteins transferred to the membranes or not.

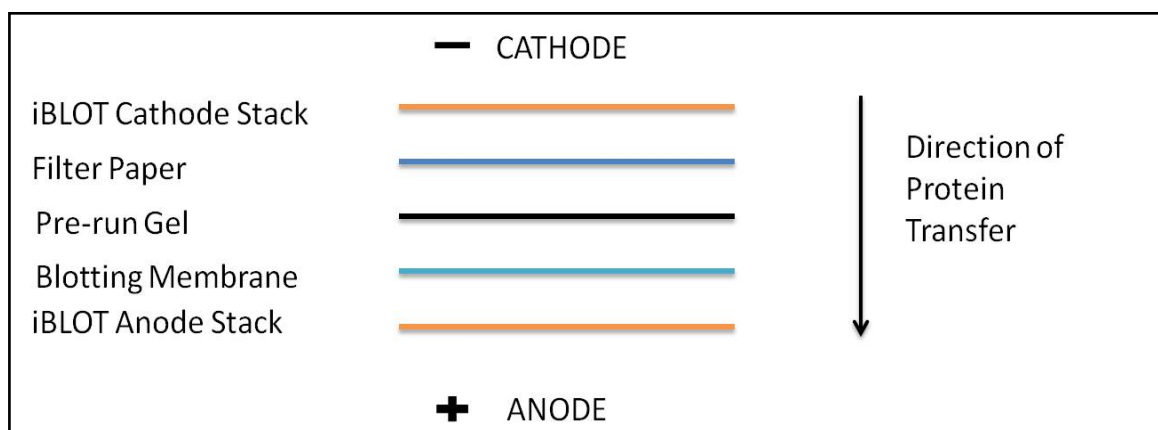


Figure 3.8. Schematic representation of blotting

### 3.9.5. Immunostaining

To avoid nonspecific binding of primary antibody, the membranes were incubated in 5 per cent non-fat dry milk solution (5 g dry milk was dissolved in 100 mL TBS-T) for 1 hour at room temperature on a shaker. The membranes were incubated in 1:2000 dilution (prepared in 5 per cent dry milk) of the anti-acetyl-histone H3 (Lys9) or Pathscan Multiplex Western Cocktail II primary antibodies overnight at 4°C on a shaker. The membranes were washed in TBS-T solution 3 times each for 5 minutes. Then the membranes were incubated in 1:5000 dilution (prepared in 5 per cent dry milk) of secondary antibody solution (Anti-rabbit IgG HRP-linked antibody) for 1 hour at room temperature on a shaker. Finally the membranes were washed with TBS-T three times for five minutes each.

### 3.9.6. Imaging

1000  $\mu$ L Lumigen TMA A solution was mixed with 1000  $\mu$ L Lumigen TMA B solution and diluted 1:1 in distilled water. The membranes were incubated in this solution for one minute at room temperature. Protein loading was controlled with  $\beta$ -actin antibody (rabbit). The blots were examined with a computer-based gel imaging instrument (DNR). The protein bands were examined with Image J software (NIH).

### 3.10. STATISTICS

PASW Statistics 18.0 (formerly SPSS Statistics) package program was used for the statistical analysis of the experiments. Mean $\pm$ SEM values were calculated for all data. Statistical significance was set at  $p < 0.05$ . For the locomotor activity parameters (distance travelled, stereotypic activity, ambulatory activity, horizontal activity, vertical activity) the differences between groups were analyzed with one-way Anova followed by Least Significant Difference (LSD) post-hoc test for multiple comparisons. Furthermore, for the apomorphine induced rotation test, the differences between groups were analyzed with one-way Anova followed by Least Significant Difference (LSD) post-hoc test for multiple comparisons. Immunohistochemistry for tyrosine hydroxylase and TUNEL assay data were analyzed using one-way Anova followed by Least Significant Difference (LSD) post-hoc test. All oxidative stress parameters (lipid peroxide level, superoxide dismutase activity, reduced glutathione activity and glutathione S-transferase activity) were analyzed with one-way Anova followed by Least Significant Difference (LSD) post-hoc test. Similarly all western blot data were analyzed with one-way Anova followed by Least Significant Difference (LSD) post-hoc test.

## 4. RESULTS

### 4.1. APOMORPHINE INDUCED ROTATION TEST

Apomorphine induced rotation test was performed in order to control the validity of the model. When the dopaminergic neurons die unilaterally in substantia nigra pars compacta, the animals demonstrate a rotational behavior contralateral to the lesion side. The number of the rotations give a clue about the severity of the model. Apomorphine induced rotation test was performed after the operation and at the end of drug treatment (Figure 4.1).

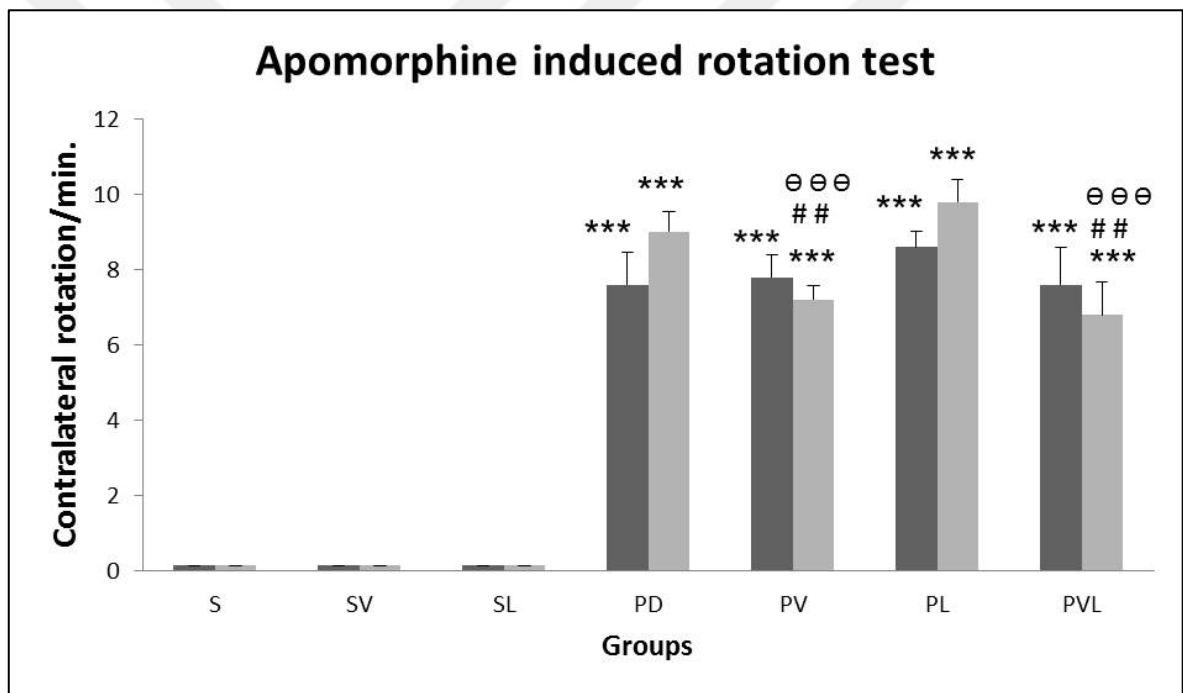


Figure 4.1. Graphs comparing apomorphine induced rotational behavior of the animals. Sham operated (S), Sham operated and VPA treated (SV), Sham operated and L-DOPA treated (SL), Nigraly 6-OHDA injected (PD), Nigraly 6-OHDA injected and VPA treated (PV), Nigraly 6-OHDA injected and L-DOPA treated (PL), Nigraly 6-OHDA injected and VPA and L-DOPA treated (PVL) groups. Data are presented as contralateral rotations per minute. Data are expressed as mean  $\pm$  SEM (\*\* $p < 0.001$  compared with S, SV and SL groups,  $###p < 0.01$ .  $####p < 0.001$  compared with PD group,  $####p < 0.001$  compared with PL group).

Sham operated groups did not show any rotational behavior. After the operation all of the 6-OHDA lesioned animals showed similar pronounced rotational behavior as compared with the sham operated control animals ( $p < 0.001$ ). After drug treatment, in PV group rotational behavior is slightly decreased as compared with PD and PL groups ( $p < 0.01$  and  $p < 0.001$  respectively). Similarly, in PVL group rotational behavior significantly decreased as compared with PD and PL groups ( $p < 0.01$  and  $p < 0.001$  respectively).

## **4.2. HISTOLOGY**

Tyrosine hydroxylase positive neurons were counted in both left and right substantia nigra pars compacta. TUNEL positive neurons were counted in both left and right substantia nigra pars compacta as well. In addition, in order to see general histopathological changes and the anatomical structure of the substantia nigra pars compacta, hematoxylin and eosin and cresyl violet stainings were performed.

### **4.2.1. Immunohistochemistry for Tyrosine Hydroxylase**

Coronal sections from all of the groups were analyzed for tyrosine hydroxylase immunoreactive neurons. Immunohistochemistry for tyrosine hydroxylase gives reliable data on the number of dopaminergic neurons. Photomicrographs demonstrate sections taken from right substantia nigra pars compacta stained with Tyrosine Hydroxylase (Figure 4.2).

The number of tyrosine hydroxylase positive neurons was not different between S, SV and SL groups. There was a pronounced loss of tyrosine hydroxylase positive neurons in 6-OHDA lesioned right substantia nigra pars compacta in PD group as compared to sham-operated groups ( $p < 0.001$ ). VPA treatment significantly increased the number of tyrosine hydroxylase positive neurons in PV group as compared to PD group ( $p < 0.001$ ) and PL group ( $p < 0.01$ ). However, the numbers of tyrosine hydroxylase positive neurons were still significantly lower in PV group as compared to S, SV and SL groups ( $p < 0.001$ ). The number of tyrosine hydroxylase positive neurons was not different between PD and PL groups. (Figure 4.3).

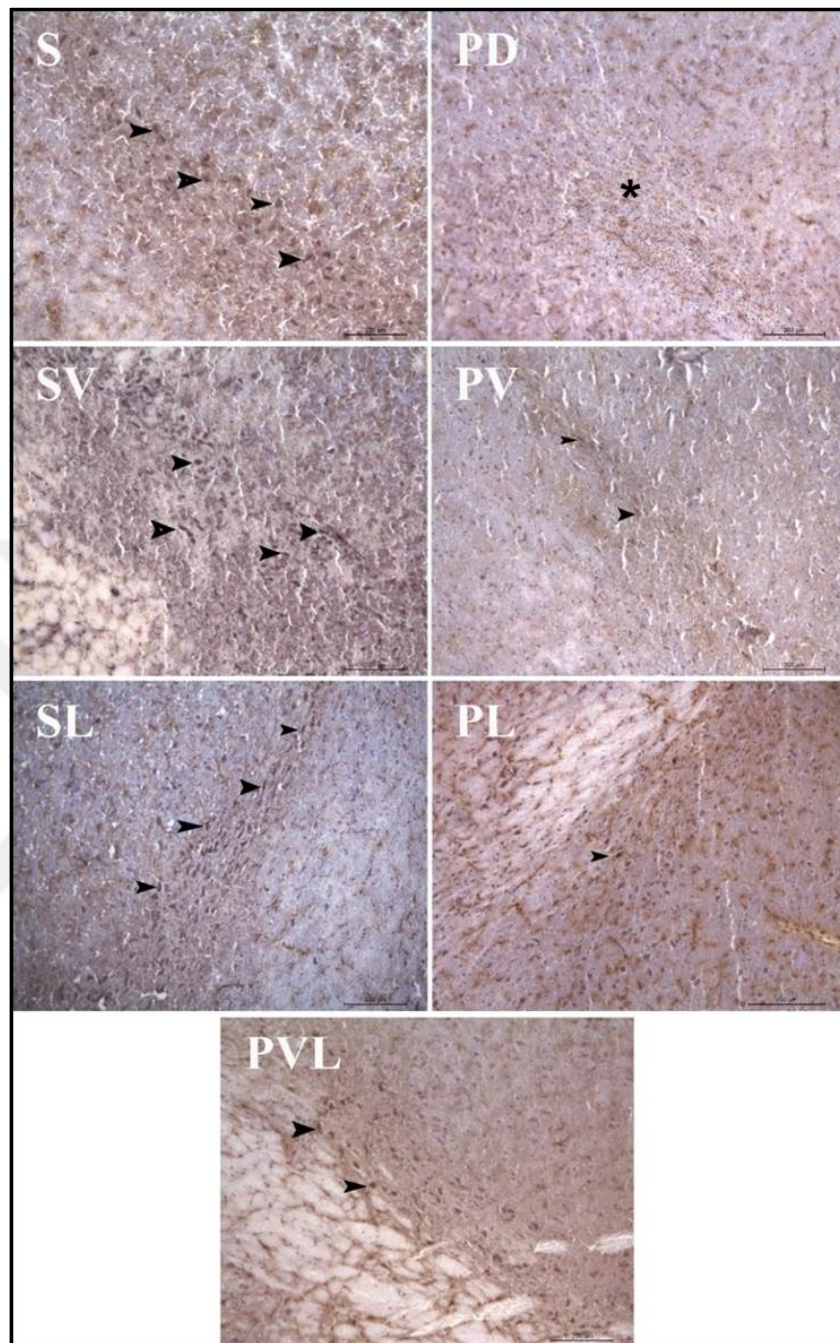


Figure 4.2. Photomicrographs demonstrate Tyrosine Hydroxylase immunoreactivity in right substantia nigra pars compacta. Sham operated (S), Sham operated and VPA treated (SV), Sham operated and L-DOPA treated (SL), Nigraly 6-OHDA injected (PD), Nigraly 6-OHDA injected and VPA treated (PV), Nigraly 6-OHDA injected and L-DOPA treated (PL), Nigraly 6-OHDA injected and VPA and L-DOPA treated (PVL) groups.

Dopaminergic neuron is demonstrated with arrow and mononuclear cell infiltration star.

The magnification is x20. Scale bar represents 200 µm.



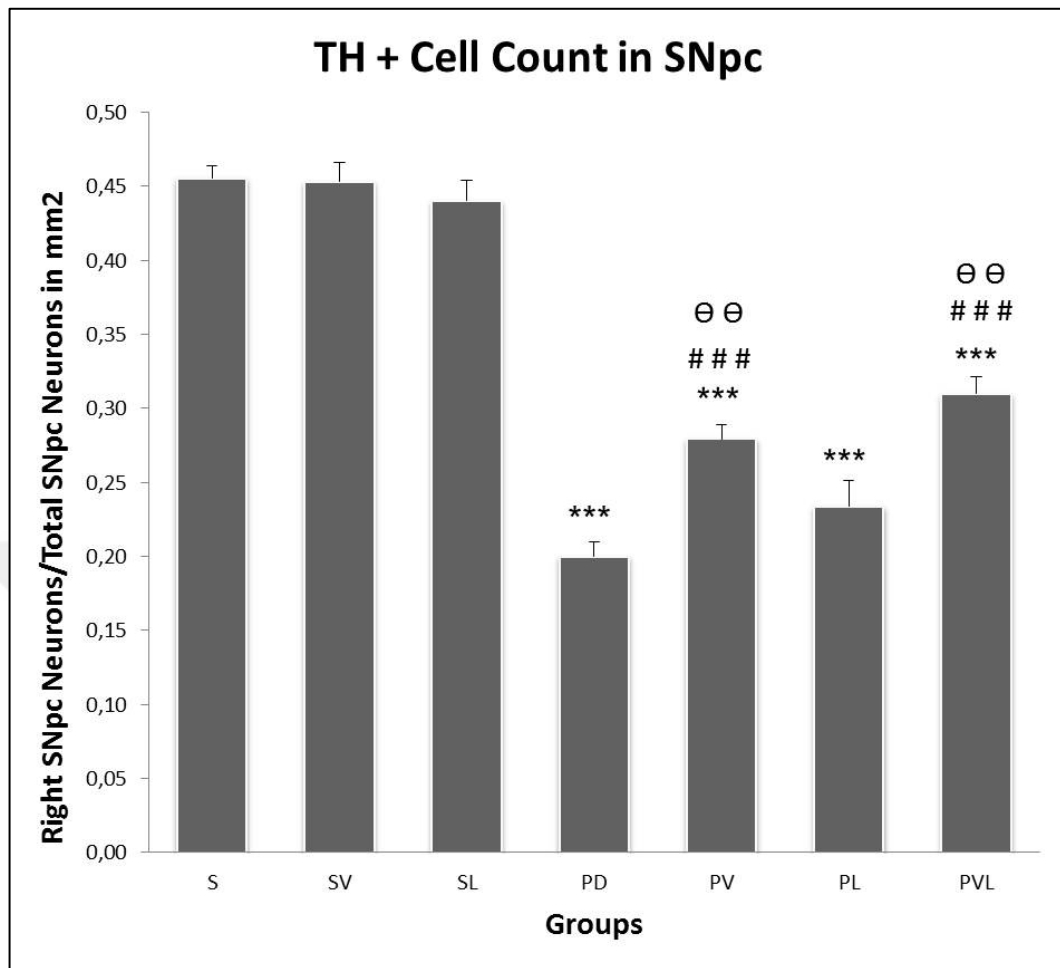


Figure 4.3. Graphs comparing Tyrosine Hydroxylase immunoreactivity in right substantia nigra pars compacta. Sham operated (S), Sham operated and VPA treated (SV), Sham operated and L-DOPA treated (SL), Nigraly 6-OHDA injected (PD), Nigraly 6-OHDA injected and VPA treated (PV), Nigraly 6-OHDA injected and L-DOPA treated (PL), Nigraly 6-OHDA injected and VPA and L-DOPA treated (PVL) groups. Data are presented as percentage of right substantia nigra pars compacta neurons compared to total neurons in right and left substantia nigra pars compacta. Data are expressed as mean  $\pm$  SEM. \*\*\* $p < 0.001$  vs S, SV, SL; ### $p < 0.001$  vs PD;  $\Theta\Theta$  $p < 0.01$  v PL.

#### 4.2.2. TUNEL Assay

Coronal sections from all of the groups were analyzed for TUNEL positive neurons. TUNEL assay gives reliable data on the number of apoptotic neurons. Photomicrographs demonstrate sections taken from right substantia nigra pars compacta (Figure 4.4).

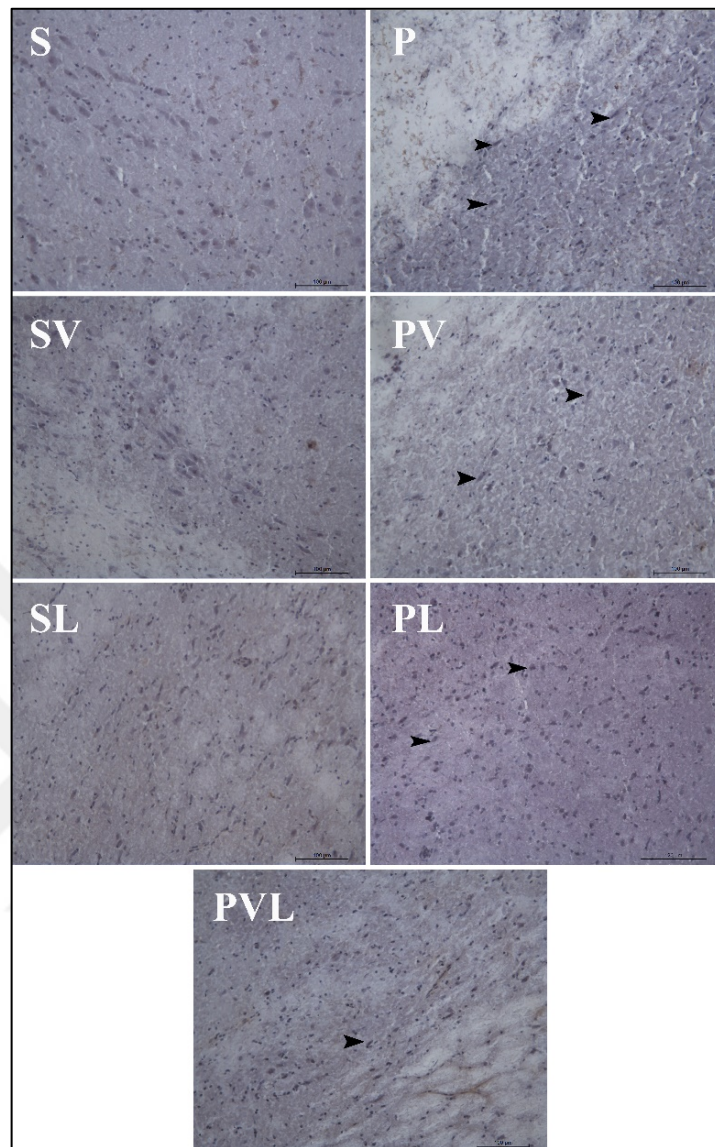


Figure 4.4. Photomicrographs demonstrate TUNEL positive neurons in right substantia nigra pars compacta. Sham operated (S), Sham operated and VPA treated (SV), Sham operated and L-DOPA treated (SL), Nigraly 6-OHDA injected (PD), Nigraly 6-OHDA injected and VPA treated (PV), Nigraly 6-OHDA injected and L-DOPA treated (PL), Nigraly 6-OHDA injected and VPA and L-DOPA treated (PVL) groups. Apoptotic neuron (TUNEL positive neuron) is demonstrated with arrow. The magnification is x20. Scale bar represents 100  $\mu\text{m}$ .

The number of TUNEL positive neurons was not different in substantia nigra pars compacta of the animals between S, SV, SL groups. 6-OHDA injection into the substantia nigra pars compacta induced apoptosis in PD group as compared to all other groups

( $p < 0.001$ ). Valproic acid treatment significantly attenuated 6-OHDA induced apoptosis in PV and PVL groups as compared to PD group ( $p < 0.001$ ). However, the number of TUNEL positive neurons was still higher in PV group as compared to S and SV groups ( $p < 0.001$ ) (Figure 4.5).

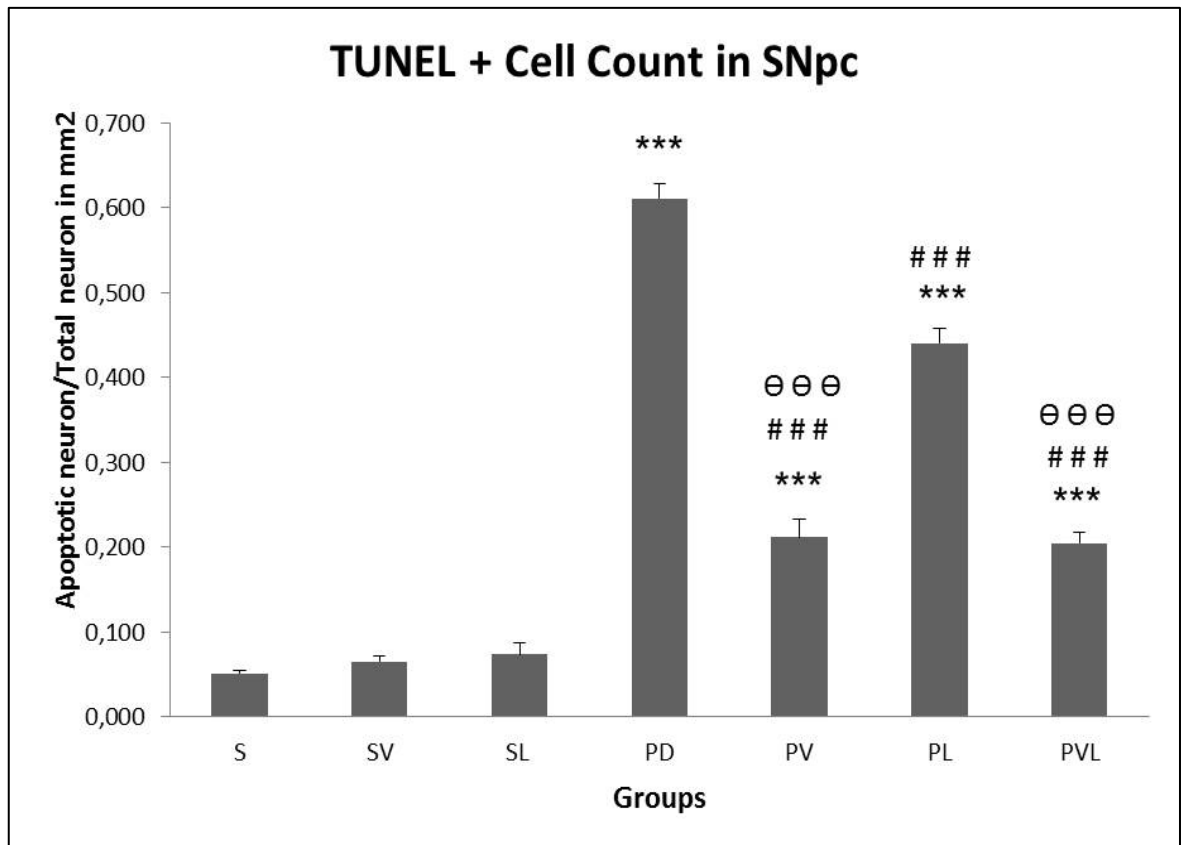


Figure 4.5. Graphs comparing TUNEL positive neurons in right substantia nigra pars compacta. Sham operated (S), Sham operated and VPA treated (SV), Sham operated and L-DOPA treated (SL), Nigraly 6-OHDA injected (PD), Nigraly 6-OHDA injected and VPA treated (PV), Nigraly 6-OHDA injected and L-DOPA treated (PL), Nigraly 6-OHDA injected and VPA and L-DOPA treated (PVL) groups. Data are presented as percentage of apoptotic neurons in right substantia nigra pars compacta compared to total neurons in right substantia nigra pars compacta. Data are expressed as mean  $\pm$  SEM. \*\*\* $p < 0.001$  vs S, SV, SL; ### $p < 0.001$  vs PD; ### $p < 0.001$  vs PL.

### 4.2.3. Hematoxylin Eosin and Cresyl Violet Stainings

Hematoxylin Eosin and cresyl violet stainings were performed in order to histopathologically examine the tissues (Figure 4.6 and Figure 4.7).

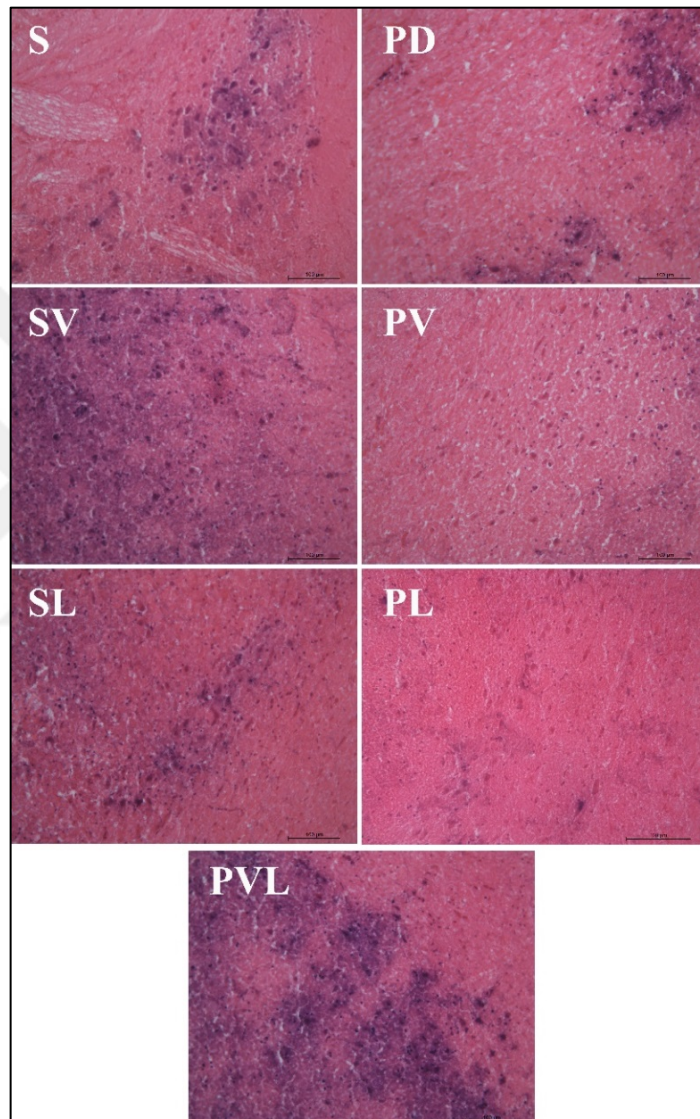


Figure 4.6. Photomicrographs demonstrate Hematoxylin Eosin staining in right substantia nigra pars compacta. Sham operated (S), Sham operated and VPA treated (SV), Sham operated and L-DOPA treated (SL), Nigraly 6-OHDA injected (PD), Nigraly 6-OHDA injected and VPA treated (PV), Nigraly 6-OHDA injected and L-DOPA treated (PL), Nigraly 6-OHDA injected and VPA and L-DOPA treated (PVL) groups. The magnification is x20. Scale bar represents 100  $\mu\text{m}$ .

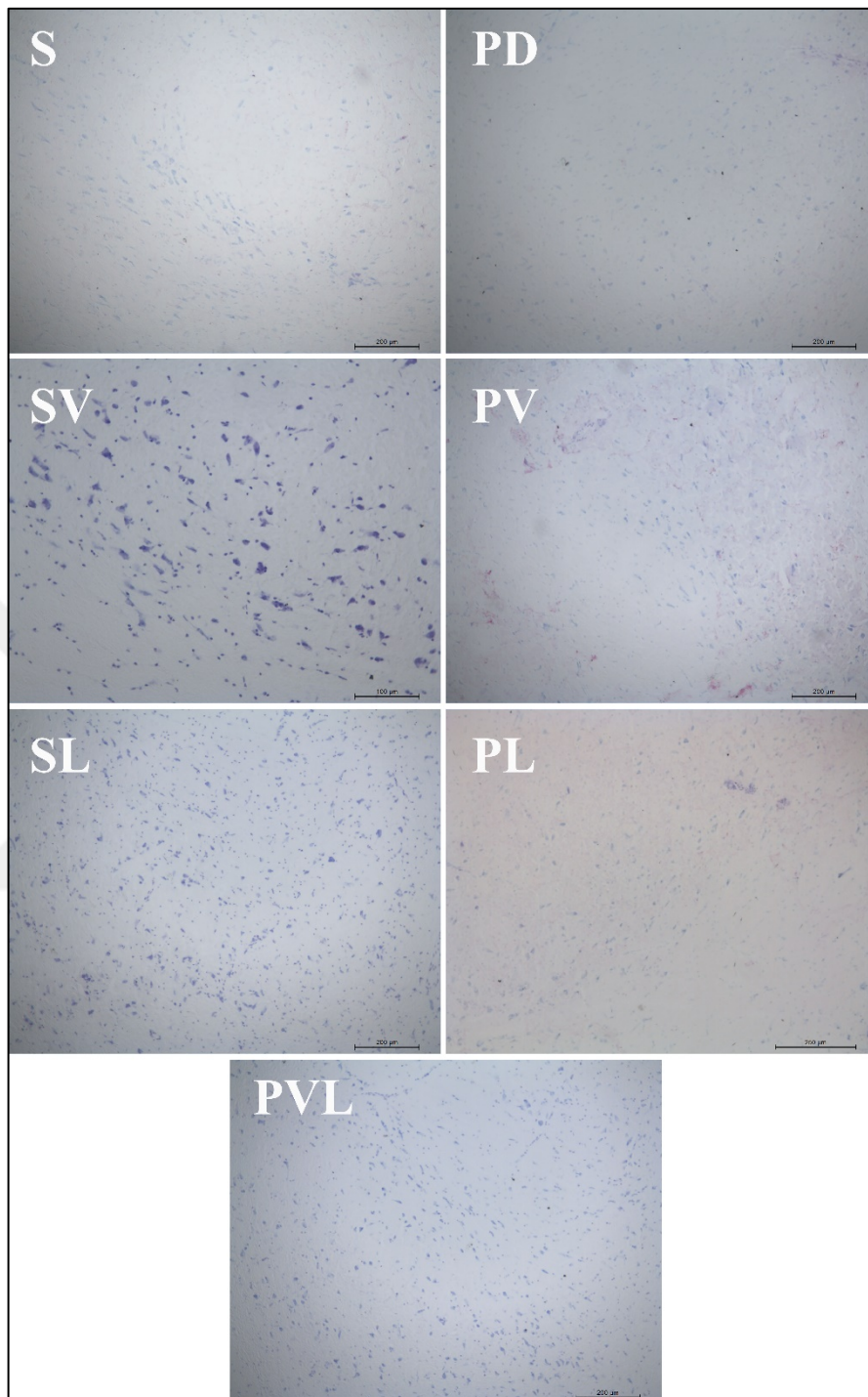


Figure 4.7. Photomicrographs demonstrate cresyl violet staining in right substantia nigra pars compacta. Sham operated (S), Sham operated and VPA treated (SV), Sham operated and L-DOPA treated (SL), Nigraly 6-OHDA injected (PD), Nigraly 6-OHDA injected and VPA treated (PV), Nigraly 6-OHDA injected and L-DOPA treated (PL), Nigraly 6-OHDA injected and VPA and L-DOPA treated (PVL) groups. The magnification is x10.

Scale bar represents 200 μm.

The coronal sections from substantia nigra pars compacta were examined in terms of histopathology, morphology and inflammatory cell infiltration. In 6-OHDA lesioned PD group there was a pronounced inflammatory cell infiltration clearly seen in tyrosine hydroxylase immunohistochemistry, was not seen in sham operated control groups. In addition, cross sections revealed that, in 6-OHDA lesioned groups higher number of glial cells were observed as compared with sham operated control groups.

### **4.3. SPONTANEOUS LOCOMOTOR ACTIVITY**

To examine the effects of valproic acid on motor activity of the animals, locomotor activities of the animals were measured with a motor activity monitoring system. Stereotypic, ambulatory, vertical, horizontal motor activities and distance travelled by the animal were measured.

#### **4.3.1. Distance Travelled**

The distance travelled by the animals did not differ between groups before the operation. In the last measurement before decapitation of the animals, in SL group levodopa treatment slightly increased locomotor activity according to the S group. On the contrary, in SV group valproic acid treatment decreased locomotor activity as compared with S group. In the last measurement before decapitation of the animals, the distance travelled by the animal was significantly decreased in PD group as compared with the S group ( $p < 0.01$ ). Although valproic acid treatment in PV group slightly increased the distance travelled by animals compared with PD group, it is still significantly lower than S group ( $p < 0.05$ ). Though there is no statistical significance, the distance travelled by the animals was higher in PL and PVL groups as compared with the PD and PV groups (Figure 4.8).

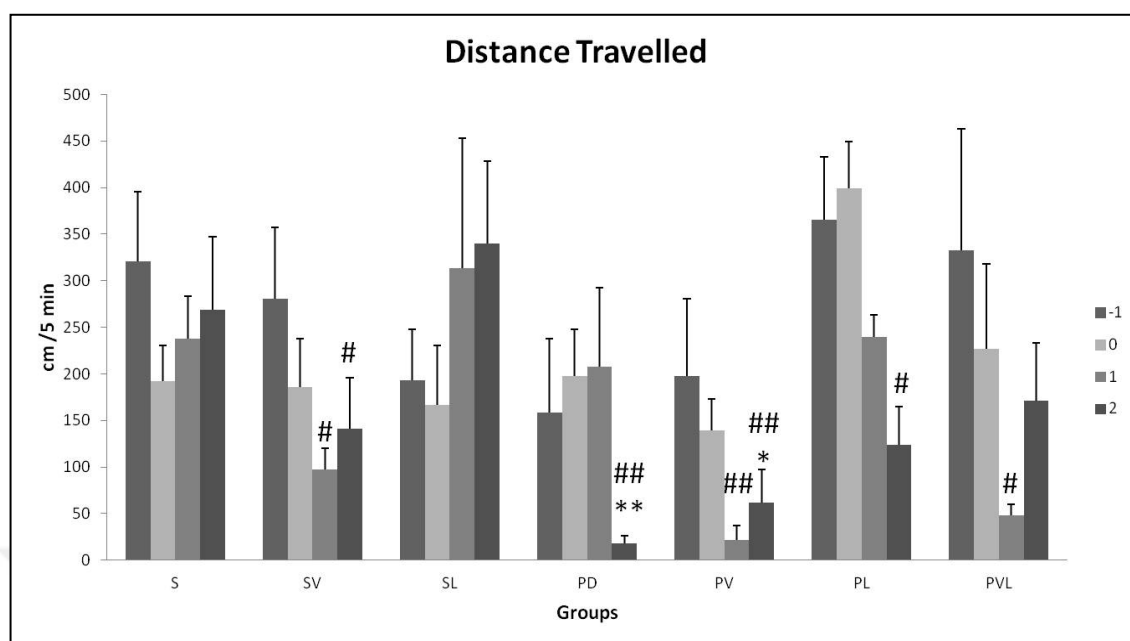


Figure 4.8. Graphs comparing distance traveled by the animals. Sham operated (S), Sham operated and VPA treated (SV), Sham operated and L-DOPA treated (SL), Nigrally 6-OHDA injected (PD), Nigrally 6-OHDA injected and VPA treated (PV), Nigrally 6-OHDA injected and L-DOPA treated (PL), Nigrally 6-OHDA injected and VPA and L-DOPA treated (PVL) groups. Data are presented as centimeter of distance travelled by the animal in 5 minutes. Data are expressed as mean  $\pm$  SEM (\* $p$ <0.05, \*\* $p$ <0.01 compared with S group, # $p$ <0.05 ## $p$ <0.01 compared with SL group).

#### 4.3.2. Stereotypic Activity

The stereotypic activity did not differ between groups before the operation. In the last measurement before decapitation of the animals, the stereotypic activity was significantly decreased in PD group as compared with the S group, SV group and SL group ( $p$ <0.05,  $p$ <0.05 and  $p$ <0.01 respectively). Similarly the stereotypic activity in PV group was lower than S group, SV group and SL group ( $p$ <0.05,  $p$ <0.05 and  $p$ <0.01 respectively). On the other hand, valproic acid treatment did not make a significant difference for stereotypic activity between PV and PD groups. Though there is no statistical significance, the stereotypic activity of the animals was higher in PL and PVL groups as compared with the PD and PV groups (Figure 4.9).

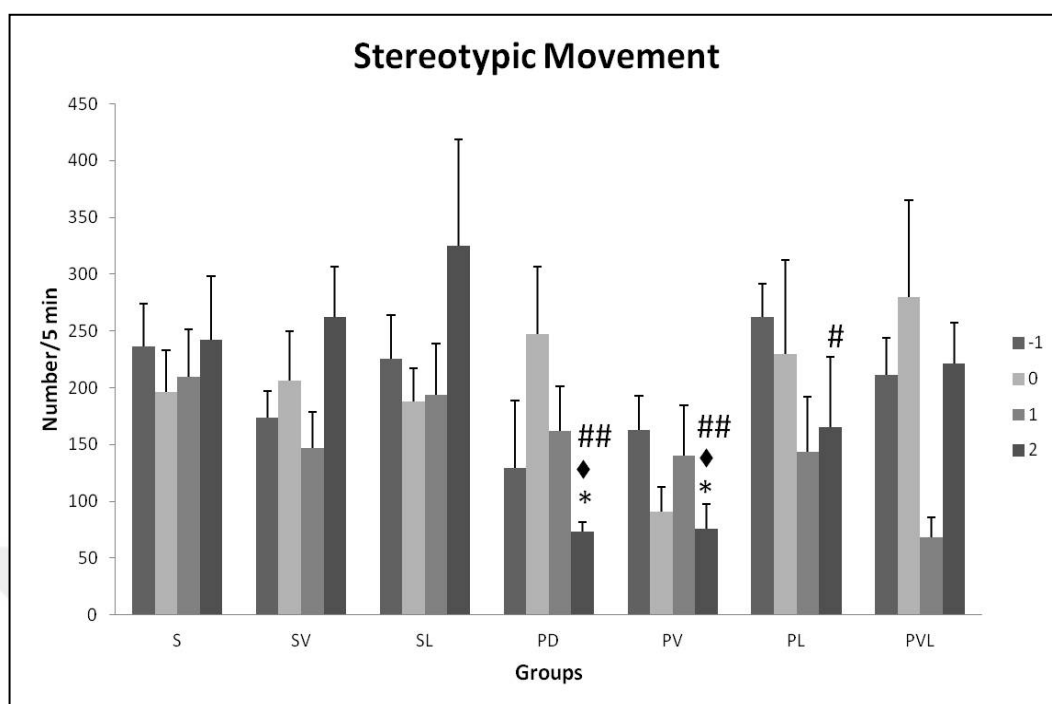


Figure 4.9. Graphs comparing stereotypic movement of animals. Sham operated (S), Sham operated and VPA treated (SV), Sham operated and L-DOPA treated (SL), Nigrally 6-OHDA injected (PD), Nigrally 6-OHDA injected and VPA treated (PV), Nigrally 6-OHDA injected and L-DOPA treated (PL), Nigrally 6-OHDA injected and VPA and L-DOPA treated (PVL) groups. Data are presented as number of stereotypic movement in 5 minutes. Data are expressed as mean  $\pm$  SEM (\* $p$ <0.05 compared with S group, \* $p$ <0.05 compared with SV group, # $p$ <0.05 ## $p$ <0.01 compared with SL group).

### 4.3.3. Ambulatory Activity

The ambulatory activity did not differ between groups before the operation. In the last measurement before decapitation of the animals, the ambulatory activity was significantly decreased in PD group as compared with the S group and SL group ( $p$ <0.01 and  $p$ <0.01 respectively). Although valproic acid treatment in PV group slightly increased the ambulatory activity compared with PD group, it is still significantly lower than S group and SL group ( $p$ <0.05 and  $p$ <0.05 respectively). Though there is no statistical significance, the ambulatory activity of the animals was higher in PL and PVL groups as compared with the PD and PV groups (Figure 4.10).



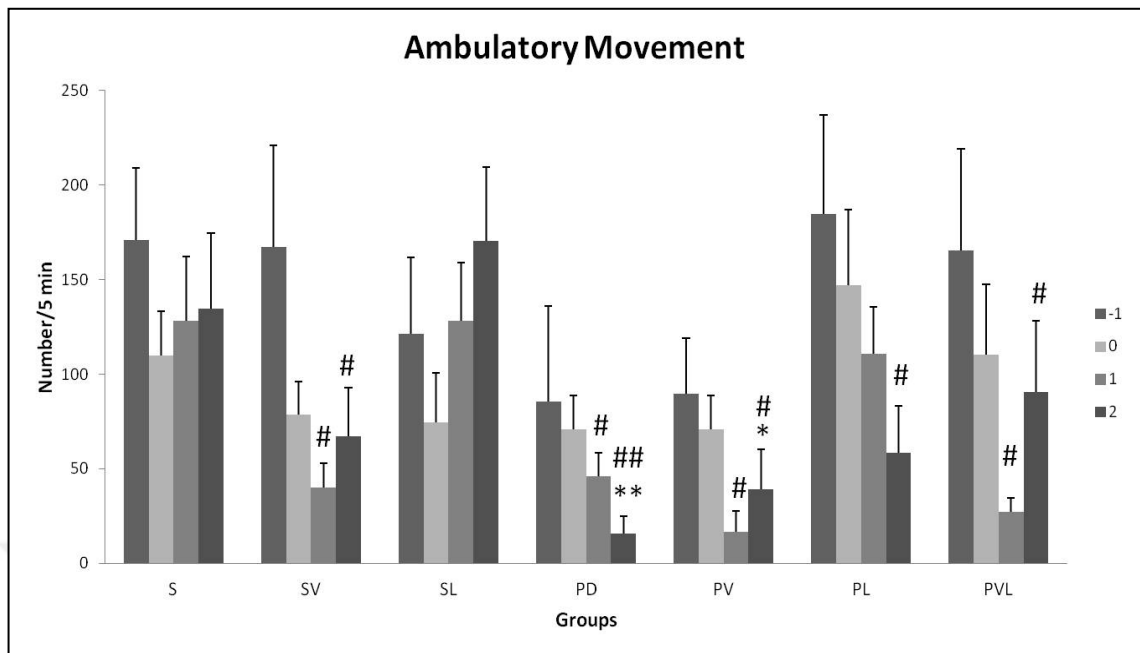


Figure 4.10. Graphs comparing ambulatory movement of animals. Sham operated (S), Sham operated and VPA treated (SV), Sham operated and L-DOPA treated (SL), Nigraly 6-OHDA injected (PD), Nigraly 6-OHDA injected and VPA treated (PV), Nigraly 6-OHDA injected and L-DOPA treated (PL), Nigraly 6-OHDA injected and VPA and L-DOPA treated (PVL) groups. Data are presented as number of ambulatory movement in 5 minutes. Data are expressed as mean  $\pm$  SEM (\* $p$ <0.05, \*\* $p$ <0.01 compared with S group, # $p$ <0.05 ## $p$ <0.01 compared with SL group).

#### 4.3.4. Horizontal Activity

The horizontal activity did not differ between groups before the operation. In the last measurement before decapitation of the animals, the horizontal activity was significantly decreased in PD group as compared with the S group and SL group ( $p$ <0.05 and  $p$ <0.01 respectively). Similarly the horizontal activity in PV group was lower than S group and SL group ( $p$ <0.05 and  $p$ <0.01 respectively). On the other hand, valproic acid treatment did not make a significant difference for horizontal activity between PV and PD groups. Though there is no statistical significance, the horizontal activity of the animals was higher in PL and PVL groups as compared with the PD and PV groups (Figure 4.11).

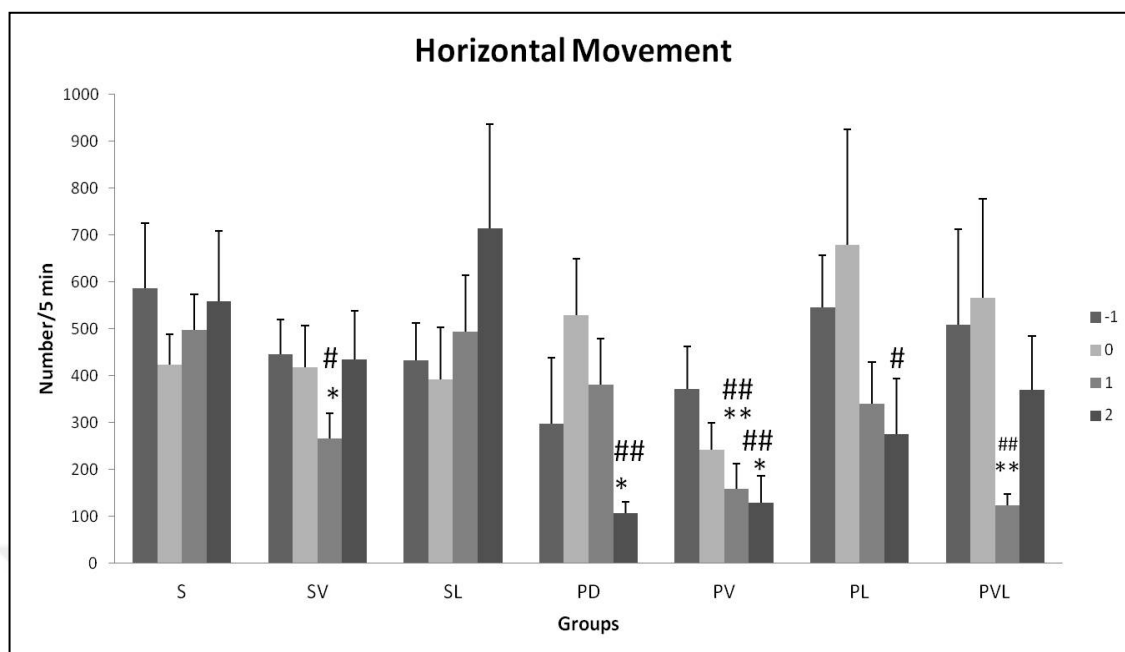


Figure 4.11. Graphs comparing horizontal movement of animals. Sham operated (S), Sham operated and VPA treated (SV), Sham operated and L-DOPA treated (SL), Nigraly 6-OHDA injected (PD), Nigraly 6-OHDA injected and VPA treated (PV), Nigraly 6-OHDA injected and L-DOPA treated (PL), Nigraly 6-OHDA injected and VPA and L-DOPA treated (PVL) groups. Data are presented as number of horizontal movement in 5 minutes. Data are expressed as mean  $\pm$  SEM (\* $p$ <0.05, \*\* $p$ <0.01 compared with S group, # $p$ <0.05 ## $p$ <0.01 compared with SL group).

#### 4.3.5. Vertical Activity

The vertical activity did not differ between groups before the operation. In the last measurement before decapitation of the animals, the vertical activity was significantly decreased in PD group as compared with the SL group ( $p$ <0.05). Similarly the vertical activity in PV group was lower than SL group ( $p$ <0.05). On the other hand, valproic acid treatment did not make a significant difference for vertical activity between PV and PD groups. Though there is no statistical significance, the vertical activity of the animals was higher in PL and PVL groups as compared with the PV group (Figure 4.12).

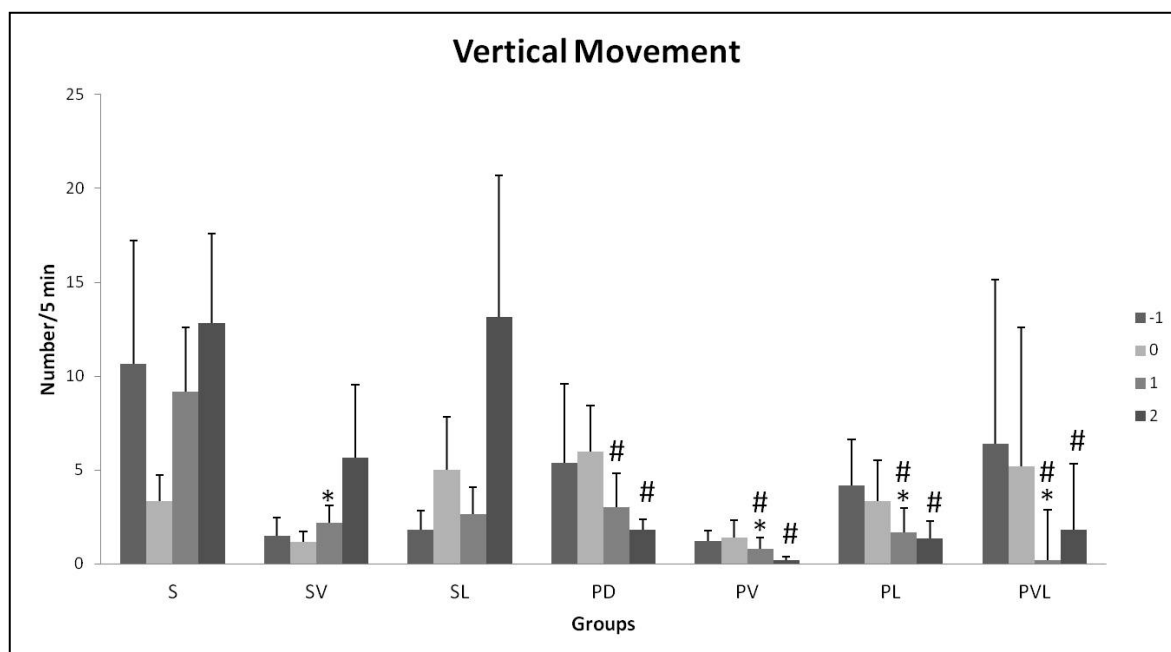


Figure 4.12. Graphs comparing vertical movement of animals. Sham operated (S), Sham operated and VPA treated (SV), Sham operated and L-DOPA treated (SL), Nigraly 6-OHDA injected (PD), Nigraly 6-OHDA injected and VPA treated (PV), Nigraly 6-OHDA injected and L-DOPA treated (PL), Nigraly 6-OHDA injected and VPA and L-DOPA treated (PVL) groups. Data are presented as number of vertical movement in 5 minutes. Data are expressed as mean  $\pm$  SEM (\* $p < 0.05$  compared with S group, # $p < 0.05$  compared with SL group.)

#### 4.4. BIOCHEMICAL ANALYSIS OF OXIDATIVE STRESS

Oxidative stress is strongly implicated in PD pathogenesis. In addition, it is well established that 6-hydroxydopamine kills dopaminergic neurons via increasing reactive oxygen species and decreasing the activities of anti-oxidant systems. Therefore, in this study lipid peroxide levels, superoxide dismutase, reduced glutathione and glutathione s-transferase activities were determined from striatal tissue of the animals.

#### 4.4.1. Lipid Peroxide (MDA) Level

MDA level in the striatum in the PD group was found to be higher than all of the groups ( $p < 0.001$ ). There was no difference between sham operated groups. In PV group, MDA level was decreased as compared with the PD and PL groups ( $p < 0.001$ ,  $p < 0.05$  respectively). There was no difference between PV and PVL groups. Similarly in PV group MDA levels were similar to sham operated groups (Figure 4.13).

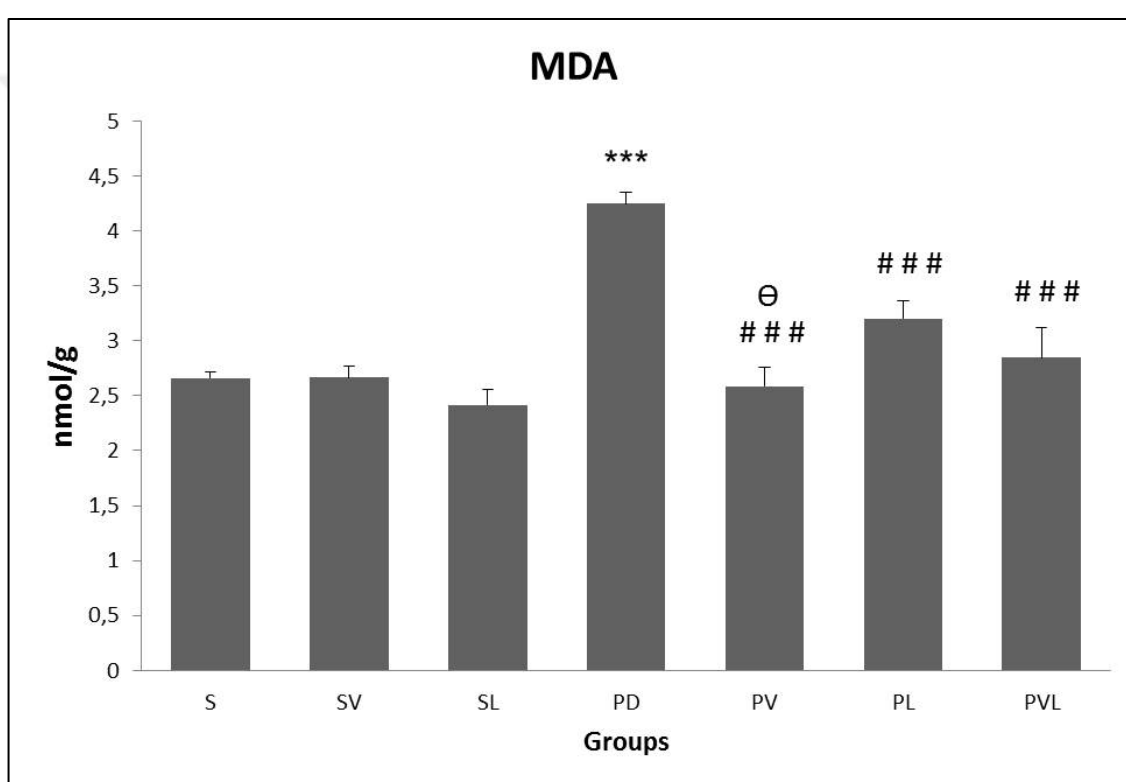


Figure 4.13. Graphs comparing MDA level in the striatum. Sham operated (S), Sham operated and VPA treated (SV), Sham operated and L-DOPA treated (SL), Nigraly 6-OHDA injected (PD), Nigraly 6-OHDA injected and VPA treated (PV), Nigraly 6-OHDA injected and L-DOPA treated (PL), Nigraly 6-OHDA injected and VPA and L-DOPA treated (PVL) groups. The data were all expressed as mean  $\pm$  SEM. One way Anova followed by LSD post-hoc test was used for statistical analysis. \*\*\* $p < 0.001$  vs S, SV, SL; ### $p < 0.001$  vs PD;  $\ominus p < 0.05$  v PL.

#### 4.4.2. Superoxide Dismutase (SOD) Activity

SOD activities in striatum in the PD group were determined to be lower than S and SV groups ( $p < 0.01$ ,  $p < 0.001$  respectively). In PV group, on the other hand, SOD activity was found to be increased as compared with the PD group ( $p < 0.01$ ). Similarly, in PL and PVL groups SOD activities were found to be increased as compared with the PD group ( $p < 0.05$ ,  $p < 0.05$  respectively). In addition, in PV group SOD activity was similar to sham operated groups (Figure 4.14).

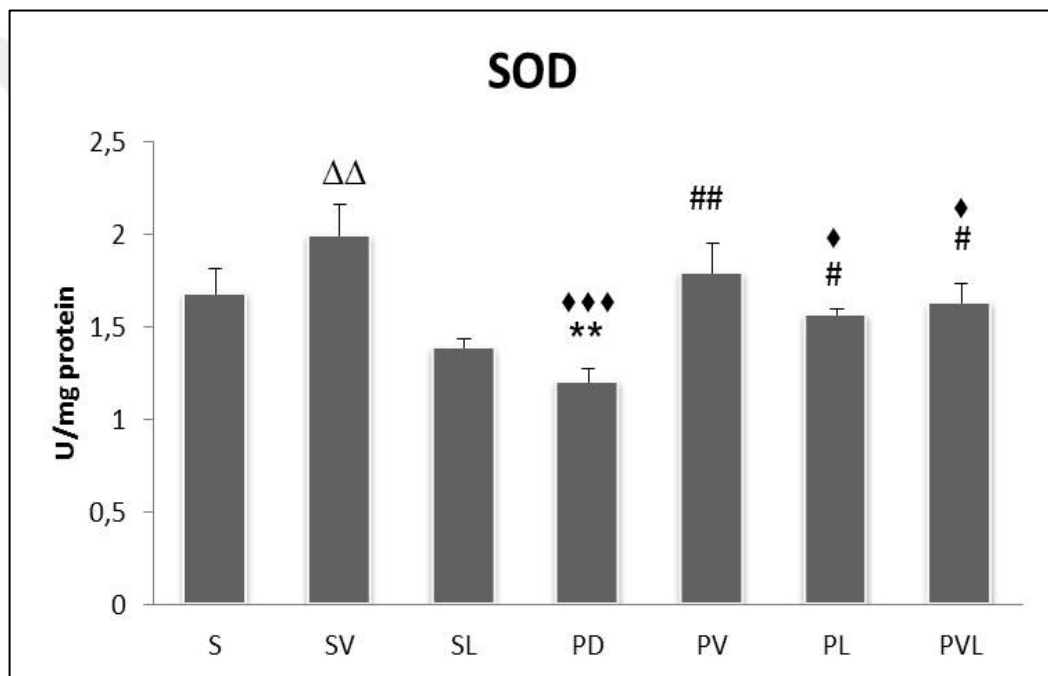


Figure 4.14. Graphs comparing SOD activity in the striatum. Sham operated (S), Sham operated and VPA treated (SV), Sham operated and L-DOPA treated (SL), Nigraly 6-OHDA injected (PD), Nigraly 6-OHDA injected and VPA treated (PV), Nigraly 6-OHDA injected and L-DOPA treated (PL), Nigraly 6-OHDA injected and VPA and L-DOPA treated (PVL) groups. The data were all expressed as mean  $\pm$  SEM. One way Anova followed by LSD post-hoc test was used for statistical analysis.  $**p < 0.01$  vs S;  $\#p < 0.05$ ,  $##p < 0.01$  vs PD;  $\blacklozenge p < 0.001$  vs SV;  $\Delta p < 0.05$ ,  $\Delta\Delta p < 0.01$  vs SL.

#### 4.4.3. Reduced Glutathione (GSH) Activity

There was no significant difference of GSH activities between sham operated groups. GSH activities in striatum in the PD group were determined to be lower than S, SV and SL groups ( $p < 0.01$ ,  $p < 0.01$ ,  $p < 0.01$  respectively). In PV and PVL groups, on the other hand, GSH activities were found to be increased as compared with the PD group ( $p < 0.05$ ,  $p < 0.01$  respectively) (Figure 4.15).

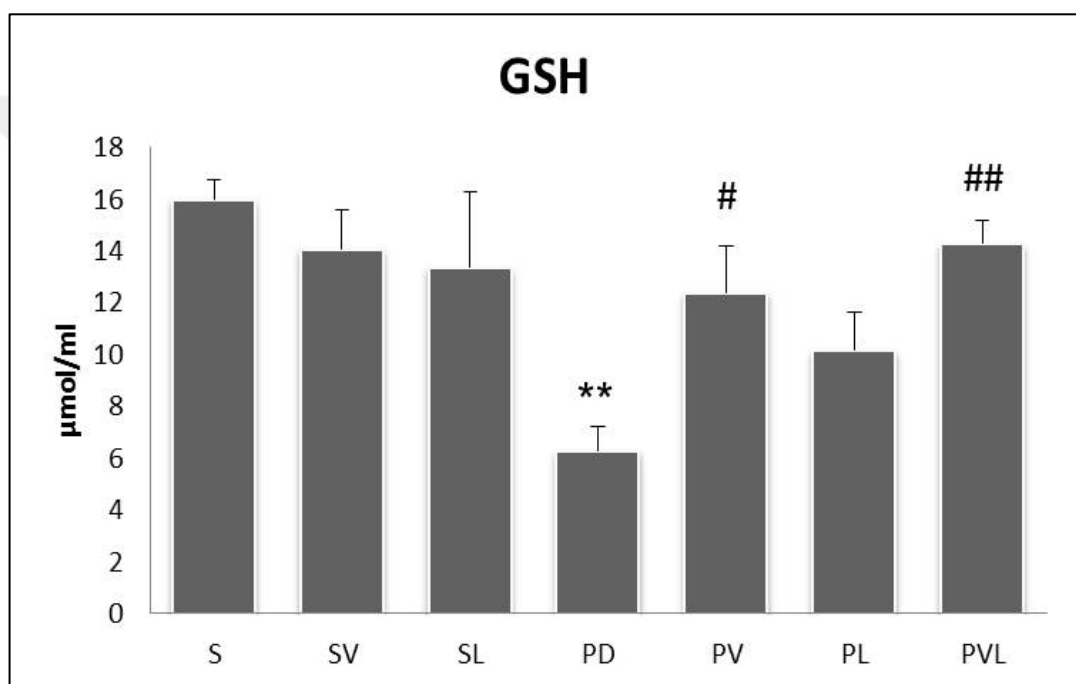


Figure 4.15. Graphs comparing GSH activity in the striatum. Sham operated (S), Sham operated and VPA treated (SV), Sham operated and L-DOPA treated (SL), Nigraly 6-OHDA injected (PD), Nigraly 6-OHDA injected and VPA treated (PV), Nigraly 6-OHDA injected and L-DOPA treated (PL), Nigraly 6-OHDA injected and VPA and L-DOPA treated (PVL) groups. The data were all expressed as mean  $\pm$  SEM. One way Anova followed by LSD post-hoc test was used for statistical analysis. \*\* $p < 0.01$  vs S, SV, SL; # $p < 0.05$ , ## $p < 0.01$  vs PD.

#### 4.4.4. Glutathione S-transferase (GST) Activity

There was no significant difference of GST activities between sham operated groups. GST activities in striatum in the PD group were determined to be lower than S and SV groups ( $p < 0.05$ ). In PV group, on the other hand, GST activities were found to be increased as compared with the PD group. ( $p < 0.01$ ). Likewise, GST activity in PV group was found to be increased as compared with the PL group. ( $p < 0.01$ ). Similarly GST activity in PV group was similar to those in sham operated groups. (Figure 4.16).

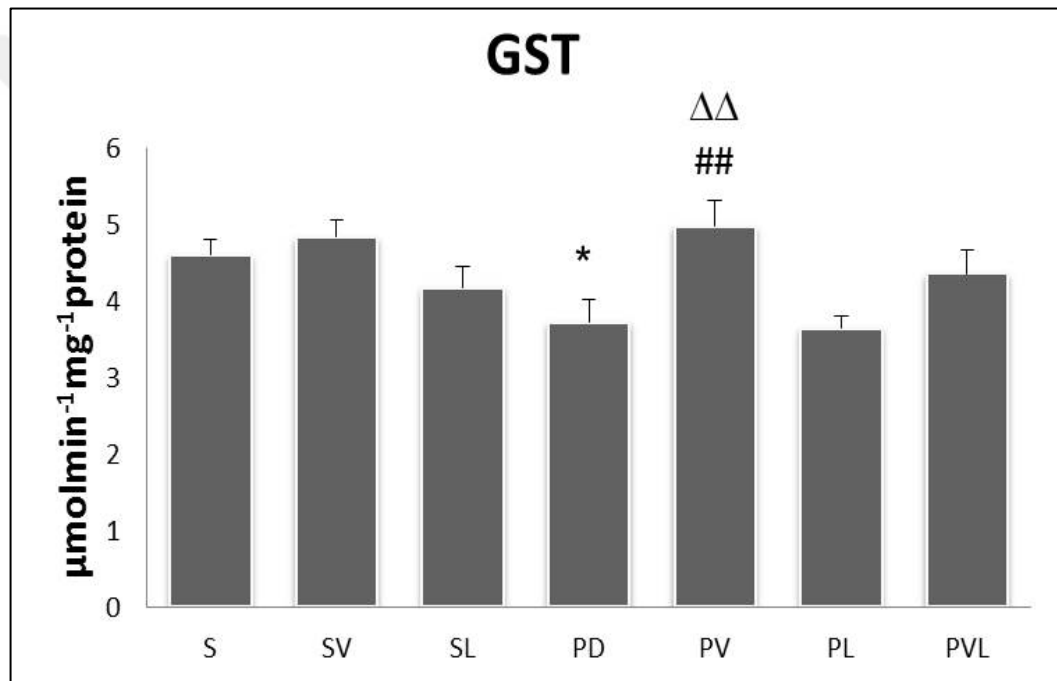


Figure 4.16. Graphs comparing GST activity in the striatum. Sham operated (S), Sham operated and VPA treated (SV), Sham operated and L-DOPA treated (SL), Nigraly 6-OHDA injected (PD), Nigraly 6-OHDA injected and VPA treated (PV), Nigraly 6-OHDA injected and L-DOPA treated (PL), Nigraly 6-OHDA injected and VPA and L-DOPA treated (PVL) groups. The data were all expressed as mean  $\pm$  SEM. One way Anova followed by LSD post-hoc test was used for statistical analysis. \* $p < 0.05$  vs S, SV; ## $p < 0.01$  vs PD;  $\Delta\Delta p < 0.01$  vs PL.

#### 4.5. WESTERN BLOTTING

Histone acetylation level was determined with western blotting method in order to see whether valproic acid exerts its effects via modulating epigenetic mechanisms. In addition, the phosphorylation levels of p90RSK and ribosomal s6 protein were determined with western blotting method since these proteins are strongly implicated in survival and proliferation of the cells. For all of the western blotting experiments, the striatal tissue of the animals were dissected out and protein isolation were performed from striatal tissues.

##### 4.5.1. Acetyl Histone H3 (Lys9)

Valproic acid is known to acetylate histone proteins at lysine 9 position. The levels of acetyl histone H3 were not different between S and SL groups. Valproic acid treatment increased the histone acetylation level in SV group as compared with S and SL groups ( $p < 0.001$ ,  $p < 0.05$  respectively). Histone acetylation level was decreased in PD group according to the sham operated S, SV and SL groups ( $p < 0.001$ ,  $p < 0.001$ ,  $p < 0.001$  respectively). Valproic acid treatment in PV and PVL groups increased histone acetylation level as compared with PD group ( $p < 0.05$ ,  $p < 0.001$  respectively). In addition, in PVL group histone acetylation level was increased as compared with PV and PL groups ( $p < 0.01$ ,  $p < 0.01$  respectively) (Figure 4.17 and 4.18).

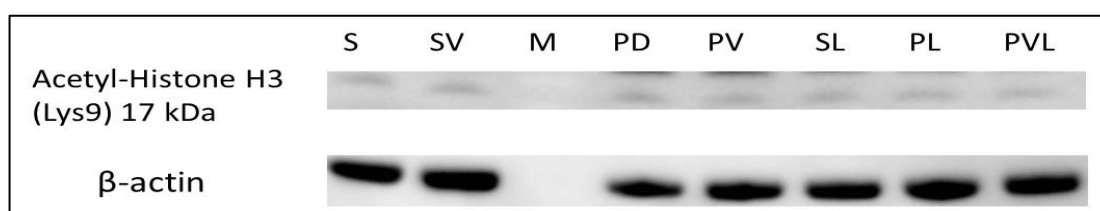


Figure 4.17. Western blot analysis for 17 kDa band of Acetyl-Histone H3 (Lys9) in striatal tissue.  $\beta$ -actin (42 kDa) was used as an internal control. M stands for marker. Sham operated (S), Sham operated and VPA treated (SV), Sham operated and L-DOPA treated (SL), Nigraly 6-OHDA injected (PD), Nigraly 6-OHDA injected and VPA treated (PV), Nigraly 6-OHDA injected and L-DOPA treated (PL), Nigraly 6-OHDA injected and VPA and L-DOPA treated (PVL) groups.



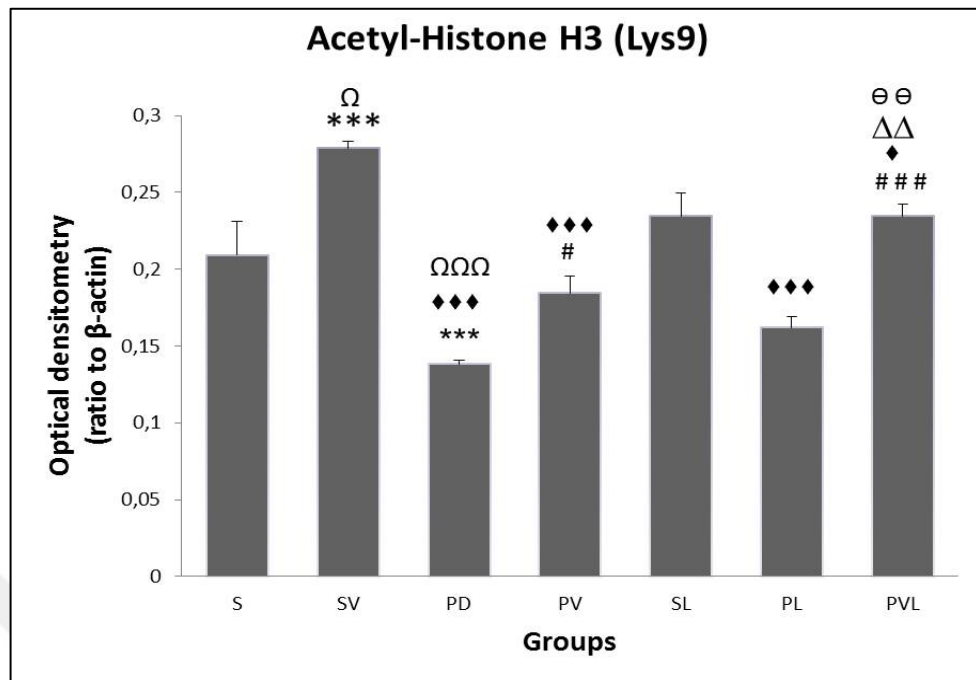


Figure 4.18. Graph comparing Acetyl-Histone H3 (Lys9) level in striatum. Sham operated (S), Sham operated and VPA treated (SV), Sham operated and L-DOPA treated (SL), Nigraly 6-OHDA injected (PD), Nigraly 6-OHDA injected and VPA treated (PV), Nigraly 6-OHDA injected and L-DOPA treated (PL), Nigraly 6-OHDA injected and VPA and L-DOPA treated (PVL) groups. The data were all expressed as mean  $\pm$  SEM of the relative intensity with respect to  $\beta$ -actin. \*\*\* $p$ <0.001 vs S; \* $p$ <0.05, \*\* $p$ <0.001 vs SV;  $\Omega$  $p$ <0.05,  $\Omega\Omega\Omega$  $p$ <0.001 vs SL; # $p$ <0.05, ### $p$ <0.001 vs PD;  $\Delta\Delta$  $p$ <0.01 vs PV;  $\Theta\Theta$  $p$ <0.01 vs PL.

#### 4.5.2. Phospho p90RSK (Ser380)

The levels of phospho p90RSK were not different between S and SL groups. Valproic acid treatment increased phospho p90RSK level in SV group as compared with S group ( $p$ <0.05). The level of phospho p90RSK was decreased in PD group according to the sham operated S, SV and SL groups ( $p$ <0.01,  $p$ <0.001,  $p$ <0.001 respectively). Valproic acid treatment in PV group increased phospho p90RSK level as compared with PD group ( $p$ <0.001) and PL group ( $p$ <0.05). In addition, in PVL group phospho p90RSK level was increased as compared with PD and PL groups ( $p$ <0.001,  $p$ <0.01 respectively). Furthermore, in PL group phospho p90RSK level was increased as compared with PD group ( $p$ <0.01) (Figure 4.19 and 4.20).

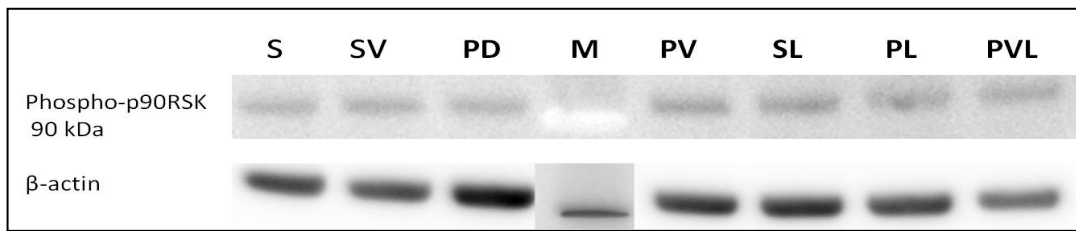


Figure 4.19. Western blot analysis for 90 kDa band of phospho p90RSK (Ser380) in striatal tissue.  $\beta$ -actin (42 kDa) was used as an internal control. M stands for marker. Sham operated (S), Sham operated and VPA treated (SV), Sham operated and L-DOPA treated (SL), Nigraly 6-OHDA injected (PD), Nigraly 6-OHDA injected and VPA treated (PV), Nigraly 6-OHDA injected and L-DOPA treated (PL), Nigraly 6-OHDA injected and VPA and L-DOPA treated (PVL) groups.

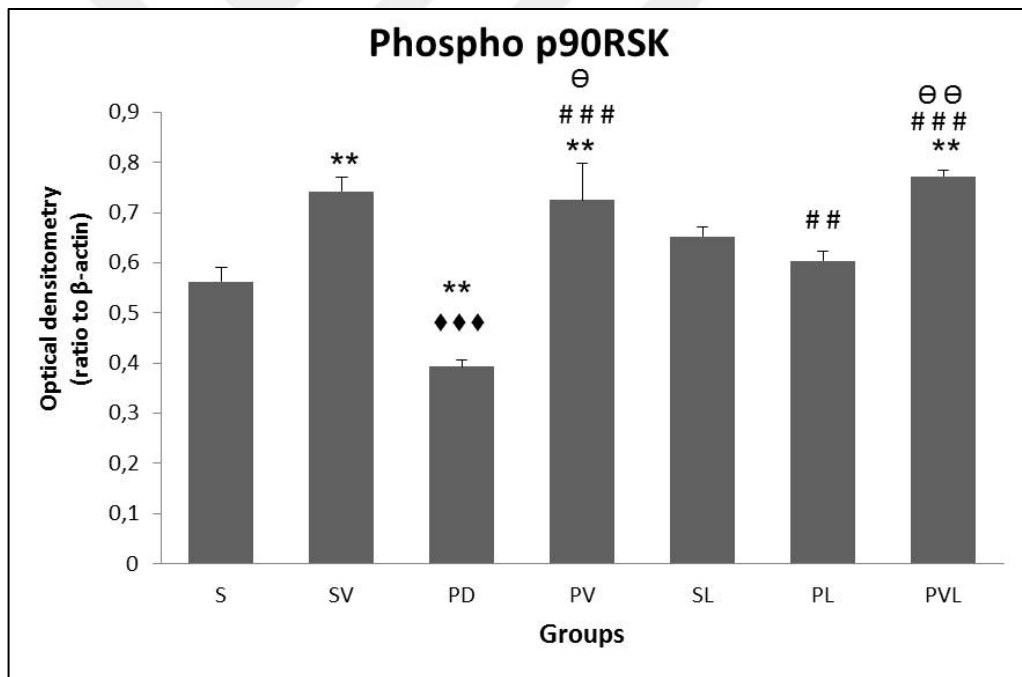


Figure 4.20. Graph comparing phospho p90RSK (Ser380) level in striatum. Sham operated (S), Sham operated and VPA treated (SV), Sham operated and L-DOPA treated (SL), Nigraly 6-OHDA injected (PD), Nigraly 6-OHDA injected and VPA treated (PV), Nigraly 6-OHDA injected and L-DOPA treated (PL), Nigraly 6-OHDA injected and VPA and L-DOPA treated (PVL) groups. The data were all expressed as mean  $\pm$  SEM of the relative intensity with respect to  $\beta$ -actin. \*\* $p$ <0.01 vs S; \*\*\* $p$ <0.001 vs SV, SL; ## $p$ <0.01, ### $p$ <0.001 vs PD;  $\Theta$  $p$ <0.05,  $\Theta\Theta$  $p$ <0.01 vs PL.

### 4.5.3. Phospho-S6 Ribosomal Protein (Ser235/236)

The levels of phospho S6 ribosomal protein (Ser235/236) were not different between S, SL and SV groups. The phosphorylation level of S6 ribosomal protein in PD group was found to be decreased as compared to SV and SL groups ( $p < 0.05$ ). On the other hand, the phosphorylation level of S6 ribosomal protein was increased in PVL group as compared with PD, PV and PL groups ( $p < 0.001$ ,  $p < 0.01$ ,  $p < 0.05$  respectively). Furthermore, the level of phospho S6 ribosomal protein was increased in PL group as compared with PD group ( $p < 0.05$ ) (Figure 4.21 and 4.22).

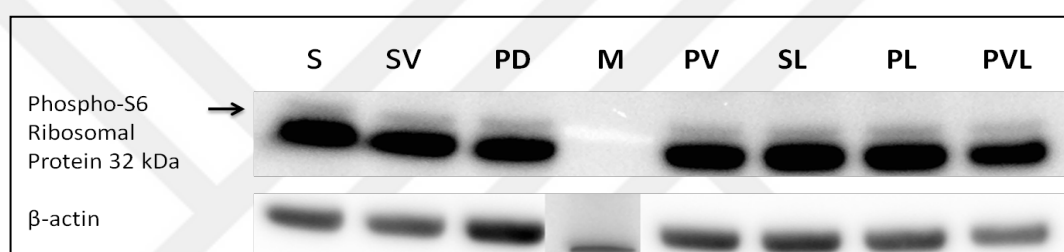


Figure 4.21. Western blot analysis for 32 kDa band of phospho S6 ribosomal protein (Ser235/236) in striatal tissue.  $\beta$ -actin (42 kDa) was used as an internal control. M stands for marker. Sham operated (S), Sham operated and VPA treated (SV), Sham operated and L-DOPA treated (SL), Nigrally 6-OHDA injected (PD), Nigrally 6-OHDA injected and VPA treated (PV), Nigrally 6-OHDA injected and L-DOPA treated (PL), Nigrally 6-OHDA injected and VPA and L-DOPA treated (PVL) groups.

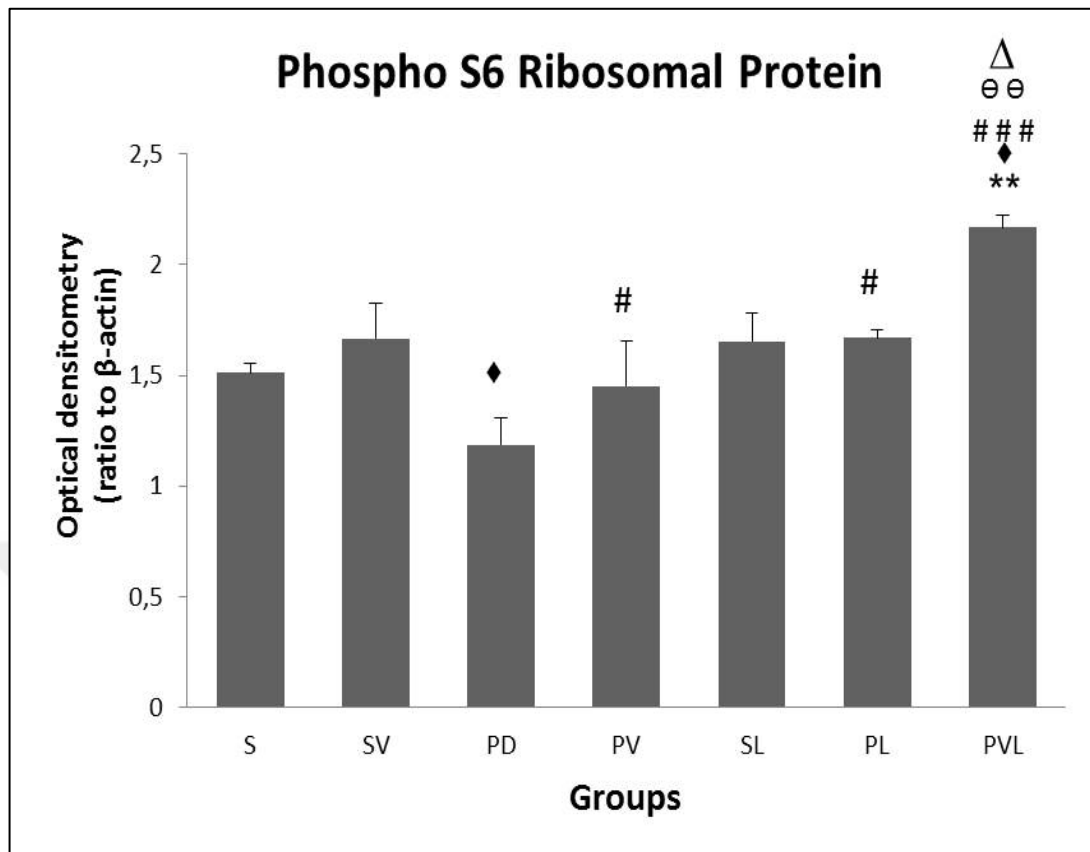


Figure 4.22. Graph comparing phospho S6 ribosomal protein (Ser235/236) level in striatum. Sham operated (S), Sham operated and VPA treated (SV), Sham operated and L-DOPA treated (SL), Nigraly 6-OHDA injected (PD), Nigraly 6-OHDA injected and VPA treated (PV), Nigraly 6-OHDA injected and L-DOPA treated (PL), Nigraly 6-OHDA injected and VPA and L-DOPA treated (PVL) groups. The data were all expressed as mean  $\pm$  SEM of the relative intensity with respect to  $\beta$ -actin. \*\* $p < 0.01$  vs S, \* $p < 0.05$  vs SV, SL; # $p < 0.05$ , ### $p < 0.001$  vs PD; ∅∅ $p < 0.01$  vs PV; △ $p < 0.05$ , vs PL.

## 5. DISCUSSION

Parkinson's Disease is widely seen in the world and the prevalence of it is increasing with the aging population. Although the pathogenesis of PD is not fully understood, it is characterized by the progressive degeneration of the dopaminergic neurons in substantia nigra pars compacta region of the brain. Degeneration of the dopaminergic neurons diminishes the dopamine amount in the striatum. Oxidative stress, mitochondrial dysfunction, protein aggregation, inflammation and lysosomal dysfunction are involved in PD pathogenesis. The major clinical signs are resting tremor, postural instability, bradykinesia and rigidity all of which affect negatively the quality of life of the patients [200, 201]. When the clinical symptoms occur, approximately 60 percent of dopamine neurons in substantia nigra pars compacta and 80 per cent of the dopamine amount in the striatum are lost. It is hypothesized that, the compensatory mechanisms in the brain such as diminished dopamine uptake may substitute for the smaller lesions in substantia nigra pars compacta. On the other hand, when there is a bigger lesion, those compensatory mechanisms are insufficient such that motor symptoms clinically occur [202].

After the clinical diagnosis, the current therapies are only symptomatic. There is currently no known neuroprotective and neurorestorative therapy for PD. The gold standard therapy levodopa is only a dopamine precursor with the ability to cross blood brain barrier and is converted into dopamine in the brain [203]. It accounts for the loss of dopamine amount in PD brains, provides a brief relief of the motor symptoms to the PD patients. On the other hand, after a while motor complications related to the usage of levodopa become apparent [204]. As the disease progresses, dyskinesia and diminished response to the medication occur. Dyskinesia is characterized as the involuntary movements such as tics and chorea which are involuntary movements of the muscles in the face and extremities. It is important to note that, as the disease progresses patients taking levodopa medication begin to be unresponsive to levodopa which is called as the off state and the responsive times (on state) are decreased during this time. For this reason physicians try to delay the usage of levodopa by using some dopamine agonists although only minority of the PD patients give response the dopamine agonists treatment [205]. Dopamine agonists also lead to serious side effects such as hallucinations, confusion and paranoia [206]. In the light of these piece of information, the only therapeutic approach in the treatment of PD has many

complications. Therefore, novel therapies, which are also neuroprotective and neurorestorative, are needed in the treatment of PD.

Valproic acid is currently used in the treatment of epilepsy, migraine and bipolar disorder. It was first synthesized by Burton in 1882 [207], although anticonvulsant properties were indicated later on. It is well tolerated, commercially available and cheap. It has a high bioavailability rate in both humans and rodents. It is indicated that, it can cross blood brain barrier rapidly by active transport mechanisms [208]. It is important to note that, valproic acid has no known drug interactions with levodopa [209]. Furthermore, recent studies demonstrate that valproic acid is also a histone deacetylase inhibitor. Increasing number of studies indicate the neuroprotective effects of histone deacetylase inhibitors in various neurodegenerative disorders. Valproic acid specifically targets class I and class IIa histone deacetylases which are strongly implicated in central nervous system [210]. Various studies indicate that, valproic acid decreases neuronal death through increasing histone 3 acetylation which increase the transcription of many anti-apoptotic proteins [211].

In this study, the main purpose was to understand the potency of valproic acid as an alternative treatment of PD because of its strong neuroprotective effects. In order to compare valproic acid's potential effects with the effects of gold standard therapeutic agent levodopa, valproic acid was included into the study as a second agent. Valproic acid and levodopa were used post acutely in a 6-hydroxydopamine animal model of Parkinson's Disease. Both of the drugs were administered to the animals intraperitoneally. It is important to note that, benserazide hydrochloride was also administered in combination with levodopa in order to decrease peripheral decarboxylation and to increase the bioavailability of levodopa. The effects of valproic acid on neuronal survival, motor activity, oxidative stress parameters, apoptotic mechanisms and histone acetylation levels in the brain were investigated. It is known that oxidative stress and apoptotic mechanisms are important in PD pathogenesis as they lead to dopaminergic neuronal death. In addition akinetic motor symptoms diminish the quality of life of the PD patients. Therefore, when developing new therapeutic approaches, the effects of novel agents on these mechanisms should also be taken into consideration as accomplished in this study.

Animal models are commonly used to investigate the molecular mechanisms of diseases and to test new therapeutic approaches. In order to test the effects of valproic acid, a neurotoxin induced animal model of PD was used in this study. 6-hydroxydopamine

targets dopamine neurons via its specific affinity to dopamine transporters on dopaminergic neurons and closely mimics PD. Once in the dopamine neurons, it increases the amount of reactive oxygen species while decreasing the activities of anti-oxidant systems, it leads to dopaminergic neuron death [212]. It also interferes with mitochondrial respiratory chain which further increases reactive oxygen species [213]. On the ground that 6-hydroxydopamine cannot cross blood brain barrier, it can be injected into substantia nigra pars compacta, medial forebrain bundle or striatum. In this study, 6-hydroxydopamine was stereotaxically injected into substantia nigra pars compacta of the brain which provides rapid degeneration of the neurons. In addition, 6-hydroxydopamine was unilaterally injected into the right substantia nigra pars compacta, while the left substantia nigra pars compacta serving as an internal control. In the literature bilateral animal models are reported to decrease the survival rate of the animals after the operation. To decrease the oxidation of 6-hydroxydopamine, the solution was freshly prepared just before the operation in ascorbic acid solution which is an anti-oxidant. The advantage of 6-hydroxydopamine PD model over other methods is that, the validity of the method can be assessed while the animals are alive by subcutaneous administration of apomorphine or amphetamine. Apomorphine is a dopamine agonist and contralateral rotations after apomorphine administration correlate with the severity of the disease [214]. In line with the literature, 6-hydroxydopamine lesioned animals showed pronounced rotational behavior, while sham operated animals did not show any rotational behavior in apomorphine induced rotation test. Valproic acid treatment slightly decreased the apomorphine induced rotations as compared to 6-hydroxydopamine lesioned and saline treated animals.

Dopaminergic neurons progressively degenerate in PD pathogenesis. 6-hydroxydopamine also leads to degeneration of dopaminergic neurons [215]. Immunohistochemical detection of tyrosine hydroxylase is the established method in PD research. Tyrosine hydroxylase is the rate limiting enzyme in the dopamine synthesis process. Therefore, tyrosine hydroxylase positive neurons give reliable data on the number of dopaminergic neurons in substantia nigra pars compacta. In line with the literature, in this study 6-hydroxydopamine injection significantly diminished tyrosine hydroxylase positive dopaminergic neurons in substantia nigra pars compacta and levodopa treatment did not change the number of tyrosine hydroxylase positive dopaminergic neurons. Although

post-acute valproic acid treatment significantly increased the number tyrosine hydroxylase positive neurons, they were still lower than sham operated groups. On the other hand, Kidd et al [187], published that valproic acid provided almost full protection from MPTP induced dopaminergic neuronal death. In that study, the authors preferred a prophylactic administration of valproic acid such that, valproic acid is injected to the animals before establishing the MPTP model of PD and also is continued afterwards. In this study, we preferred a post-acute treatment with valproic acid. Our results suggested that, post-acute treatment of valproic acid with the dose and time window used in this study may provide a partial protection from toxic insults, while levodopa does not change the number of dopaminergic neurons.

Although controversial studies are present in terms of apoptosis in nigral degeneration, various studies indicate the involvement of apoptosis in neuron degeneration, in humans, in vivo and in vitro models of PD [216]. TUNEL method is widely used for detecting apoptotic cells. It is a highly reliable method for detecting apoptosis as it labels DNA double strand breaks. Various studies demonstrate TUNEL positive neurons in 6-hydroxydopamine animal models [217, 218]. Many studies indicate that, valproic acid provides protection via increasing the amount of anti-apoptotic proteins such as BCL-2 and BCL-XL [219]. In this study, sham operated animals demonstrated trace amounts of apoptotic neurons. In line with the literature, 6-hydroxydopamine caused significantly increased amounts of TUNEL positive neurons in substantia nigra pars compacta as compared with sham operated groups. Valproic acid treatment significantly diminished the apoptotic neurons in substantia nigra pars compacta as compared with 6-hydroxydopamine lesioned and saline treated animals. Valproic acid treatment also significantly diminished the apoptotic neurons as compared with 6-hydroxydopamine lesioned and levodopa treated animals. On the other hand, the number of apoptotic neurons were still higher than sham operated groups. These results suggested that, valproic acid treatment may provide an effective protection to dopaminergic neurons from toxic insults through interfering apoptotic mechanisms.

In this study, cresyl violet and hematoxylin eosin stainings were also performed in order to morphologically examine tissues. Interestingly, 6-hydroxydopamine caused increased accumulation of glial cells in the lesioned area, which is not seen in sham operated animals. It has been observed that valproic acid treatment diminished those cells. In the



literature, Hirsch et al [220], demonstrated that both astrocytes and microglia are activated in PD animal model which subsequently release inflammatory agents leading to neuronal death. In addition valproic acid is known to reduce inflammatory agents by increasing the apoptosis of microglial cells [221, 222].

Oxidative stress is a key player in the degeneration of the dopaminergic neurons in PD. Because of the specific structure of the dopamine neurons, they are especially vulnerable to toxic insults and reactive oxygen species [223]. 6-hydroxydopamine is known to increase reactive oxygen species such as hydroxyl radicals [224]. 6-hydroxydopamine also increases hydrogen peroxide [225]. In addition 6-hydroxydopamine is known to interfere with the free radical scavengers [226]. Furthermore, 6-hydroxydopamine decreases superoxide dismutase and glutathione peroxidase [227]. It has been demonstrated that overexpression of anti-oxidants such as superoxide dismutase and glutathione peroxidase diminishes 6-hydroxydopamine induced cell death [228, 229]. Therefore, targeting mechanisms that halt reactive oxygen species and increase the function of anti-oxidant systems should be an important approach in developing novel therapies for PD. Jornada et al [230], demonstrated that valproic acid halts reactive oxygen species by increasing the activities of superoxide dismutase and catalase. In the model used in this study, 6-hydroxydopamine led to increased amounts of oxidative stress in dopaminergic neurons. As in the literature, in the current study 6-hydroxydopamine injection decreased activities of anti-oxidant systems superoxide dismutase, glutathione S-transferase and reduced glutathione as compared to sham operated animals. Decreased activities of anti-oxidant enzymes leads to increased amounts of reactive oxygen species which damages lipids and produces lipid peroxidation products such as malondialdehyde. In line with the literature, in this study, 6-hydroxydopamine injection increased malondialdehyde level as compared to sham operated animals. On the other hand, valproic acid treatment decreased malondialdehyde level and increased the activities of superoxide dismutase, glutathione S-transferase and reduced glutathione as compared to 6-hydroxydopamine lesioned and saline treated animals. Furthermore, valproic acid treatment decreased malondialdehyde level and increased the activities of superoxide dismutase, glutathione S-transferase and reduced glutathione as compared to 6-hydroxydopamine lesioned and levodopa treated animals. These results suggest that valproic acid may halt 6-hydroxydopamine induced

oxidative stress. Therefore, valproic may have beneficial effects in the treatment of PD by diminishing oxidative stress and increasing the anti-oxidant capacity of the neurons.

The major clinical symptom of the PD is the motor abnormalities due to the disrupted balance of the direct and indirect pathways of the basal ganglia. 6-hydroxydopamine is known to decrease motor activity of the animals in both unilateral [231] and bilateral [232] models of PD. In this study, the locomotor activity parameters were also investigated with an activity monitoring system [233]. Distance travelled is the measurement of the area travelled by the animal in the activity cage as centimeter. Stereotypic activity is the number of times the rat licking the fore legs, moving them over its head and bites its own fur. Ambulatory activity is the number of squares crossed in the activity cage. Vertical activity is the number of times the rat stands on its hind feet. In the present study all of the locomotor activity parameters were decreased in 6-hydroxydopamine lesioned animals since the balance between direct and indirect pathways of the basal ganglia was disrupted in Parkinson's Disease. The relatively low dose of levodopa used in this study, in order not to induce dyskinetic behavior, still increased the locomotor activity parameters as compared to 6-hydroxydopamine lesioned and saline treated animals. This is due to increased activation of the direct pathway of the basal ganglia by dopaminergic agents. Similarly, levodopa treatment in sham operated animals increased locomotor activity parameters as compared to other sham operated animals. Although valproic acid treatment significantly improved the impaired locomotor activity parameters as compared to 6-hydroxydopamine lesioned and saline treated animals, they were still lower than sham operated groups. Likewise, locomotor activity parameters were lower in sham operated and valproic acid treated animals as compared to both sham operated saline treated and sham operated and levodopa treated animals. One explanation may be that, valproic acid also increases the level of GABA which is an inhibitory transmitter and has a negative effect on locomotor activity of the animals [234-236]. Iadarola et al, demonstrated that 200-400 mg/kg of valproic acid increases GABA in rat brains, which includes the dosage used in this study [237]. On the other hand, Biggs et al, published that different doses of valporic acid leads to biphasic effect on GABA levels. They demonstrated that 100 mg/kg valproic acid decreased GABA amount in the brain by half, on the other hand, 400 mg/kg valproic acid increased amount of GABA in the brain by 200 per cent [238]. According to

these results, the effects of different doses of valproic acid on locomotor activity may be investigated in PD models.

Epigenetics is the alterations in the gene expression that are not due to alterations in DNA sequence. In neurodegenerative studies valproic acid is one of the most widely studied histone deacetylase inhibitor. Increasing number of studies are investigating the potent neuroprotective effects of valproic acid in many neurodegenerative diseases such as Alzheimer's Disease, Huntington's Disease, spinal muscular atrophy and cerebral ischemia [239-242]. As shown in the previous in vitro and in vivo Parkinson's Disease studies, valproic acid may have potential protective mechanisms by inducing antiapoptotic, antioxidant, anti-inflammatory, and histone deacetylase inhibitory mechanisms. It is known that systemic administration of relatively high doses of valproic acid results in hyper acetylation in the brain by increasing the level of Acetyl-Histone H3 (Lys9) [243]. It has been demonstrated that valproic acid has neuroprotective effects in a rotenone model of PD through increasing histone 3 acetylation level in the brain [244]. Similarly, valproic acid also provides protection from 6-hydroxydopamine induced neuronal death [245]. Furthermore, in a recent in vivo PD study, the neuroprotective effects of valproic acid mediated HDAC inhibition and histone 3 acetylation has been implicated prophylactically [187]. It is interesting to note that,  $\alpha$ -synuclein aggregation was found to be associated with hypo-acetylation of histone 3. It is suggested that  $\alpha$ -synuclein aggregation represses the transcription of certain genes by decreasing histone acetylation eventually causing neuronal death [246]. In the present study, valproic acid treatment in 6-hydroxydopamine lesioned animals slightly increased Histone 3 acetylation as compared to the 6-hydroxydopamine lesioned and saline treated animals. Likewise, valproic acid treatment in sham operated animals slightly increased Histone 3 acetylation as compared to the sham operated saline treated and sham operated and levodopa treated animals. Although not significant, there was a slight increase of Histone 3 acetylation in sham operated and levodopa treated animals compared to sham operated animals. Interestingly, levodopa treatment is found to be related to Histone 3 acetylation [247]. These results suggested that valproic acid may exert its effects via modulating epigenetics mechanisms.

In order to understand the molecular mechanisms of valproic acid in detail, the phosphorylation level of p90RSK and ribosomal s6 protein were investigated in this study. p90RSK is strongly implicated in cell survival and proliferation processes. It is regulated

under the MAPK pathway. Upon a stimulus, the phosphorylation of ERK1/2 in turn phosphorylates p90RSK proteins at several sites. Phosphorylated and activated RSK proteins translocate into nucleus and phosphorylate proteins such as ribosomal S6 protein. Phosphorylated ribosomal S6 protein in turn increases the transcription of the proteins involved in cell cycle progression and synaptic plasticity [248]. Therefore, phosphorylation level of p90RSK and ribosomal S6 protein is very important in cell survival processes [249, 250]. Of note, p90RSK also halts apoptotic mechanisms by inhibiting proapoptotic protein BAD [251]. It has been demonstrated that, while ribosomal S6 kinase phosphorylates ribosomal S6 protein at all sites, p90RSK phosphorylates ribosomal S6 protein at Ser 235/236 [168]. Therefore, in the current study, an antibody specific to these phosphorylation sites was selected. In this study, valproic acid treatment in 6-hydroxydopamine lesioned animals significantly increased the phosphorylation of p90RSK protein as compared to the 6-hydroxydopamine lesioned and saline treated animals. Likewise, valproic acid treatment in 6-hydroxydopamine lesioned animals slightly increased the phosphorylation of ribosomal S6 protein as compared to the 6-hydroxydopamine lesioned and saline treated animals. These results suggested that, valproic acid may provide protection from 6-hydroxydopamine induced toxic insults by stimulating the activation of proteins involved in cell proliferation, differentiation and survival processes. Interestingly, levodopa treatment in 6-hydroxydopamine lesioned animals also increased the phosphorylation of p90RSK and ribosomal S6 protein as compared to the 6-hydroxydopamine lesioned and saline treated animals. It is known that, levodopa treatment increases the phosphorylation of ERK1/2 proteins which is upstream of p90RSK and ribosomal S6 proteins [252, 253]. It is thought that, long term treatment of levodopa leads to dyskinetic behavior via phosphorylation of ERK1/2. In the current study, combined treatment of 6-hydroxydopamine lesioned animals with valproic acid and levodopa, further increased the phosphorylation of p90RSK and ribosomal S6 proteins, suggesting a synergistic effect of both agents.

## 6. CONCLUSION

Millions of patients suffer from PD in the world and prevalence is also increasing with the aging population. Currently only symptomatic therapies are present in the treatment of PD. Therefore, novel neuroprotective and neurorestorative therapeutic approaches are needed. The current study demonstrates that, valproic acid may have beneficial effects in the treatment of PD. The dosage and duration of valproic acid used in this study, partially protected dopaminergic neurons by slightly increasing tyrosine hydroxylase positive dopaminergic neurons and decreasing apoptotic neurons. In addition, valproic acid treatment diminished oxidative stress parameters and increased the activities of antioxidant mechanisms. Furthermore, in this study, it was demonstrated that valproic acid stimulates the phosphorylation of proteins which are involved in cell survival and proliferation processes. On the other hand, valproic acid had limited effects on impaired locomotor activity parameters as compared with levodopa. Overall data suggested that, valproic acid may have beneficial effects in the treatment of PD in combination with levodopa and it is worth investigating. However, due to the fact that PD is a highly complex disorder involving many pathologic mechanisms at the same time, further studies should be conducted to determine the limitations and detailed mechanisms of the effects of valproic acid in the treatment of PD.

## REFERENCES

1. R. L. Albin, A. B. Young and J. B. Penney. The Functional Anatomy of Basal Ganglia Disorders. *Trends in Neurosciences*, 12:366-376, 1989.
2. J. J. Jankovic, and E. Tolosa. *Parkinson's Disease and Movement Disorders*, Fourth Edition, Lippincott Williams and Wilkins, 2002.
3. J. W. Mink. The basal ganglia: Focused Selection and Inhibition of Competing Motor Programs. *Progress in Neurobiology*, 50:381-425, 1996.
4. G. Chevalier and J. M. Deniau. Disinhibition as a Basic Process in the Expression of Striatal Functions. *Trends in Neurosciences*, 13:277-280, 1990.
5. A. D. Smith and J. P. Bolam. The Neural Network of the Basal Ganglia as Revealed by the Study of Synaptic Connections of Identified Neurones. *Trends in Neurosciences*, 13:259-265, 1990.
6. C. R. Gerfen and C. J. Wilson. *The Basal Ganglia. Integrated Systems of the CNS, Part III*. Elsevier Science, 1996.
7. S. P. Wise, E.A. Murray and C. R. Gerfen. The Frontal Cortex-Basal Ganglia System in Primates. *Critical Reviews in Neurobiology*, 10:317-356, 1996.
8. H. J. Groenewegen. The Basal Ganglia and Motor Control. *Neural Plasticity*, 10:1-2, 2003
9. E. R. Kandel, J. H. Schwartz, T. M. Jessell, S. A. Siegelbaum and A. J. Hudspeth. *Principles of Neural Science*, McGraw-Hill Education, 2012.
10. A. Parent and L. N. Hazrati. Functional Anatomy of the Basal Ganglia. I. The Cortico-Basal Gangliathalamo-Cortical Loop. *Brain Research Reviews*, 20:91-127, 1995.

11. R. Levy, L. N. Hazrati, M. T. Herrero, M. Vila, O.K. Hassani, M. Mouroux, M. Ruberg, H. Asensi, Y. Agid, J. Féger, J. A. Obeso, A. Parent and E. C. Hirsch. Re-Evaluation of the Functional Anatomy of the Basal Ganglia in Normal and Parkinsonian States. *Neuroscience*, 76:335-343, 1997.
12. A. Lieberman. Depression in Parkinson's Disease a Review. *Acta Neurologica Scandinavica*, 113:1-8, 2006.
13. J. Parkinson. An Essay on the Shaking Palsy. *Journal of Neuropsychiatry and Clinical Neurosciences*, 14:223-236, 2002.
14. A. Bjorklund and S. B. Dunnett. Dopamine Neuron Systems in the Brain: an Update. *Trends in Neurosciences*, 30:194-202, 2007
15. O. Hornykiewicz. The Discovery of Dopamine Deficiency in the Parkinsonian Brain. *Journal of Neural Transmission*, 70:9-15, 2006
16. P. M. Antony, N. J. Diederich, R. Krüger and R. Balling. The Hallmarks of Parkinson's Disease. *Febs Journal*, 23:5981-5993, 2013.
17. J Jankovic. Parkinson's Disease: Clinical Features and Diagnosis. *Journal of Neurology, Neurosurgery, and Psychiatry*, 79:368-376, 2008.
18. K. R. Chaudhuri, D. G. Healy and A. H. V Schapira. Non-Motor Symptoms of Parkinson's Disease: Diagnosis and Management. *Lancet Neurology*, 5:235-245, 2006.
19. N. Caballol, M. J. Marti and E. Tolosa. Cognitive Dysfunction and Dementia in Parkinson Disease. *Movement Disorders*, 22:358-366, 2007.
20. C. Ramaker, J. Marinus and A. M. Stiggelbout. Systematic Evaluation of Rating Scales for Impairment and Disability in Parkinson's Disease. *Journal of Movement Disorders*, 17:867-876, 2002.

21. C. G. Goetz, S. Fahn and P. Martinez-Martin. Movement Disorder Society-Sponsored Revision of the Unified Parkinson's Disease Rating Scale (MDS-UPDRS): Process, Format, and Clinimetric Testing Plan. *Journal of Movement Disorders*, 22:41-47, 2007.
22. A. Berardelli, J. C. Rothwell and P. D. Thompson. Pathophysiology of Bradykinesia in Parkinson's Disease. *Brain*, 124:2131-2146, 2001.
23. F. J. G. Vingerhoets, M. Schulzer and D. B. Calne. Which Clinical Sign of Parkinson's Disease Best Reflects the Nigrostriatal Lesion? *Annals of Neurology*, 41:58-64, 1997.
24. L. C. Parr-Brownlie and B. I. Hyland. Bradykinesia Induced by Dopamine D2 Receptor Blockade is Associated with Reduced Motor Cortex Activity in the Rat. *The Journal of Neuroscience*, 25:5700-5709, 2005.
25. L.M. Shulman, C. Singer and J. A. Bean. Internal Tremor in Patients with Parkinson's Disease. *Journal of Movement Disorders*, 11:3-7, 1996.
26. E. Broussolle, P. Krack and S. Thobois. Contribution of Jules Froment to the Study of Parkinsonian Rigidity. *Journal of Movement Disorders*, 22:909-914, 2007.
27. B. R. Bloem. Postural Instability in Parkinson's Disease. *Clinical Neurology and Neurosurgery*, 94:41-45, 1992.
28. A. L. Adkin, J. S. Frank and M. S. Jog. Fear of Falling and Postural Control in Parkinson's Disease. *Journal of Movement Disorders*, 18:496-502, 2003.
29. R. Matison, R. Mayeux and J. Rosen. "Tip-of-the-Tongue" Phenomenon in Parkinson's Disease. *Neurology*, 32:567-570, 1982.
30. V. Biousse, B. C. Skibell and R. L. Watts. Ophthalmologic Features of Parkinson's Disease. *Neurology*, 62:177-180, 2004.



31. K. R. Chaudhuri, G. H. Daniel and A. H. V. Schapira. Non-Motor Symptoms of Parkinson's Disease: Diagnosis and Management. *The Lancet Neurology*, 5:235-245, 2006.
32. D. J. Burn. Beyond the Iron Mask: Towards Better Recognition and Treatment of Depression Associated with Parkinson's Disease. *Journal of Movement Disorders*, 17:445-454, 2002.
33. D. Aarsland, K. Andersen and J. P. Larsen. Risk of Dementia in Parkinson's Disease: A Community-Based, Prospective Study. *Neurology*, 56:730-736, 2001.
34. M. A. Hely, J. G. L. Morris and W. G. J. Reid. Sydney Multicenter Study of Parkinson's Disease: Non-L-Dopa-Responsive Problems Dominate at 15 Years. *Journal of Movement Disorders*, 20:190-199, 2005.
35. M. P. Laakso, K. Partanen and P. Riekkinen. Hippocampal Volumes in Alzheimer's Disease, Parkinson's Disease with or without Dementia: An MRI Study. *Neurology*, 46:678-681, 1996.
36. D. Weintraub, A. D. Siderowf and M. N. Potenza. Association of Dopamine Agonist Use with Impulse Control Disorders in Parkinson Disease. *Archives of Neurology*, 63:969-973, 2006.
37. D. Garcia-Borreguero, O. Larosa and M. Bravo. Parkinson's Disease and Sleep. *Sleep Medicine Reviews*, 7:115-129, 2003.
38. C. H. Schenck, S.R. Bundlie and M.W. Mahowald. Delayed Emergence of a Parkinsonian Disorder in 38 per cent of 29 Older Men Initially Diagnosed with Idiopathic Rapid Eye Movement Sleep Behavior Disorder. *Neurology*, 46:388-393, 1996.

39. R. D. Abbott, G. W. Ross and L.R. White. Excessive Daytime Sleepiness and the Future Risk of Parkinson's Disease. *Journal of Movement Disorders*, 20:101-110, 2005.
40. C. Magerkurth, R. Schnitzer and S. Braune. Symptoms of Autonomic Failure in Parkinson's Disease: Prevalence and Impact on Daily Life. *Clinical Autonomic Research*, 15:76-82, 2005.
41. R. F. Pfeiffer. Gastrointestinal Dysfunction in Parkinson's Disease. *The Lancet Neurology*, 2:107-116, 2003.
42. A. J. Stoessl. Etiology of Parkinson's Disease. *Journal of the Neurological Sciences*, 26:5-12, 1999.
43. B. Thomas and M. F. Beal. Parkinson's disease. *Human Molecular Genetics*, 16:183-194, 2007.
44. C. Klein, R. Chuang, C. Marras and A. E. Lang. The Curious Case of Phenocopies in Families with Genetic Parkinson's Disease. *Journal of Movement Disorders*, 26:1793-1802, 2011.
45. M. G. Spillantini, R. A. Crowther, R. Jakes, M. Hasegawa, and M. Goedert.  $\alpha$ -Synuclein in Filamentous Inclusions of Lewy Bodies from Parkinson's Disease and Dementia with Lewy Bodies. *Proceedings of the National Academy of Sciences of the United States of America*, 95:6469-6473, 1998.
46. L. Yavich, H. Tanila, S. Vepsalainen and P. Jakala. Role of alpha-synuclein in Presynaptic Dopamine Recruitment. *The Journal of Neuroscience*, 24:11165-11170, 2004.
47. M. H. Polymeropoulos, C. Lavedan, E. Leroy, S. E. Ide, A. Dehejia, A. Dutra, B. Pike, H. Root, J. Rubenstein and R. Boyer. Mutation in the Alpha-Synuclein Gene Identified in Families with Parkinson's Disease. *Science*, 276:2045-2047, 1997.

48. S. M. Solano, D. W. Miller, S. J. Augood, A. B. Young, and J. B. Penney. Expression of Alpha-Synuclein, Parkin, and Ubiquitin Carboxy-Terminal Hydrolase L1 mRNA in Human Brain: Genes Associated with Familial Parkinson's Disease. *Annals of Neurology*, 47:201-210, 2000.
49. A. A. Cooper, A. D. Gitler, A. Cashikar, C. M. Haynes, K. J. Hill, B. Bhullar, K. Liu, K. Xu, K. E. Strathearn, and F. Liu. Alpha-Synuclein Blocks ER-Golgi Traffic and Rab1 Rescues Neuron Loss in Parkinson's Models. *Science*, 313:324-328, 2006.
50. L. J. Martin, Y. Pan, A. C. Price, W. Sterling, N. G. Copeland, N. A. Jenkins, D. L. Price and M. K. Lee. Parkinson's Disease Alpha-Synuclein Transgenic Mice Develop Neuronal Mitochondrial Degeneration and Cell Death. *The Journal of Neuroscience*, 26:41-50, 2006.
51. H. J. Lee, F. Khoshaghideh, S. Lee and S. J. Lee. Impairment of Microtubule-Dependent Trafficking by Overexpression of Alpha-Synuclein. *The Journal of Neuroscience*, 24:3153-3162, 2006.
52. T. Kitada, S. Asakawa, N. Hattori, H. Matsumine, Y. Yamamura, S. Minoshima, M. Yokochi, Y. Mizuno and N. Shimizu. Mutations in the Parkin Gene Cause Autosomal Recessive Juvenile Parkinsonism. *Nature*, 392:605-608, 1998.
53. H. Shimura, N. Hattori, S. Kubo, Y. Mizuno, S. Asakawa, S. Minoshima, N. Shimizu, K. Iwai, T. Chiba and K. Tanaka. Familial Parkinson Disease Gene Product, Parkin, is a Ubiquitin-Protein Ligase. *Nature Genetics*, 25:302-305, 2000.
54. T. M. Dawson. Parkin and Defective Ubiquitination in Parkinson's Disease. *Journal of Neural Transmission*, 70:209-213, 2006.
55. A. C. Belin and D. Galter. S18Y, UCH-L1 and Parkinson's Disease. *European Neurological Review*, 3:41-44, 2008.

56. E. M. Valente, P. M. Abou-Sleiman, V. Caputo, M. M. Muqit, K. Harvey, S. Gispert, Z. Ali, D. Del Turco, A. R. Bentivoglio and D. G. Healy. Hereditary Early-Onset Parkinson's Disease Caused by Mutations in PINK1. *Science*, 304:1158-1160, 2004.
57. A. Petit, T. Kawarai, E. Paitel, N. Sanjo, M. Maj, M. Scheid, F. Chen, Y. Gu, H. Hasegawa and S. Salehi-Rad, S. Wild-Type PINK1 Prevents Basal and Induced Neuronal Apoptosis, a Protective Effect Abrogated by Parkinson Disease-Related Mutations. *Journal of Biological Chemistry*, 280:34025-34032, 2005.
58. V. Bonifati, P. Rizzu, M. J. van Baren, O. Schaap, G. J. Breedveld, E. Krieger, M. C. Dekker, F. Squitieri, P. Ibanez and M. Joesse. Mutations in the DJ-1 Gene Associated with Autosomal Recessive Early-Onset Parkinsonism. *Science*, 299:256-259, 2003.
59. L. Zhang, M. Shimoji, B. Thomas, D. J. Moore, S. W. Yu, N. I. Marupudi, R. Torp, I. A. Torgner, O. P. Ottersen, T. M. Dawson. Mitochondrial Localization of the Parkinson's Disease Related Protein DJ-1: Implications for Pathogenesis. *Human Molecular Genetics*, 14:2063-2073, 2005.
60. T. Taira, Y. Saito, T. Niki, S. M. Iguchi-Ariga, K. Takahashi, K. and H. Ariga. DJ-1 Has a Role in Antioxidative Stress to Prevent Cell Death. *EMBO Reports*, 5:213-218, 2004.
61. S. Shendelman, A. Jonason, C. Martinat, T. Leete and A. Abeliovich. DJ-1 is a Redox-Dependent Molecular Chaperone That Inhibits Alpha-Synuclein Aggregate Formation. *PLOS Biology*, 2:1764-1773, 2004.
62. M. S. Goldberg, A. Pisani, M. Haburcak, T. A. Vortherms, T. Kitada, C. Costa, Y. Tong, G. Martella, A. Tschertter and A. Martins. Nigrostriatal Dopaminergic Deficits and Hypokinesia Caused by Inactivation of the Familial Parkinsonism-Linked Gene DJ-1. *Neuron*, 45:489-496, 2005.

63. A. Zimprich, S. Biskup, P. Leitner, P. Lichtner, M. Farrer, S. Lincoln, J. Kachergus, M. Hulihan, R. J. Uitti and D. B. Calne. Mutations in LRRK2 Cause Autosomal-Dominant Parkinsonism with Pleomorphic Pathology. *Neuron*, 44:601-607, 2004.
64. X. Zhu, S. L. Siedlak, M. A. Smith, G. Perry and S. G. Chen. LRRK2 Protein is a Component of Lewy Bodies. *Annals of Neurology*, 60:617-618, 2006.
65. C. M. Tanner. Advances in Environmental Epidemiology. *Movement Disorders*, 25:58-62, 2010.
66. D.B. Hancock, E.R. Martin and J.M. Stajich. Smoking, Caffeine, and Nonsteroidal Anti-Inflammatory Drugs in Families with Parkinson Disease. *Archives of Neurology*, 64:576-580, 2007.
67. J.A. Firestone, T. Smith-Weller, G. Franklin, P. Swanson, W.T. Longstreth and H. Checkoway. Pesticides and Risk of Parkinson Disease: A Population-Based Case-Control Study. *Archives of Neurology*, 62:91-95, 2005.
68. M. Chin-Chan, J. Navarro-Yepes and B. Quintanilla-Vega. Environmental Pollutants As Risk Factors for Neurodegenerative Disorders: Alzheimer and Parkinson Diseases. *Frontiers in Cellular Neuroscience*, 9:1-22, 2015.
69. A. Reeve, E. Simcox and D. Turnbull. Ageing and Parkinson's Disease: Why is Advancing Age the Biggest Risk Factor? *Ageing Research Reviews*, 14:19-30, 2014.
70. J. V. Hindle. Ageing, Neurodegeneration and Parkinson's Disease. *Age and Ageing*, 39:156-161, 2010.
71. M. J. Zigmond R and E. Burke. *The Fifth Generation of Progress American College of Neuropsychopharmacology, Chapter 123: Pathophysiology of Parkinson's Disease Neuropsychopharmacology*. Lippincott, Williams, and Wilkins, Philadelphia, Pennsylvania, 2002.

72. J.M. Fearnley and A. J. Lees. Ageing and Parkinson's Disease: Substantia Nigra Regional Selectivity. *Brain*, 114:2283, 1991.
73. P. Calabresi, D. Centonze, and G. Bernardi. Electrophysiology of Dopamine in Normal and Denervated Striatal Neurons. *Trends in Neurosciences*, 23:57-63, 2000.
74. Y. Agid, F. Agid and M. Ruberg. Biochemistry of Neurotransmitters in Parkinson's Disease. *Movement Disorders*, 2:166-230, 1987.
75. P. J. Whitehouse, J. C. Hedreen and C. L. White. Basal Forebrain Neurons in the Dementia of Parkinson Disease. *Annals of Neurology*, 13:243-248, 1983.
76. F. H. Lewy. Paralysis Agitans. Pathologishe Anatomie. Lewandowsky Med. *Handbook Der Neurologie*, Springer Berlin, 1912.
77. W. R. Gibb, T. Scott T, A. J. Lees. Neuronal Inclusions of Parkinson's Disease. *Journal of Movement Disorders*, 6:2-11, 1991.
78. S. Engelender, Z. Kaminsky and X. Guo. Synphilin-1 Associates with Alpha-Synuclein and Promotes the Formation of Cytosolic Inclusions. *Nature Genetics*, 22:110-114, 1999.
79. S. M. Solano, D. W. Miller, S. J. Augood, A. B. Young and J. B. Penney. Expression of  $\alpha$ -Synuclein, Parkin, and Ubiquitin Carboxy-Terminal Hydrolase L1 mRNA in Human Brain: Genes Associated with Familial Parkinson's Disease. *Annals of Neurology*, 47:201-210, 2000.
80. P.T. Lansbury and A. Brice. Genetics of Parkinson's Disease and Biochemical Studies of Implicated Gene Products. *Current Opinion in Cell Biology*, 14:653-660, 2002.
81. D. J. Moore, A. B. West, V. L. Dawson and T. M. Dawson. Molecular Pathophysiology of Parkinson's Disease. *Annual Review of Neuroscience*, 28:57-87, 2005.

82. A. Abeliovich, Y. Schmitz, I. Farinas, D. Choi-Lundberg and W. H. Ho. Mice Lacking  $\alpha$ -Synuclein Display Functional Deficits in the Nigrostriatal Dopamine System. *Neuron*, 25:239-252, 2000.
83. M. B. Feany and W. W. Bender. A Drosophila Model of Parkinson's Disease. *Nature*, 404:394-398, 2000.
84. Y. Chu, H. Dodiya, P. Aebische, C. W. Olanow and J. H. Kordower. Alterations in Lysosomal and Proteasomal Markers in Parkinson's Disease: Relationship to Alphasynuclein Inclusions. *Neurobiology of Disease*, 35:385-398, 2009.
85. L. G. Friedman, M. L. Lachenmayer and J. Wang. Disrupted Autophagy Leads to Dopaminergic Axon and Dendrite Degeneration and Promotes Presynaptic Accumulation of Alpha-Synuclein and LRRK2 in the Brain. *The Journal of Neuroscience*, 32:7585-7593, 2012.
86. M. Vila, J. Bove, B. Dehay, N. Rodriguez-Muela and P. Boya. Lysosomal Membrane Permeabilization in Parkinson Disease. *Autophagy*, 7:98-100, 2011.
87. J. Bove, M. Martinez-Vicente and M. Vila. Fighting Neurodegeneration with Rapamycin: Mechanistic Insights. *Nature Reviews Neuroscience*, 12:437-452, 2011.
88. P. L. McGeer and E. G. McGeer. Inflammation and Neurodegeneration in Parkinson's Disease. *Parkinsonism and Related Disorders*, 10:3-7, 2004.
89. H. Chen, S. M. Zhang, M. A. Herman, M. A. Schwarzschild, W. C. Willett, G. A. Colditz, F. E. Speizer and A. Acherio. Nonsteroidal Anti-Inflammatory Drugs and the Risk of Parkinson Disease. *Archives of Neurology*, 60:1059-1064, 2003.
90. T. Yamada, P. L. McGeer and E. G. McGeer. Relationship of Complement Activated Oligodendrocytes to Reactive Microglia and Neuronal Pathology in Neurodegenerative Disease. *Dementia*, 2:71-77, 1991.

91. E. Koutsilieris, C. Scheller, E. Grunblatt, K. Nara, J. Li and P. Riederer. Free Radicals in Parkinson's Disease. *Journal of Neurology*, 249:1-5, 2002.
92. P. L. McGeer, K. Yasojima and E. G. McGeer. Inflammation in Parkinson's Disease. *Advances in Neurology*, 86:83-89, 2001.
93. J. W. Langston, P. Ballard, J.W. Tetrud and I. Irwin. Chronic Parkinsonism in Humans Due to a Product of Meperidine-Analog Synthesis. *Science*, 219:979-980, 1983.
94. A. H. Schapira, J. M. Cooper, D. Dexter, J. B. Clark, P. Jenner and C. D. Marsden. Mitochondrial Complex I Deficiency in Parkinson's Disease. *Journal of Neurochemistry*, 54:823-827, 1990.
95. K. F. Winklhofer and C. Haass. Mitochondrial Dysfunction in Parkinson's Disease. *Biochimica et Biophysica Acta*, 1802:29-44, 2010.
96. A. Bender, K. J. Krishnan, C. M. Morris, G. A. Taylor, A. K. Reeve, R. H. Perry, E. Jaros, J. S. Hersheson, J. Betts and T. Klopstock. High Levels of Mitochondrial DNA Deletions in Substantia Nigra Neurons in Aging and Parkinson Disease. *Nature Genetics*, 38:515-517, 2006.
97. Y. Kraytsberg, E. Kudryavtseva, A. C. McKee, C. Geula, N. W. Kowall and K. Khrapko. Mitochondrial DNA Deletions are Abundant and Cause Functional Impairment in Aged Human Substantia Nigra Neurons. *Nature Genetics*, 38:518-520, 2006.
98. D. R. Green and G. Kroemer. The Pathophysiology of Mitochondrial Cell Death. *Science*, 305:626-629, 2004.
99. E. Birben, U. M. Sahiner, C. Sackesen, S. Erzurum and O. Kalayci. Oxidative Stress and Antioxidant Defense World. *World Allergy Organization Journal*, 5:9-19, 2012.



100. I. N. Zelko, T. J. Mariani and R.J. Folz. Superoxide Dismutase Multigene Family: A Comparison of the CuZn-SOD (SOD1), Mn-SOD (SOD2), and EC-SOD (SOD3) Gene Structures, Evolution, and Expression. *Free Radical Biology and Medicine*, 33:337-349, 2002.
101. H. N. Kirkman, M. Rolfo, A.M. Ferraris and G.F. Gaetani. Mechanisms of Protection of Catalase by NADPH. Kinetics and Stoichiometry. *Journal of Biological Chemistry*, 274:13908-13914, 1999.
102. L. Flohé. Glutathione Peroxidase. *Basic Life Sciences*, 49:663-668, 1988.
103. J.E. Ladner, J.F. Parsons, C.L. Rife, G.L. Gilliland and R.N. Armstrong. Parallel Evolutionary Pathways for Glutathione Transferases: Structure and Mechanism of the Mitochondrial Class Kappa Enzyme rGSTK1-1. *Biochemistry*, 43:52-61, 2004.
104. J. Poirier D. Dea, A. Baccichet and C. Thiffault. Superoxide Dismutase Expression in Parkinson's Disease. *Annals of the New York Academy of Sciences*, 738:116-120, 1994.
105. S. J. Kish, C. L. Morito and O. Hornykiewicz. Glutathione Peroxidase Activity in Parkinson's Disease. *Neuroscience Letters*, 58:343-346, 1985.
106. L. M. Ambani, M. H. Van Woert and S. Murphy. Brain Peroxidase and Catalase in Parkinson's Disease. *Archives of Neurology*, 32:114-118, 1975.
107. T. L. Perry, D. V. Godin and S. Hansen. Parkinson's Disease: A Disorder due to Nigral Glutathione Deficiency? *Neuroscience Letters*, 33:305-310, 1982.
108. K. Jellinger, W. Paulus, I. Grundke-Iqbal, P. Riederer and M. B. Youdim. Brain Iron and Ferritin in Parkinson's and Alzheimer's Diseases. *Journal of Neural Transmission Parkinson's Disease and Dementia*, 2:327-340, 1990.

109. E. Floor and M. G. Wetzel. Increased Protein Oxidation in Human Substantia Nigra Pars Compacta in Comparison with Basal Ganglia and Prefrontal Cortex Measured with an Improved Dinitrophenylhydrazine Assay. *Journal of Neurochemistry*, 70:2682-2675, 1998.
110. Z. I. Alam, A. Zenner and S. A. Daniel. Oxidative DNA Damage in the Parkinsonian Brain: An Apparent Selective Increase in 8-Hydroxyguanine Levels in Substantia Nigra. *Journal of Neurochemistry*, 69:1196-1203, 1997.
111. D. T. Dexter, C. J. Carter, F. R. Wells, F. Javoy-Agid, Y. Agid, A. Lees, P. Jenner and C. D. Marsden. Basal Lipid Peroxidation in Substantia Nigra is Increased in Parkinson's Disease. *Journal of Neurochemistry*, 52:381-389, 1989.
112. P. Jenner. Oxidative Stress in Parkinson's Disease. *Annals of Neurology*, 53:26-36, 2003.
113. G. Cohen, R. Farooqui and N. Kesler. Parkinson's Disease: A New Link Between Monoamine Oxidase and Mitochondrial Electron Flow. *Proceedings of the National Academy of Science of the United States of America*, 94:4890-4894, 1997.
114. E. Sofic, K. W. Lange, K. Jellinger and P. Riederer. Reduced and Oxidized Glutathione in the Substantia Nigra of Patients with Parkinson's Disease. *Neuroscience Letters*, 142:128-130, 1992.
115. P. G. Clarke. Developmental Cell Death: Morphological Diversity and Multiple Mechanisms. *Anatomy and Embryology*, 181:195-213, 1990.
116. J. F. Kerr, A. H. Wyllie and A. R. Currie. Apoptosis: A Basic Biological Phenomenon with Wide-Ranging Implications in Tissue Kinetics. *British Journal of Cancer*, 26:239-257, 1972.

117. L. K. Klaidman, S. K. Mukherjee and J. D. Adams. Oxidative Changes in Brain Pyridine Nucleotides and Neuroprotection Using Nicotinamide. *Biochimica et Biophysica Acta*, 1525:136-148, 2001
118. R. J. Youle and A. Strasser. The BCL-2 Protein Family: Opposing Activities That Mediate Cell Death. *Nature Reviews Molecular Cell Biology*, 9:47-59, 2008.
119. M. C. Wei, W. X. Zong, E. H.Y. Cheng, T. Lindsten, V. Panoutsakopoulou, A. J. Ross, K. A. Roth, G. R. MacGregor, C. B. Thompson and S. J. Korsmeyer. Proapoptotic BAX and BAK: A Requisite Gateway to Mitochondrial Dysfunction and Death. *Science*, 292:727-730, 2001.
120. S. W. G. Tait and D. R. Green. Mitochondria and Cell Death: Outer Membrane Permeabilization and Beyond. *Nature Reviews Molecular Cell Biology*, 11:621-632, 2010.
121. A. Oberst, C. Pop, A. G. Tremblay, V. Blais, J. B. Denault, G. S. Salvesen and D. R. Green. Inducible Dimerization and Inducible Cleavage Reveal a Requirement for Both Processes in Caspase-8 Activation. *Journal of Biological Chemistry*, 285:16632-16642, 2010.
122. P. L. McGeer, S. Itagaki, H. Akiyama and E. G. McGeer. Rate of Cell Death in Parkinsonism Indicates Active Neuropathological Process. *Annals of Neurology*, 24:574-576, 1988.
123. S. Kosel, R. Egensperger, U. Eitzen, P. Mehraein and M. B. Graeber. On the Question of Apoptosis in the Parkinsonian Substantia Nigra. *Acta Neuropathologica*, 93:105-108, 1997.
124. K. A. Jellinger. Cell Death Mechanisms in Parkinson's Disease. *Journal of Neural Transmission*, 107:1-29, 2000.

125. H. Mochizuki, K. Goto, H. Mori and Y. Mizuno. Histochemical Detection of Apoptosis in Parkinson's Disease. *Journal of the Neurological Sciences*, 137:120-123, 1996.
126. N. A. Tatton, A. Maclean-Fraser, W. G. Tatton, D. P. Perl and C. W. Olanow. A Fluorescent Double-Labeling Method to Detect and Confirm Apoptotic Nuclei in Parkinson's Disease. *Annals of Neurology*, 44:142-148, 1998.
127. M. M. Tompkins, E. J. Basgall, E. Zamrini, W. D. Hill. Apoptotic-Like Changes in Lewy-Body-Associated Disorders and Normal Aging in Substantia Nigral Neurons. *American Journal of Pathology*, 150:119-131, 1997.
128. P. Anglade, S. Vyas and F. Javoy-Agid. Apoptosis and Autopsy in Nigral Neurons of Patients with Parkinson's Disease. *Histology And Histopathology*, 12:25-31, 1997.
129. A. Hartmann, S. Hunot, P. P. Michel, S. Vyas, B. A. Faucheux, A. Mouatt-Prigent, H. Turmel, A. Srinivasan, M. Ruberg, G. I. Evan and Y. Agid. Caspase-3: A Vulnerability Factor and Final Effector in Apoptotic Death of Dopaminergic Neurons in Parkinson's Disease. *Proceedings of the National Academy of Sciences of the United States of America*, 97:2875-2880, 2000.
130. J. K. Andersen. Does Neuronal Loss in Parkinson's Disease Involve Programmed Cell Death? *Bioessays*, 23:640-646, 2001.
131. I. Hassouna, H. Wickert, M. Zimmerman and F. Gillardon. Increase in Bax Expression in Substantia Nigra Following 1-Methyl-4-Phenyl-Tetrahydropyridine (MPTP) Treatment of Mice. *Neuroscience Letters*, 204:85-88, 1996.
132. M. Gomez-Lazaro, M. F. Galindo, C. G. Concannon, M. F. Segura, F. J. Fernandez-Gomez, N. Llecha, J. X. Comella, J. H. M. Prehn and J. Jordan. 6-Hydroxydopamine Activates the Mitochondrial Apoptosis Pathway Through P38 MAPK-Mediated, P53-Independent Activation of Bax and PUMA. *Journal of Neurochemistry*, 104:1599-1612, 2008.

133. M. Vila, V. Jackson-Lewis, S. Vukosavic, R. Djaldetti, G. Liberatore, D. Offen, S. J. Korsmeyer and S. Przedborski. Bax Ablation Prevents Dopaminergic Neurodegeneration in the 1-Methyl-4-Phenyl- 1,2,3,6-Tetrahydropyridine Mouse Model of Parkinson's Disease. *Proceedings of the National Academy of Sciences of the United States of America*, 98:2837-2842, 2001.
134. M. Yamada, T. Oligino, M. Mata, J. R. Goss, J. C. Glorioso and D. J. Fink. Herpes Simplex Virus Vector-Mediated Expression of Bcl-2 Prevents 6-Hydroxydopamine-Induced Degeneration of Neurons in the Substantia Nigra in Vivo. *Proceedings of the National Academy of Sciences of the United States of America*, 96:4078-4083, 1999.
135. W. Birkmayer and O. Hornykiewicz. The L-3,4-Dioxyphenylalanine (DOPA)-Effect in Parkinson-Akinesia. *Wiener klinische Wochenschrift*, 73:787-788, 1961.
136. T. T. Myöhänen, N. Schendzielorz and P. T. Männistö. Distribution of Catechol-O-Methyltransferase (COMT) Proteins and Enzymatic Activities in Wild-Type and Soluble COMT Deficient Mice. *Journal of Neurochemistry*, 113:1632-1643, 2010.
137. U. Bonuccelli and R. Ceravolo. The Safety of Dopamine Agonists in the Treatment of Parkinson's Disease. *Expert Opinion on Drug Safety*, 7:111-127, 2008.
138. M.D. Gottwald and M. J. Aminoff. New Frontiers in the Pharmacological Management of Parkinson's Disease. *Drugs Today*, 44:531-545, 2008.
139. J. L. Jaggi, A. Umemura, H. I. Hurtig, A. D. Siderowf, A. Colcher, M. B. Stern and G. H. Baltuch. Bilateral Stimulation of the Subthalamic Nucleus in Parkinson's Disease: Surgical Efficacy and Prediction of Outcome. *Stereotactic and Functional Neurosurgery*, 82:104-114, 2004.
140. M. C. Rodriguez-Oroz, I. Zamarbide, J. Guridi, M. R. Palmero and J. A. Obeso. Efficacy of Deep Brain Stimulation of the Subthalamic Nucleus in Parkinson's Disease 4 Years After Surgery: Double Blind and Open Label Evaluation. *Journal of Neurology, Neurosurgery and Psychiatry*, 75:1382-1385, 2004.

141. J. L. Eberling, W. J. Jagust, C. W. Christine, P. Starr, P. Larson, K. S. Bankiewicz and M. J. Aminoff. Results From a Phase I Safety Trial of hAADC Gene Therapy for Parkinson Disease. *Neurology*, 70:1980-1983, 2008.
142. M. G Kaplitt, A. Feigin, C. Tang, H. L. Fitzsimons, P. Mattis, P. A. Lawlor, R. J. Bland, D. Young, K. Strybing, D. Eidelberg and M. J. During. Safety and Tolerability of Gene Therapy with an Adeno-Associated Virus (AAV) Borne GAD Gene for Parkinson's Disease: An Open Label, Phase I Trial. *Lancet*, 369:2097-2105, 2007.
143. W. J. Marks, J. L. Ostrem, L. Verhagen, P. A. Starr, P. S. Larson, R. A. E. Bakay, R. Taylor, D. A. Cahn-Weiner, A. J. Stoessl, C. W. Olanow and R. T. Bartus. Safety and Tolerability of Intraputaminial Delivery of CERE-120 (Adeno-Associated Virus Serotype 2-Neurturin) to Patients with Idiopathic Parkinson's Disease: An Open-Label, Phase I Trial. *The Lancet Neurology*., 7:400-408, 2008.
144. W. Dauer and S. Przedborski. Parkinson's Disease Mechanisms and Models. *Neuron*, 39:889-909, 2003.
145. G. Jonsson and C. Sachs. Effects of 6-hydroxydopamine on the Uptake and Storage of Noradrenaline in Sympathetic Adrenergic Neurons. *European Journal of Pharmacology*, 9:141-155, 1970.
146. B. S. Jeon, V. Jackson-Lewis and R. E. Burke. 6-hydroxydomine Lesion of the Rat Substantia Nigra: Time Course and Morphology of Cell Death. *Neurodegeneration*, 4:131-137, 1995.
147. H. Sauer and W. H. Oertel. Progressive Degeneration of Nigrostriatal Dopamine Neurons Following Intrastratial Terminal Lesions with 6-Hydroxydopamine: A Combined Retrograde Tracing and Immunocytochemical Study in the Rat. *Neuroscience*, 59:401-415, 1994.

148. R. Heikkila and G. Cohen. Further Studies on the Generation of Hydrogen Peroxide by 6-hydroxydopamine. Potentiation by Ascorbic Acid. *Molecular Pharmacology*, 8:241-248, 1972.
149. S. Hall, J. N. Rutledge and T. Schallert. MRI, Brain Iron and Experimental Parkinson's Disease. *Journal of the Neurological Sciences*, 113:198-208, 1992.
150. R. Kumar, M. L. Agarwal and P. K. Seth. Free Radical-Generated Neurotoxicity of 6-hydroxydopamine. *Journal of Neurochemistry*, 64:1703-1707, 1995.
151. Y. He, T. Lee and S. K. Leong. 6-Hydroxydopamine Induced Apoptosis of Dopaminergic Cells in the Rat Substantia Nigra. *Brain Research*, 858:163-166, 2000.
152. R. Betarbet, T. B. Sherer and T. Greenamyre. Animal Models of Parkinson's Disease. *Bioessays*, 24:308-318, 2002.
153. U. Ungerstedt. Postsynaptic supersensitivity after 6-hydroxydopamine Induced Degeneration of the Nigro-Striatal Dopamine System. *ACTA Physiologica Scandinavica Supplement*, 367:69-93, 1971.
154. R. Deumens, A. Blokland and J. Prickaerts. Modeling Parkinson's Disease in Rats: An Evaluation of 6-OHDA Lesions of the Nigrostriatal Pathway Experimental *Neurology*, 175:303-317, 2002.
155. A. R. Cools, R. Brachten, D. Heeren, A. Willemsen and B. Ellenbroek. Search After Neurobiological Profile of Individual-Specific Features of Wistar Rats. *Brain Research Bulletin*, 24:49-69, 1990.
156. J. W. Langston, L. S. Forno, J. Tetrad, A. G. Reeves, J. A. Kaplan and D. Karluk. Evidence of Active Nerve Cell Degeneration in the Substantia Nigra of Humans Years After 1-Methyl-4-Phenyl-1,2,3,6-Tetrahydropyridine Exposure. *Annals of Neurology*, 46:598-605, 1999.

157. K. F. Tipton and T. P. Singer. Advances in our Understanding of the Mechanisms of the Neurotoxicity of MPTP and Related Compounds. *Journal of Neurochemistry*, 61:1191-1206, 1993.
158. N. W. Kowall, P. Hantraye, E. Brouillet, M. F. Beal, A. C. McKee and R. J. Ferrante. MPTP Induces Alpha-Synuclein Aggregation in the Substantia Nigra of Baboons. *Neuroreport*, 11:211-213, 2000.
159. H. H. Liou, M. C. Tsai, C. J. Chen, J. S. Jeng, Y. C. Chang, S. Y. Chen and R. C. Chen. Environmental Risk Factors and Parkinson's Disease: A Case-Control Study in Taiwan. *Neurology*, 48:1583-1588, 1997.
160. R. Betarbet, T. B. Sherer, G. MacKenzie, M. Garcia-Osuna, A. V. Panov and J. T. Greenamyre. Chronic Systemic Pesticide Exposure Reproduces Features of Parkinson's Disease. *Nature Neuroscience*, 3:1301-1306, 2000.
161. Y. Matsuoka, M. Vila, S. Lincoln, A. McCormack, M. Picciano, J. LaFrancois, X. Yu, D. Dickson, J. W. Langston, E. McGowan, M. Farrer, J. Hardy, K. Duff, S. Przedborski and D. A. Di Monte. Lack of Nigral Pathology in Transgenic Mice Expressing Human Alpha-Synuclein Driven by the Tyrosine Hydroxylase Promoter. *Neurobiology of Disease*, 8:535-539, 2001.
162. C. Lo Bianco, J. L. Ridet, B. L. Schneider, N. Deglon and P. Aebischer. Alpha - Synucleinopathy and Selective Dopaminergic Neuron Loss in a Rat Lentiviral-Based Model of Parkinson's Disease. *Proceedings of the National Academy of Sciences of the United States of America the United States of America*, 99:10813-10818, 2002.
163. R. Anjum and J. Blenis. The RSK Family of Kinases: Emerging Roles in Cellular Signalling. *Nature Reviews Molecular Cell Biology*, 9:747-758, 2008.
164. S. W. Jones, E. Erikson, J. Blenis, J. L. Maller and R. L. Erikson. A Xenopus Ribosomal Protein S6 Kinase Has Two Apparent Kinase Domains that are Each



- Similar to Distinct Protein Kinases. *Proceedings of the National Academy of Sciences of the United States of America*, 85:3377-3381, 1988.
165. J. Xing, D. D. Ginty and M. E. Greenberg. Coupling of the Ras-MAPK Pathway to Gene Activation by RSK2, a Growth Factor-Regulated CREB Kinase. *Science*, 273:959-963, 1996.
166. L. Zhang, Y. Ma, J. Zhang, J. Cheng and J. Du. A New Cellular Signaling Mechanism for Angiotensin II Activation of NF-Kappab; an Ikappab-Independent, RSK-Mediated Phosphorylation of P65. *Arteriosclerosis, Thrombosis and Vascular Biology*, 25:1148-1153, 2005.
167. D. Shahbazian, P. P. Roux, V. Mieulet, M. S. Cohen, B. Raught, J. Taunton, J. W. B. Hershey, J. Blenis, M. Pende and N. Sonenberg. The mTOR/ PI3K and MAPK Pathways Converge on eIF4B to Control its Phosphorylation and Activity. *EMBO Journal*, 25:2781-2791, 2006.
168. P. P. Roux, D. Shahbazian, H. Vu, M. K. Holz, M. S. Cohen, J. Taunton, N. Sonenberg and J. Blenis. Ras/ERK Signaling Promotes Site-Specific Ribosomal Protein S6 Phosphorylation via RSK and Stimulates Cap-Dependent Translation. *Journal of Biological Chemistry*, 282:14056-14064, 2007.
169. Y. Tan, H. Ruan, M. R. Demeter and M. J. Comb. p90RSK Blocks Bad-Mediated Cell Death via a Protein Kinase C-Dependent Pathway. *The Journal of Biological Chemistry*, 274:34859-34867, 1999.
170. D. Neise, D. Sohn, A. Stefanski, H. Goto, M. Inagaki, S. Wesselborg, W. Budach, K. Stuhler and R. U. Janicke. The p90 Ribosomal S6 Kinase (RSK) Inhibitor BI-D1870 Prevents Gamma Irradiation-Induced Apoptosis and Mediates Senescence via RSK and p53-Independent Accumulation of p21WAF1/CIP1. *Cell Death and Disease*, 4:1-11, 2013.

171. X. B. Meng, G. B. Sun, M. Wang, J. Sun, M. Qin and X. B. Sun. P90RSK and Nrf2 Activation via MEK1/2-ERK1/2 Pathways Mediated by Notoginsenoside R2 to Prevent 6-Hydroxydopamine-Induced Apoptotic Death in SH-SY5Y Cells. *Evidence-Based Complementary and Alternative Medicine*, 2013:1-15, 2013.
172. A. Biever, E. Valjent and E. Puighermanal. Ribosomal Protein S6 Phosphorylation in the Nervous System: From Regulation to Function. *Frontiers in Molecular Neuroscience*, 8:1-14, 2015.
173. J. A. Hutchinson, N. P. Shanware, H. Chang and R. S. Tibbetts. Regulation of Ribosomal Protein S6 Phosphorylation by Casein Kinase 1 and Protein Phosphatase 1. *The Journal of Biological Chemistry*, 286:8688-8696, 2011.
174. A. Portela and M. Esteller. Epigenetic Modifications and Human Disease. *Nature Biotechnology*, 28:1057-68, 2010.
175. O. Kovalchuk. Epigenetic Research Sheds New Light on the Nature of Interactions Between Organisms and Their Environment. *Environmental and Molecular Mutagenesis*, 49:1-3, 2008.
176. N. A. Kaidery, S. Tarannum and B. Thomas. Epigenetic Landscape of Parkinson's Disease: Emerging Role in Disease Mechanisms and Therapeutic Modalities. *Neurotherapeutics*, 10:698-708, 2013.
177. Z. Konsoula and F. A. Barile. Epigenetic Histone Acetylation and Deacetylation Mechanisms in Experimental Models of Neurodegenerative Disorders. *Journal of Pharmacological and Toxicological Methods*, 66:215-220, 2012.
178. G. P. Delcuve, D. H. Khan, and J. R. Davie. Roles of Histone Deacetylases in Epigenetic Regulation: Emerging Paradigms from Studies with Inhibitors. *Clinical Epigenetics*, 4:2-13, 2012.

179. S. L. Berger. The Complex Language of Chromatin Regulation During Transcription. *Nature*, 447:407-412, 2007.
180. S. Sharma and R. Taliyan. Targeting Histone Deacetylases: A Novel Approach in Parkinson's Disease. *Hindawi Publishing Corporation Parkinson's Disease*, 2015:1-11, 2015.
181. N. Gurvich, O. M. Tsygankova, J. L. Meinkoth and P. S. Klein. Histone Deacetylase is a Target of Valproic Acid-Mediated Cellular Differentiation. *Cancer Research*, 64:1079-1086, 2004.
182. T. Uo, T. D. Veenstra and R. S. Morrison. Histone Deacetylase Inhibitors Prevent p53-Dependent and p53-Independent Bax-Mediated Neuronal Apoptosis through Two Distinct Mechanisms. *The Journal of Neuroscience*, 29:2824-2832, 2009.
183. R. L. Macdonald and G. K. Bergey. Valproic Acid Augments GABA-Mediated Postsynaptic Inhibition in Cultured Mammalian Neurons. *Brain Research*, 170:558-562, 1979.
184. R. L. Macdonald and K. M. Kelly. Antiepileptic Drug Mechanisms of Action. *Epilepsia*, 36:2-12, 1995.
185. M. H. M. Baf, M. N. Subhash, K. M. Lakshmana and B. S. S. R. Rao. Sodium Valproate Induced Alterations in Mono Amine Levels In Different Regions Of The Rat Brain. *Neurochemistry International*, 24:67-72, 1994.
186. P. S. Chen, G. S. Peng, G. Li, S. Yang, X. Wu, C. C. Wang, B. Wilson, R. B. Lu, P. W. Gean, D. M. Chuang and J. S. Hong. Valproate Protects Dopaminergic Neurons in Midbrain Neuron/Glia Cultures by Stimulating the Release of Neurotrophic Factors from Astrocytes. *Molecular Psychiatry*, 11:1116-1125, 2006.

187. S. K. Kidd and J. S. Schneider. Protective Effects Of Valproic Acid on the Nigrostriatal Dopamine System in a 1-Methyl-4-Phenyl-1,2,3,6-Tetrahydropyridine Mouse Model of Parkinson's Disease. *Neuroscience*, 194:189-194, 2011.
188. G. Díaz-Véliz, S. Mora, P. Gómez, M. T. Dossi, J. Montiel, C. Arriagada, F. Aboitiz and J. Segura-Aguilar. Behavioral Effects of Manganese Injected in the Rat Substantia Nigra are Potentiated by Dicumarol, a DT-Diaphorase Inhibitor. *Pharmacology, Biochemistry and Behavior*, 77:245-251, 2004.
189. G. Paxinos and C. Watson. *The Rat Brain in Stereotaxic Coordinates*, Academic Press Inc., California, USA, 1997
190. L. Chagniel, C. Robitaille, M. Lebel and M. Cyr. Striatal Inhibition Of Calpains Prevents Levodopa-Induced Neurochemical Changes and Abnormal Involuntary Movements in the Hemiparkinsonian Rat Model. *Neurobiology of Disease*, 45:645-655, 2012.
191. İ. T. Uzbay. *Psikofarmakolojinin Temelleri ve Deneysel Araştırma Teknikleri*. Çizgi Tıp Yayınevi, Ankara, 2004.
192. K. A. Tayarani-Binazir, M. J. Jackson, I. Strang, M. Jairaj, S. R. and P. Jenner. Benserazide Dosing Regimen Affects the Response to L-3,4-Dihydroxyphenylalanine in the 6-Hydroxydopamine-Lesioned Rat. *Behavioural Pharmacology*, 23:126-133, 2012
193. S. M. Hsu, L. Raine and H. Fanger. Use of Avidin-Biotin Peroxidase Complex (ABC) in Immunoperoxidase Techniques: A Comparison Between ABC and Unlabeled Antibody (PAP) Procedures. *Journal of Histochemistry and Cytochemistry*, 29:577-580, 1981.
194. J. D. Bancroft and A. Stevens. *Theory and Practice of Histological Techniques*, Fourth Edition, Churchill Livingstone, 1996.

195. O. H. Lowry, N. J. Rosebrough, A. L. Farr and R. J. Randall. Protein Measurement with the Folin Phenol Reagent. *The Journal of Biological Chemistry*, 193:265-257, 1951
196. Z. A. Placer, L. L. Cushmann and B. C. Johnson. Estimation of Products of Lipid Peroxidation in Biochemical Systems. *Analytical Biochemistry*, 16:359-364, 1966.
197. Y. Sun, L. W. Oberley and Y. A. Li. Simple Method for Clinical Assay of Superoxide Dismutase. *Clinical Chemistry*, 34:497-500, 1988.
198. G. L. Elmann, K. D. Courtney, V. Andres and R. M. Featherstone. A New and Rapid Colorimetric Determination of Acetylcholinesterase Activity. *Biochemical Pharmacology*, 7:88-95, 1961.
199. W. H. Habig, M. J. Pabst and W. B. Jakoby. Glutathione s-transferases. The First Enzymatic Step in Mercapturic Acid Formation. *The Journal of Biological Chemistry*, 249:7130-7139, 1974.
200. A. E. Lang and A. M. Lozano. Parkinson's Disease. First of Two Parts. *The New England Journal of Medicine*, 339:1044-1053, 1998.
201. A. E. Lang and A. M. Lozano. Parkinson's Disease. Second of Two Parts. *The New England Journal of Medicine*, 339:1130-1143, 1998.
202. M. J. Zigmond. Chemical Transmission in the Brain: Homeostatic Regulation and its Functional Implications. *Progress in Brain Research*, 100:115-122, 1994.
203. G. C. Cotzias, P. S. Papavasiliou and R. Gellene. Modification of Parkinsonism Chronic Treatment with L-dopa. *The New England Journal of Medicine*, 280:337-345, 1969.
204. A. Barbeau. The Clinical Physiology of Side Effects in Long Term L-dopa *Therapeutic Advances in Neurological Disorders*, 5:347-365, 1974.

205. A. J. Lees. Comparison of Therapeutic Effects of Levodopa, Levodopa and Selegiline, and Bromocriptine in Patients with Early, Mild Parkinson's Disease Three Year Interim Report. *British Medical Journal*, 307:469-472, 1993.
206. D. B. Calne, C. Plotkin, A. C. Williams, J. G. Nutt, A. Neophytides and P. F. Teychenne. Long Term Treatment of Parkinsonism with Bromocriptine. *Lancet*, 8067:735-738, 1978.
207. B. S. Burton. On the Propyl Derivatives and Decomposition Products of Ethylacetoacetate. *Journal of the American Chemical Society*, 3:385-395, 1882.
208. H. H. Frey and W. Löscher. Distribution of Valproate Across the Interface Between Blood and Cerebrospinal Fluid. *Neuropharmacology*, 17:637-642, 1978.
209. Drugs, "Valproic Acid Drug Interactions", <http://www.drugs.com/drug-interactions/valproic-acid.pdf> [retrieved 13 May 2016].
210. A. G. Kazantsev and L. M. Thompson. Therapeutic Application of Histone Deacetylase Inhibitors for Central Nervous System Disorders. *Nature Reviews*, 7:854-868, 2008.
211. L. Lva, Y. Sunb, X. Hana, C. C. Xub, Y. P. Tanga and Q. Dong. Valproic Acid Improves Outcome After Rodent Spinal Cord Injury Potential Roles of Histone Deacetylase Inhibition. *Brain Research*, 1396:60-68, 2011.
212. D. Blum, S. Torch, N. Lambeng, M. F. Nissou, A. L. Benabid, R. Sadoul and J. M. Verna. Molecular Pathways Involved in the Neurotoxicity of 6-OHDA, Dopamine and MPTP Contribution to the Apoptotic Theory in Parkinson's Disease. *Progress in Neurobiology*, 65:135-172, 2001.
213. Y. Glinka, K. F. Tipton and M. B. Youdim. Nature of Inhibition of Mitochondrial Respiratory Complex I by 6- hydroxydopamine. *Journal of Neurochemistry*, 66:2004-2010, 1996.

214. D. Kirik, C. Winkler and A. Bjorklund. Growth and Functional Efficacy of Intrastriatal Nigral Transplants Depend on the Extent of Nigrostriatal Degeneration. *The Journal of Neuroscience*, 21:2889-2896, 2001.
215. W. S. Choi, S. Y. Yoon, T. H. Oh, E. J. Choi, K. L. OMalley and Y. J. Oh. Two Distinct Mechanisms are Involved in 6-hydroxydopamine and MPP<sup>+</sup> Induced Dopaminergic Neuronal Cell Death Role of Caspases, ROS, and JNK. *Journal of Neuroscience Research*, 57:86-94, 1999.
216. G. Walkinshaw and C. M. Waters. Neurotoxin Induced Cell Death in Neuronal PC12 Cells is Mediated by Induction of Apoptosis. *Neuroscience*, 63:975-987, 1994.
217. Y. He, T. Lee and S. K. Leong. 6-Hydroxydopamine Induced Apoptosis of Dopaminergic Cells in the Rat Substantia Nigra. *Brain Research*, 858:163-166, 2000.
218. C. L. Zuch, V. K. Nordstroem, L. A. Briedrick, G. R. Hoernig, A. C. Granholm and P. C. Bickford. Time Course of Degenerative Alterations in Nigral Dopaminergic Neurons Following a 6-Hydroxydopamine Lesion. *Journal of Comparative Neurology*, 427:440-454, 2000.
219. L. K. Tsai, M. S. Tsai, C. H. Ting and H. Li. Multiple Therapeutic Effects of Valproic Acid in Spinal Muscular Atrophy Model Mice. *Journal of Molecular Medicine*, 86:1243-1254, 2008.
220. E. C. Hirsch, T. Breidert, E. Rousset, S. Hunot, A. Hartmann and P. P Michel. The Role of Glial Reaction and Inflammation in Parkinson's Disease. *Annals of the New York Academy of Sciences*, 991:214-228, 2003.
221. T. Suuronen, J. Huuskonen, R. Pihlaja, S. Kyrylenko and A. Salminen. Regulation of microglial inflammatory response by histone deacetylase inhibitors. *Journal of Neurochemistry*, 87:407-416, 2003.

222. P. S. Chen, C. C. Wang, C. D. Bortner, G. S. Peng, X. Wu, H. Pang, R. B. Lu, P. W. Gean, D. M. Chuang and J. S. Hong. Valproic Acid and Other Histone Deacetylase Inhibitors Induce Microglial Apoptosis and Attenuate Lipopolysaccharide-Induced Dopaminergic Neurotoxicity. *Neuroscience*, 149:203-212, 2007.
223. G. R. Uhl. Hypothesis The Role of Dopaminergic Transporters in Selective Vulnerability of Cells in Parkinson's Disease. *Annals of Neurology*, 43:55-56, 1998.
224. E. Tiffany-Castiglioni, R. P. Saneto, P. H. Proctor and J. R. Perez-Polo. Participation of Active Oxygen Species in 6-hydroxydopamine Toxicity to a Human Neuroblastoma Cell Line. *Biochemical Pharmacology*, 31:181-188, 1982.
225. F. Abad, R. Maroto, M. G. Lopez, P. Sanchez-Garcia and A. G. Garcia. Pharmacological Protection Against the Cytotoxicity of 6-hydroxydopamine and H<sub>2</sub>O<sub>2</sub> in Chromaffin Cells. *The European Journal of Pharmacology*, 293:55-64, 1995.
226. A. S. Permual, W. K. Tordzro, M. Katz, V. Jackson-Lewis, T. B. Cooper, S. Fahn and J. L. Cadet. Regional Effects of 6-hydroxydopamine on Free Radical Scavengers in the Rat Brain. *Brain Research*, 504:139-141, 1989.
227. L. Hritcu, A. Ciobica and V. Artenie. Effects of Right Unilateral 6-Hydroxydopamine Infusion Induced Memory Impairment and Oxidative Stress Relevance for Parkinson's Disease. *Central European Journal of Biology*, 3:250-257, 2008.
228. M. Asanuma, H. Hirata and J. L. Cadet. Attenuation of 6-hydroxydopamine-Induced Dopaminergic Nigrostriatal Lesions in Superoxide Dismutase Transgenic Mice. *Neuroscience*, 85:907-917, 1998.
229. J. C. Bensadoun, O. Mirochnitchenko, M. Inouye, P. Aebischer and A. D. Zurn. Attenuation of 6-OHDA Induced Neurotoxicity in Glutathione Peroxidase Transgenic Mice. *European Journal Of Neuroscience*, 10:3231-3236, 1998.



230. L. K. Jornada, S. S. Valvassori, A. V. Steckert, M. Moretti, F. Mina, C. L. Ferreira, C. O. Arent, F. Dal-Pizzol and J. Quevedo. Lithium and Valproate Modulate Antioxidant Enzymes and Prevent Ouabain-Induced Oxidative Damage in an Animal Model of Mania. *The Journal of Psychiatric Research*, 45:162-168, 2011.
231. M. Rodriguez Diaz, P. Abdala, P. Barroso-Chinea, J. Obeso and T. Gonzalez Hernandez. Motor Behavioural Changes After Intracerebroventricular Injection of 6-Hydroxydopamine in the Rat an Animal Model of Parkinson's Disease. *Behavioural Brain Research*, 122:79-92, 2001.
232. K. Sakai and D. M. Gash. Effect of Bilateral 6-OHDA Lesions of the Substantia Nigra on Locomotor Activity in the Rat. *Brain Research*, 633:144-150, 1994.
233. G. E. Meredith and U. J. Kang. Behavioral Models of Parkinson's Disease in Rodents A New Look at an Old Problem. *Movement Disorders*, 21:1595-1606, 2006.
234. W. Löscher. Valproate Enhances GABA Turnover in the Substantia Nigra. *Brain Research*, 501:198-203, 1989.
235. Y. Godin, L. Heiner, J. Mark and P. Mandel. Effects of di-n-propylacetate, an Anticonvulsive Compound, on GABA Metabolism. *Journal of Neurochemistry*, 16: 869-873, 1969.
236. S. Simler, L. Ciesielski, M. Klein and P. Mandel. Anticonvulsant and Antiaggressive Properties of Di-n-propylacetate After Repeated Treatment. *Neuropharmacology*, 21:133-140, 1982.
237. M. J. Iadarola and K. Gale. Dissociation Between Drug Induced Increases in Nerve Terminal and Non-Nerve Terminal Pools of GABA in vivo. *European Journal of Pharmacology*, 59:125-129, 1979.
238. C. S. Biggs, B. R. Pearce, L. J. Fowler and P. S. Whitton. Regional Effects of Sodium Valproate on Extracellular Concentrations of 5-hydroxytryptamine, Dopamine,

- and Their Metabolites in the Rat Brain: an in vivo Microdialysis Study. *Journal of Neurochemistry*, 59:1702-1708, 1992.
239. H. Qing, G. He, P. T. Ly, C. J. Fox, M. Staufenbiel and F. Cai. Valproic Acid Inhibits Abeta Production Neuritic Plaque Formation and Behavioral Deficits in Alzheimer's Disease Mouse Models. *Journal of Experimental Medicine*, 205:2781-2789, 2008.
240. A. McCampbell, A. A. Tay, L. Whitty, E. Penney, J. S. Steffan and K. H. Fischbeck. Histone Deacetylase Inhibitors Reduce Polyglutamine Toxicity. *Proceedings of the National Academy of Sciences of the United States of America the United States of America*, 98:15179-15184, 2001.
241. C. C. Weihl, A. M. Connolly and A. Pestronk. Valproate May Improve Strength and Function in Patients with Type III/IV Spinal Muscle Atrophy. *Neurology*, 67:500-501, 2006.
242. M. Ren, Y. Leng, M. Jeong, P. R. Leeds and D. M. Chuang. Valproic Acid Reduces Brain Damage Induced by Transient Focal Cerebral Ischemia in Rats Potential Roles of Histone Deacetylase Inhibition and Heat Shock Protein Induction. *Journal of Neurochemistry*, 89:1358-1367, 2004.
243. M. Fukuchi, T. Nii, N. Ishimaru, A. Minamino, D. Hara, I. Takasaki, A. Tabuchi and M. Tsuda. Valproic acid Induces Up or Down Regulation of Gene Expression Responsible for the Neuronal Excitation and Inhibition in Rat Cortical Neurons Through its Epigenetic Actions. *The Journal of Neuroscience Research*, 65:35-43, 2009.
244. B. Monti, V. Gatta, F. Piretti, S. S. Raffaelli, M. Virgili and A. Contestabile. Valproic Acid is Neuroprotective in the Rotenone Rat Model of Parkinson's Disease Involvement of  $\alpha$ -synuclein. *Neurotoxicity Research*, 17:130-41, 2010.

245. B. Monti, D. Mercatelli and A. Contestabile. Valproic Acid Neuroprotection in 6-OHDA Lesioned Rat a Model for Parkinson's Disease. *Herbert Open Access Journals*, 1:1-4, 2012.
246. E. Kontopoulos, J. D. Parvin and M. B. Feany.  $\alpha$ -synuclein Acts in the Nucleus to Inhibit Histone Acetylation and Promote Neurotoxicity. *Human Molecular Genetics*, 15:3012-3023, 2006.
247. A. P. Nicholas, F. D. Lubin and P. J. Hallett. Striatal Histone Modifications in Models of Levodopa Induced Dyskinesia. *Journal of Neurochemistry*, 106:486-94, 2008.
248. E. V. Wong, A. W. Schaefer, G. Landreth and V. Lemmon. Involvement of p90rsk in Neurite Outgrowth Mediated by the Cell Adhesion Molecule L1. *Journal of Biological Chemistry*, 271:18217-18223, 1996.
249. B. A. Ballif and J. Blenis. Molecular Mechanisms Mediating Mammalian Mitogen-Activated Protein Kinase (MAPK) Kinase (MEK)-MAPK Cell Survival Signals. *Cell Growth and Differentiation*, 12:397-408, 2001.
250. A. Shimamura, B. A. Ballif, S. A. Richards and J. Blenis. Rsk1 Mediates a MEK-MAP Kinase Cell Survival Signal. *Current Biology*, 10:127-135, 2000.
251. S. R. Boston, R. Deshmukh, S. Strome, U. D. Priyakumar, A. D. MacKerell and P. Shapiro. Characterization of ERK Docking Domain Inhibitors that Induce Apoptosis by Targeting Rsk 1 and Caspase 9. *BioMedCentral Cancer*, 11:1-12, 2011.
252. N. Pavon, A. B. Martin, A. Mendialdua and R. Moratalla. ERK Phosphorylation and Fosb Expression are Associated with L-DOPA-Induced Dyskinesia in Hemiparkinsonian Mice. *Biological Psychiatry*, 59:64-74, 2006.
253. J. E. Westin, L. Vercaammen, E. M. Strome, C. Konradi and M. A. Cenci. Spatiotemporal Pattern of Striatal ERK1/2 Phosphorylation in a Rat Model of L-

DOPA-Induced Dyskinesia and the Role of Dopamine D1 Receptors. *Biological Psychiatry*, 62:800-810, 2007.

